INFLUENCE OF PARTIAL-FLOW PARTICULATE FILTER ON DIESEL VEHICLE THERMAL EFFICIENCY AND EMISSION CHARACTERISTICS USING B20

PLAN TEEKATASN COSH

A THESIS REPORT SUBMITTED IN PARTIAL FULFILLMENT

OF THE REQUIREMENTS FOR THE DEGREE OF

MASTER OF ENGINEERING IN AUTOMOTIVE AND

ADVANCED TRANSPORTATION ENGINEERING

SCHOOL OF ENGINEERING

KING MONGKUT'S INSTITUTE OF TECHNOLOGY LADKRABANG

YEAR 2023

KMITL-2023-EN-M-277-139

THESIS TITLE	Influence of partial-flow particulate filter on diesel vehicle thermal efficiency and emission characteristics using B20
STUDENT NAME	Mr. Plan Teekatasn Cosh
STUDENT ID	64601180
DEGREE	Master of Engineering
PROGRAM	Automotive and Advanced Transportation Engineering
ADVISOR	Assoc.Prof. Dr. Supat Kittiratsatcha
CO-ADVISOR	Dr. Kobsak Sriprapha
CO-ADVISOR	Prof. Dr. Katsunori Hanamura

ABSTRACT

Diesel vehicles' exhaust hazardous gas emissions and solid particle emissions are the primary issues due to tightening emissions regulations. The utilization of renewable energy sources as a viable alternative is a potential solution to mitigate emissions. Biodiesel derived from palm oil and ethanol, characterized by its significant oxygen content, is produced from agricultural resources. In this research, the analysis focused on the metallic fleece material utilized in a partial flow diesel particulate filter (P-DPF) and the particulate matter (PM) present within an exhaust after-treatment system comprising a diesel oxidation catalyst (DOC) and P-DPF. The purpose of this research is to investigate and observe the influence of biodiesel fuels (B20) on the P-DPF and its impact on vehicle thermal efficiency and emission characteristics. The specific goals include achieving the most reduction in the quantity of PM as much as possible in diesel exhaust gas compared to systems without an after-treatment system and proving that soot oxidation occurs inside P-DPF. The experiment encompassed three different driving conditions on chassis dynamometer which allowed to get the result for the simulation of an actual driving cycle. The utilization of B20 alongside exhaust pipe-installed after-treatment systems has minimal impact on the performance of both diesel engines and

vehicles. Employing after-treatment systems led to a notable decrease in particulate matter emissions, averaging 51% to 69%, compared to using biodiesel fuels alone. Furthermore, the results demonstrate that the soot accumulated within the P-DPF undergoes oxidation via the catalytic action of NO_2, facilitated by exhaust temperatures surpassing 250 °C upon exiting the P-DPF under the conditions of constant vehicle speeds and an engine load of 140 Nm.

Keywords: Biodiesel, P-DPF, After-treatment systems, Soot oxidation, PM

ACKNOWLEDGEMENT

First, I would like to begin by conveying my sincere gratitude for the esteemed scholarship bestowed upon me by the Thailand Advance Institute of Science and Technology, as well as the Tokyo Institute of Technology (TAIST-Tokyo Tech). Their generous support has been instrumental in facilitating the accomplishment of this research endeavor, and I am truly thankful for the opportunities and resources they have provided.

I would like to extend my heartfelt appreciation to my advisor, Assoc. Prof. Dr. Supat Kittiratsatcha from King Mongkut's Institute of Technology Ladkrabang. I am also grateful for the assistance and input provided by my co-advisors, Dr. Kobsak Sriprapha from the National Science and Technology Development Agency and Assoc. Prof. Dr. Katsunori Hanamura from Tokyo Institute of Technology. Additionally, I would like to acknowledge the support and supervision of Assoc. Prof. Dr. Preechar Karin and Dr. Mek Srilomsak from the Department of Mechanical Engineering at King Mongkut's Institute of Technology Ladkrabang, for their patience, care, knowledge and guiding me through the various challenges during this period of research. Their constructive suggestions have played a significant role in shaping this study.

Special mention to the members of KMITL laboratory: P'Palm, P'Bird, P'Bank, Phyo Wai, Leo, Myat, and Ms. Zwemon. We have experienced numerous experiments, data analysis, seminars, meetings, and more, and it would not have been possible without the contributions of each team member. Another special mention to the members of Hanamura laboratory: Prof. Dr. Katsunori Hanamura, Mr. Teerapat Suteerapongpun, Mr.Phyozin Koko, and others that I have not mentioned for their grateful support and knowledge during my time as an exchange student in Japan.

To my AE-15 mates, we only meet a few times during our studies, but I am delighted that we have exchanged experiences with numerous lectures and exams. I also wish everyone well and blessings in their future undertakings. Once again, thank you for coming, and I'm pleased we got to know one another despite the fact that we largely met online.

Finally and most importantly, I am deeply grateful to my parents, my friends and my special person for their endless support, encouragement, and understanding throughout my

academic journey. This thesis owes its existence to the valuable contributions and inspiration of numerous individuals.

Plan Teekatasn Cosh

7th June 2023

TABLE OF CONTENTS

CHAPTER 1

INTRODUCTION

1.1 Research Background

1.1.1 Problematic of particulate matter in Thailand

Diesel combustion engines, also known as compression ignition engines, are extensively utilized due to their notable fuel economy and thermal efficiency. Diesel fuel use is double that of gasoline consumption and accounts for a major share of overall petroleum usage [1]. However, the main disadvantage of diesel engines is the release of particulate matter (PM). In the context of urban areas like Bangkok, Thailand, vehicles contribute to over 40% of the total $PM_{2.5}$ emissions. The air quality issues observed in the atmosphere of Bangkok are widely acknowledged to stem from the substantial emissions generated by high levels of traffic. These emissions have a significant adverse effect on the health of individuals residing in the area. Moreover, considering the escalating global climate crisis, the presence of high concentrations of $PM_{2.5}$ in Thailand is recognized as having significant consequences for the well-being and overall quality of life of the local population [2]. This is a major problem because of the well-known dangers and negative consequences of diesel PM on public health and the environment. The damaging effects of diesel PM are widely recognized, underscoring the crucial need for extensive mitigation strategies [3-4]. In Thailand, automotive share is very popular in the country, as shown in **Figure 1.1**, these light-duty truck automotive share can create PM when the vehicle getting old, which can be another reason that support the total PM2.5 emissions over 40% from vehicle in Bangkok, Thailand.

1.1.2 Emissions from diesel vehicles

The diesel engine is a type of internal combustion engine that operates on the principle of auto-ignition. It involves the mixing of fuel and air within the engine, followed by the compression of this mixture in the combustion chamber. This compression process leads to the generation of high temperatures, enabling the diesel fuel to ignite spontaneously upon injection into the cylinder. Consequently, the diesel engine utilizes the thermal energy

generated during combustion to extract the chemical energy present in diesel fuel and convert it into useful mechanical power [8]. In an ideal scenario where thermodynamic equilibrium is achieved, the complete combustion of diesel fuel within the engine's combustion chambers would result in the production of only carbon dioxide (CO_2) and water (H_2O). However, several factors such as the air-fuel ratio, ignition timing, turbulence in the combustion chamber, combustion form, air-fuel concentration, and combustion temperature prevent this ideal condition from being realized. Consequently, the combustion process generates a range of harmful byproducts. Among the most significant and commonly observed exhaust emissions from combustion ignition engines (C.I. engines), as shown in **Figure 1.2**, are carbon monoxides (CO) produced by incomplete oxidation of fuel carbon when there is insufficient oxygen to thoroughly oxidize the fuel, unburnt hydrocarbons (HC) are made up of unburned fuels because of inadequate temperature near the cylinder wall, nitrogen oxides (NO_x) is formed when nitrogen-containing air is burnt at high flame temperatures, Sulphur oxides (SO and SO_2) are formed by the sulfates included in fuels. , as well as particulates matter, soot, and smoke that are resulted from combustion process. These emissions are a result of complex interactions within the combustion process and represent significant environmental and health concerns [6-8].

1.1.3 Particulate Matter (PM)

Particulate matter (PM) in diesel engines is mostly caused by incomplete combustion of hydrocarbons found in fuel and lubricating oil. Studies of Kittelson [9] have revealed that the typical composition of PM emitted by heavy-duty diesel engines includes approximately 41% carbon, 7% unburned fuel, 25% unburned oil, 14% sulfate and water, and 13% ash and miscellaneous components. Further research by Agarwal [10] has identified various components within PM, such as elemental carbon (approximately 31%), sulfates and moisture (around 14%), unburned fuel (about 7%), unburned lubricating oil (approximately 40%), and trace amounts of metals and other substances. Diesel PM particles are generally spherical, with diameters ranging from 15 to 40 nm, and more than 90% of these particles are smaller than 1 μm in diameter. The formation of PM emissions is influenced by factors like combustion and expansion processes, fuel quality (including sulfur and ash content), lubrication oil quality

and consumption, combustion temperature, and exhaust gas cooling [11]. These factors collectively contribute to the characteristics and composition of diesel PM emissions.

1.1.3.1 Formation

To comprehend PM and its reduction, the formation of PM must be examined. The formation of PM involves a series of essential steps, illustrated in **Figure 1.3**. Firstly, during pyrolysis, the fuel undergoes incomplete combustion or a lack of oxygen, leading to the breakdown of the fuel into precursor compounds known as polycyclic aromatic hydrocarbons (PAHs). Subsequently, nucleation occurs, where these precursors further break down and form nuclei. These nuclei then undergo surface growth, whereby additional mass accumulates on the surface of nucleated soot particles, resulting in the formation of primary particles. Finally, primary particles unite to form bigger agglomerates that surpass the size of the primary particles through coalescence and agglomeration [12]. The compositions of agglomerate particles, depicted in **Figure 1.4**, primarily comprise small carbon particles known as soot. Adhered to the surface of soot are hydrocarbons, which can be effectively removed using organic solvents. Additionally, the agglomerate particles may contain sulfate (SO_4) particles, which can be eliminated through contact with water. It should be noted that the composition of PM agglomerates may also include liquid droplets, condensed hydrocarbons, and extra SO_4 particles [13]. Additionally, as shown in **Figure 1.5**, PM particle sizes are classified as follows: PM_{10}, D(diameter) < 10 μm; $PM_{2.5}$ or tiny particles D < 2.5 μm; $PM_{0.1}$ or ultrafine particles D < 0.10 μm; and nanoparticles, D < 0.05 μm or 50 nm.

1.1.3.2 Microstructure, morphology, and nanostructure

The microstructure of PM can be investigated through the utilization of advanced imaging techniques such as Scanning Electron Microscopy (SEM). SEM provides high-resolution, three-dimensional images of the scanned surfaces, enabling a detailed examination of the PM microstructure. Furthermore, to analyze the morphology and nanostructure of individual primary particles within the PM, Transmission Electron Microscopy (TEM) was employed. TEM allows for examination at various magnifications higher than SEM, providing insights into the intricate characteristics and fine-scale features of PM particles. To perform quantitative analysis of the morphology and nanostructure, the image processing software ImageJ was employed.

Figure 1.6 shows the micrograph images of diesel PM for diesel PM. The software facilitated the examination of individual ovular primary particles, allowing for precise measurement of their sizes. By gathering this data, it became possible to generate size distributions for the particulate matter (PM). **Figure 1.7** illustrates the utilization of ImageJ for the accurate counting of single primary particles, while **Figure 1.8** showcases the stepwise analysis process involving fringe length and interplanar spacing using the ImageJ software. These ImageJ studies and measurements give vital insights into the features and properties of PM, allowing for a more complete knowledge of its composition and structure. Hay Mon Oo et. al. [15] conducted an analysis of particulate matter (PM) emissions from both gasoline direct injection (GDI) and diesel direct injection (DDI) engines, comparing them with model soot (carbon black). The researchers utilized TEM) to analyze the morphology and nanostructure of soot particles. The findings indicated that carbon black primary particles were the largest, averaging around 31 nm. The PM emitted from diesel direct injection (DDI) and gasoline direct injection (GDI) engines had slightly smaller primary particle sizes, measuring around 26 nm and 24 nm, respectively. Moreover, the fringe analysis revealed that carbon black exhibited a more graphitic nature, characterized by reduced inter-planar spacing and longer fringes.

1.1.3.3 Elemental composition

The investigation of the elemental composition of diesel particulate matter (PM) involved the analysis of its aggregate particles using electron dispersive X-ray spectroscopy (EDS). Qualitative and quantitative elemental analysis was conducted utilizing transmission electron microscopy (TEM-EDS). Additionally, the SEM equipment, equipped with an EDS function, was employed to determine the elemental composition of diesel PM. These advanced techniques provided valuable insights into the elemental constituents of PM, contributing to a comprehensive understanding of its composition, as shown in **Figure 1.9(a) and (b)**, Karin P. et. al. [16-17] used TEM-EDS for the analysis of diesel PM and SEM-EDS for analysis of engine oil, respectively. In their study, Hay Mon Oo et al. [15] utilized TEM-EDS to analyze the elemental composition of the soot samples, as shown in **Figure 1.10(a) to (c)**, revealing that carbon was the primary component in all samples. The quantitative analysis of the particulate matter indicated that GDI-PMs consisted of approximately 95% carbon by weight, with an oxygen content of 5% by weight. Similarly, DDI PMs were composed of 96%

carbon fraction, while carbon black (N330), used as a model soot, consisted of 98% carbon by weight.

1.1.3.4 Oxidation

The removal of PM from the exhaust gas of internal combustion engines (ICEs) is crucial for safeguarding human health. To assess the reaction activity and oxidation characteristics of PM, researchers have employed Thermo-gravimetric Analysis (TGA) and Temperature Program Oxidation (TPO). One effective technology for reducing particle emissions from diesel engines is the implementation of Diesel Particulate Filters (DPFs). These filters play a vital role in capturing and oxidizing PM, making them an essential component in the overall process of PM mitigation.

In a study by Karin P., Boonsakda J., Siricholathum K., et al. [18], the kinetics of particulate matter (PM) oxidation were investigated using thermo-gravimetric analysis (TGA). The researchers focused on studying the oxidation kinetics of carbon black, diesel PMs, and biodiesel PMs on DPF powders under isothermal conditions at temperatures of 500°C, 550°C, and 600°C, assessing the TGA mass conversion behavior. Interestingly, the findings revealed that PMs from biodiesel engines exhibited a higher oxidation rate compared to PMs from diesel engines and carbon black. Notably, the fastest oxidation rate was observed at 600°C. Additionally, the researchers successfully examined the PM oxidation kinetics using conventional cordierite DPF powders through TGA analysis.

In their study, Leistner K. et al. [19] conducted a comprehensive investigation on the kinetic analysis of soot oxidation using different nitrogen oxide species, namely NO_2, NO, and a combination of NO and O_2. The researchers emphasized the significance of studying the reaction kinetics between soot and nitrogen oxides, as it holds crucial implications for the development of effective aftertreatment technologies for diesel engines. The findings highlighted that the oxidation of soot by NO_2 involves the formation of multiple surface complexes, and the presence of NO is attributed to the instability of C*(NO_2) below 200°C, which is then converted to C*(NO) upon NO_2 adsorption. Moreover, the researchers observed that the oxidation of carbon (C) by NO_2 benefits from a higher availability of oxygen (O) atoms

compared to the C + NO reaction. Additionally, they noted that the C + NO_2 reaction is less influenced by the adsorption step compared to the C + NO reaction.

1.1.4 The significance of exhaust after-treatment

Considering the growing need for stricter regulations on diesel emissions, it has become imperative to adjust in conventional combustion methods, introduce additives to the fuel, or implement exhaust gas treatment measures [20].

1.1.4.1 Diesel Oxidation Catalyst (DOC)

Diesel oxidation catalysts (DOCs) are utilized in the exhaust line of diesel engines to minimize hydrocarbon (HC) and carbon monoxide (CO) emissions. A diagram in **Figure 1.11** illustrates the structure of a diesel oxidation catalyst, featuring narrow channels with catalyst-coated porous walls. This design enables continuous diffusion and reactions, effectively reducing HC and CO pollutants at the DOC outlet. Kabir M. N. et al. [21] propose a novel model for designing and controlling DOCs, based on fluid flow principles. The model focuses on a single channel with its surrounding monolith wall, considering the species involved in HC and CO reduction. The study successfully predicts outlet gas temperature, as well as mole fractions of CO, H_2, and C_3H_6. The model exhibits good agreement between simulation and experimental results, accurately capturing species concentration and temperature in the diesel oxidation catalyst.

In their work, Reşitoğlu İ.A., Altinişik K., and Keskin A. [6] provide an insightful explanation on the capabilities of DOCs. These catalysts play a crucial role in oxidizing HC and CO emissions, thereby reducing diesel particulate emissions. They also contribute to enhancing the NO_2:NO_x ratio, making them suitable for catalytic heating during diesel particulate filter (DPF) regeneration. DOCs are typically constructed with a monolith honeycomb structure, featuring a washcoat of noble metals, such as platinum (Pt) and palladium (Pd), which are widely employed as metal-based catalysts for oxidation reactions. Notably, DOCs exhibit key characteristics, such as light-off temperature and conversion efficiency. Moreover, the utilization of alternative fuels has the potential to enhance the conversion efficiency of DOCs while simultaneously reducing the presence of harmful pollutants like sulfates and sulfuric acid. These findings offer valuable insights into the properties and advantages of DOCs,

highlighting their importance in mitigating emissions from diesel engines and their potential for further optimization using alternative fuels.

1.1.4.2 Full-Flow Diesel Particulate Filter (F-DPF)

A diesel particulate filter (DPF) is a type of diesel exhaust after-treatment system designed to address the issue of PM emissions, primarily composed of soot, released from the engine. Its purpose is to capture and prevent the release of PM into the atmosphere, thereby mitigating environmental pollution. Normally, the DPF will be installed downstream of the exhaust pipeline side next to the DOC. F-DPF used so far in passenger cars consists of porous ceramics. Ceramic particulate filters, as shown in **Figure 1.12**, consist of a honeycomb structure made of silicon carbide or Cordierite, which has a large number of parallel, mostly square channels. As the filter becomes increasingly saturated with soot, a layer of soot forms on the surface of the channel walls. This provides highly efficient surface filtration for the following operating phase [22]. Furthermore, Reşitoğlu İ.A., Altinişik K., and Keskin A. [6] also provide the explanation for DPF, wall flow silicon carbide (SiC) filter is widely used as DPF worldwide, and catalyzed DPFs (CDPF) can eliminate the need for DOC upstream of the filter.

1.1.4.3 Partial-Flow Diesel Particulate Filter (P-DPF)

The focus of this study revolves around the Partial-Flow Diesel Particulate Filter (P-DPF), which is designed to effectively trap and oxidize particulate matter (PM) to reduce emissions. As its name implies, the P-DPF provides partial filtration while maintaining the original electronic control system of the vehicle, making it a convenient and versatile solution. By installing the P-DPF on the vehicle's exhaust pipe, its ability to capture and neutralize PM is maximized, contributing to improved air quality and environmental sustainability The P-DPF, illustrated in **Figure 1.13**, adopts a metallic foil/fleece design that enables the trapping and combustion of soot, facilitating further soot collection and regeneration. Importantly, it maintains a low operating back pressure while exhibiting high soot trapping efficiency. Although the trapping efficiency of the P-DPF is lower (approximately 50%) compared to the full-flow DPF, its combination with a DOC can result in a remarkable reduction of PM by up to 70%. Moreover, the soot accumulated within the fleece material undergoes combustion facilitated

by the NO_2 generated by the upstream catalyst, leading to the regeneration of the filter and allowing for additional soot collection [23].

1.1.4.4 Regeneration process of DPF

The regeneration of diesel particulate filters (DPFs) can be achieved through two main processes: active regeneration and passive regeneration. Active regeneration involves controlled oxidation of trapped soot using oxygen (O_2) at high temperatures. This process is periodically initiated when the soot accumulation in the filter reaches a predetermined limit of approximately 45%, indicated by a pressure drop across the DPF [24]. However, active regeneration is often considered unfavorable due to the adverse effects of high regeneration temperatures and the increased energy requirements for heating, leading to higher production costs. On the other hand, passive regeneration of DPFs utilizes catalysts embedded within the filter to oxidize particulate matter (PM) at exhaust gas temperatures, without the need for additional fuel. The presence of nitrogen dioxide (NO_2) promotes continuous oxidation within a temperature range of 200 to 450 °C, resulting in a simpler, quieter, and more fuel-efficient process [25]. Catalyzed DPFs incorporating platinum (Pt) catalysts demonstrate comparable conversion efficiency to wall flow silicon carbide (SiC) filters. They eliminate the necessity for a diesel oxidation catalyst (DOC) upstream, enabling lower oxidation temperatures and enhanced conversion rates when using biodiesel or fuel additives [6].

1.2 Objectives of this research

The objective of this thesis research is to provide comprehensive information on the partial-flow diesel particulate filter (P-DPF) and its impact on vehicle performance, including fuel consumption, thermal efficiency, and diesel emissions. The specific goals include achieving the most reduction in the quantity of particulate matter (PM) mass as much as possible in exhaust gas of a retrofit diesel vehicle compared to systems without an after-treatment system.

In Chapter 2, the focus is on characterizing diesel vehicle soot obtained from the exhaust pipe. This involves investigating the morphology of agglomerate structures, primary particle size, fringe length distribution, interplanar spacing, and elemental analysis using transmission electron microscopy (TEM) to see how after-treatment systems (DOC and P-DPF)

effect the vehicle soot. Chapter 3 aims to assess how B20 and after-treatment equipment influence diesel emissions, soot emissions, and brake thermal efficiency of vehicle. This analysis is conducted using a 2.5-liter direct-injection diesel pickup truck under various engine speeds and loads. In Chapter 4, the research investigates fuel economy, exhaust emissions, and particulate matter using the same vehicle, fuels, and after-treatment equipment as in Chapter 3. However, the vehicle is operated on the New European Driving Cycle (NEDC), which includes four urban driving cycles (UDCs) with low vehicle speed, low engine load, and low exhaust gas temperature, followed by one extra-urban driving cycle (EUDC) involving more aggressive and higher-speed driving. Finally, in Chapter 5, the focus shifts to investigating the phenomenon of soot oxidation in the passive regeneration of diesel particulate filters. This is achieved by real-time monitoring exhaust temperatures, pressure drop profiles, and emissions.

Overall, the objective of this thesis is to provide a comprehensive understanding of the P-DPF's impact on vehicle performance, assess its effectiveness in reducing soot emissions, and explore the phenomenon of soot oxidation in passive regeneration.

1.3 Scope of this research

1) Use the 2.5-liter direct injection diesel pickup truck to investigate vehicle thermal efficiency under various engine speeds with constant engine load.

2) Use B20 as a commercial form and as a main fuel for every experiment with diesel engine pickup truck.

3) Use after-treatment equipment: Ceria coated DOC, Pt coated P-DPF, and Pt coated long P-DPF to analyze the diesel emission reduction and soot oxidation.

4) The microstructure, nanostructures, and elemental composition were analyzed through Scanning Electron Microscopy (SEM), Transmission Electron Microscopy (TEM), and energy dispersive X-ray spectroscopy (EDS).

Figures

Figure 1.1 Light-duty truck use for automotive share [5]

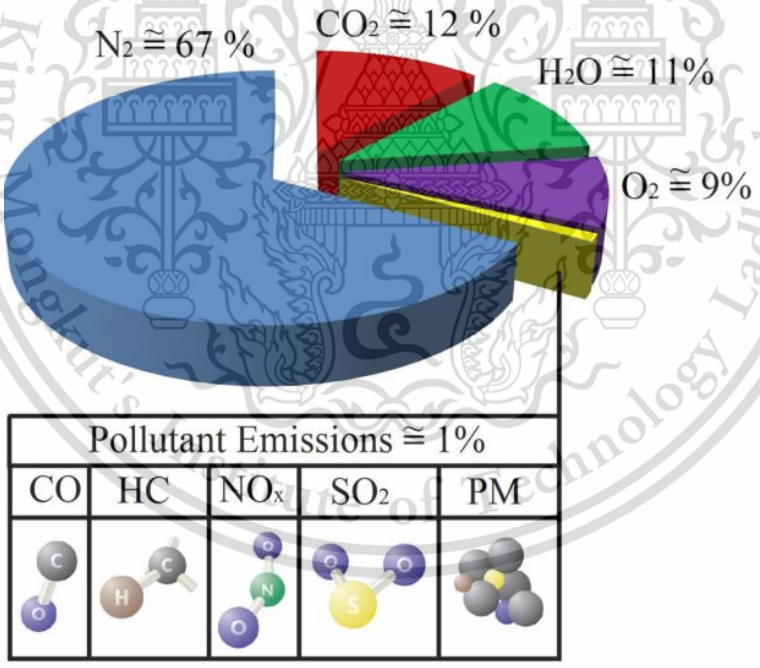

Figure 1.2 Diesel exhaust composition [6]

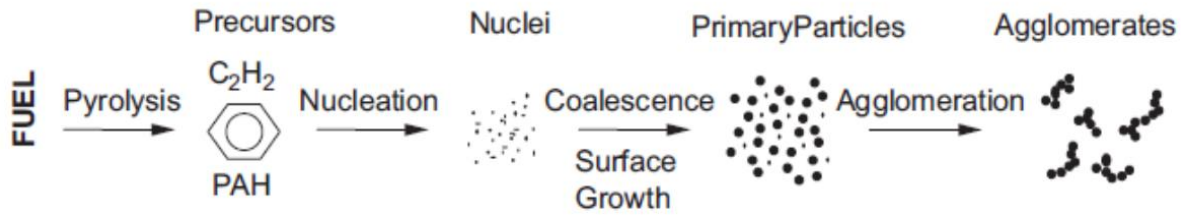

Figure 1.3 The formation of particulate matter [12]

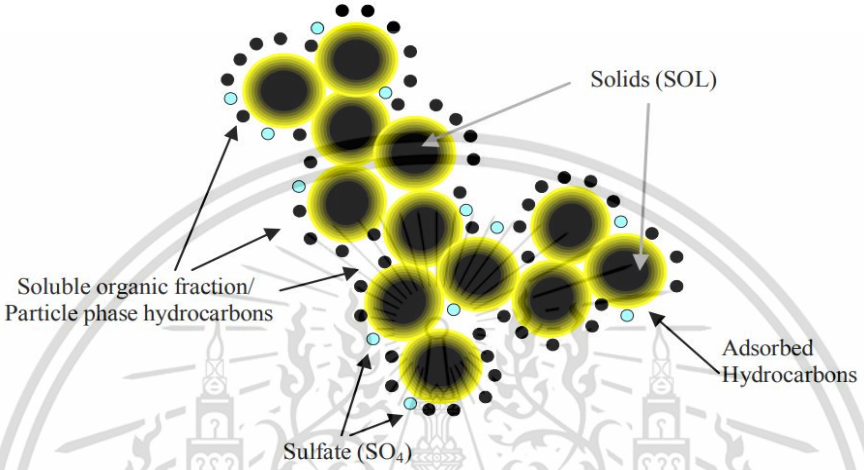

Figure 1.4 A schematic illustration of Particulate Matter [13]

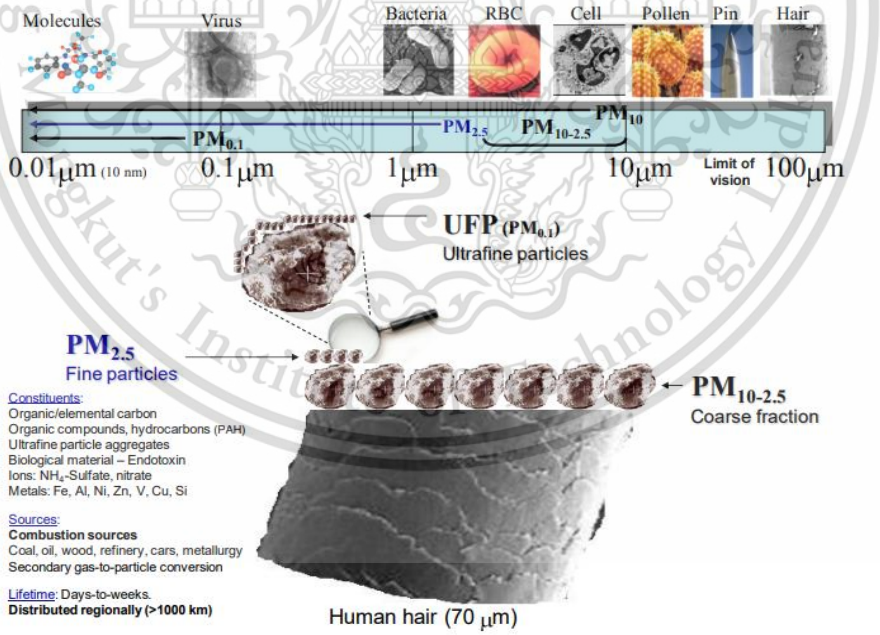

Figure 1.5 Size distribution of particulate matter [14]

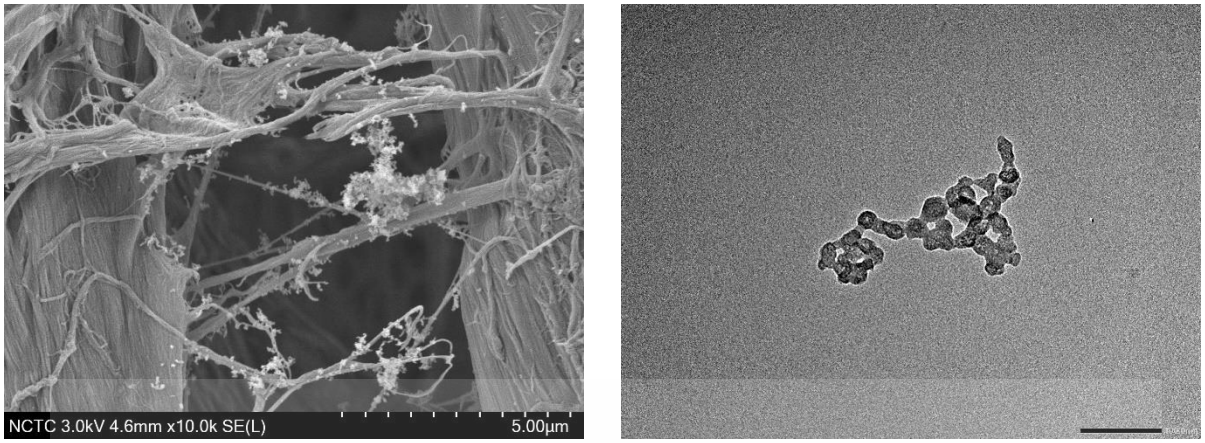

(a) (b)

Figure 1.6 Micrograph of diesel PM (a) SEM image, (b) TEM image

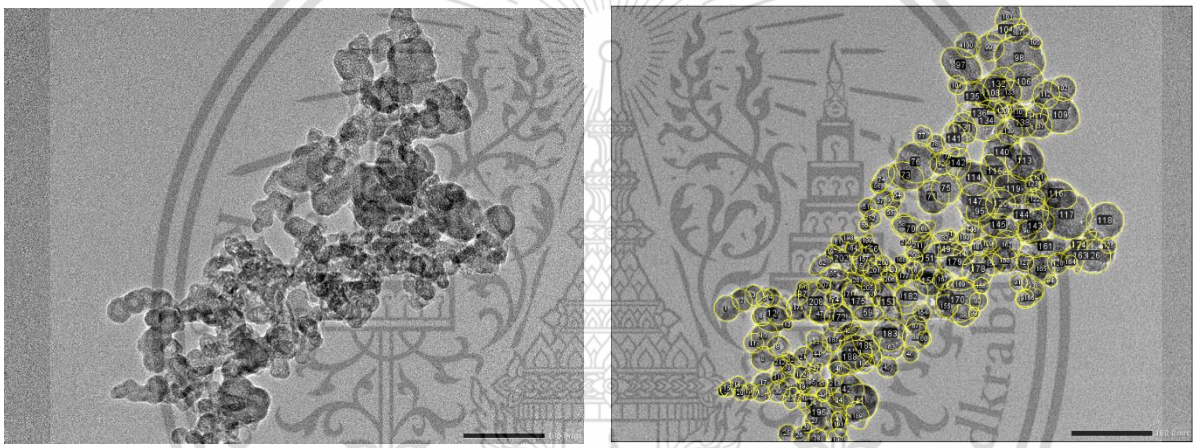

Figure 1.7 Example of diesel PM analysis on single primary particles by using ImageJ

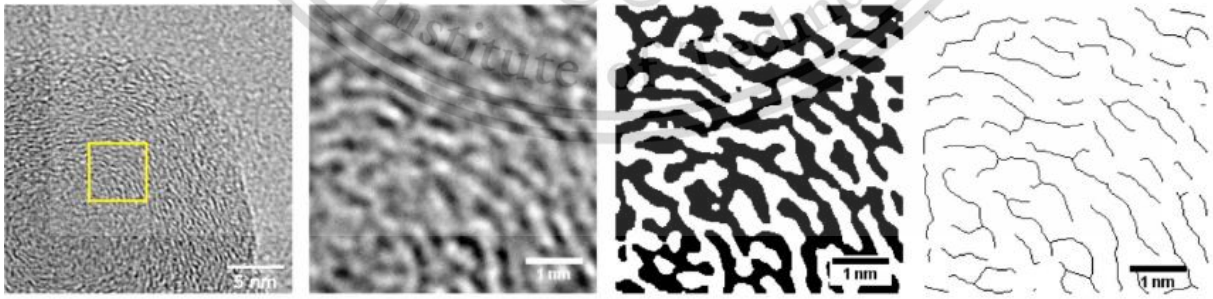

(a) (b) (c) (d)

Figure 1.8 Stepwise analysis process involving fringe length and interplanar spacing using the ImageJ software (a) selection of cropping area, (b) specified area that cropping, (c) polarizing of specified area, and (d) skeletonized image of cropping area [15]

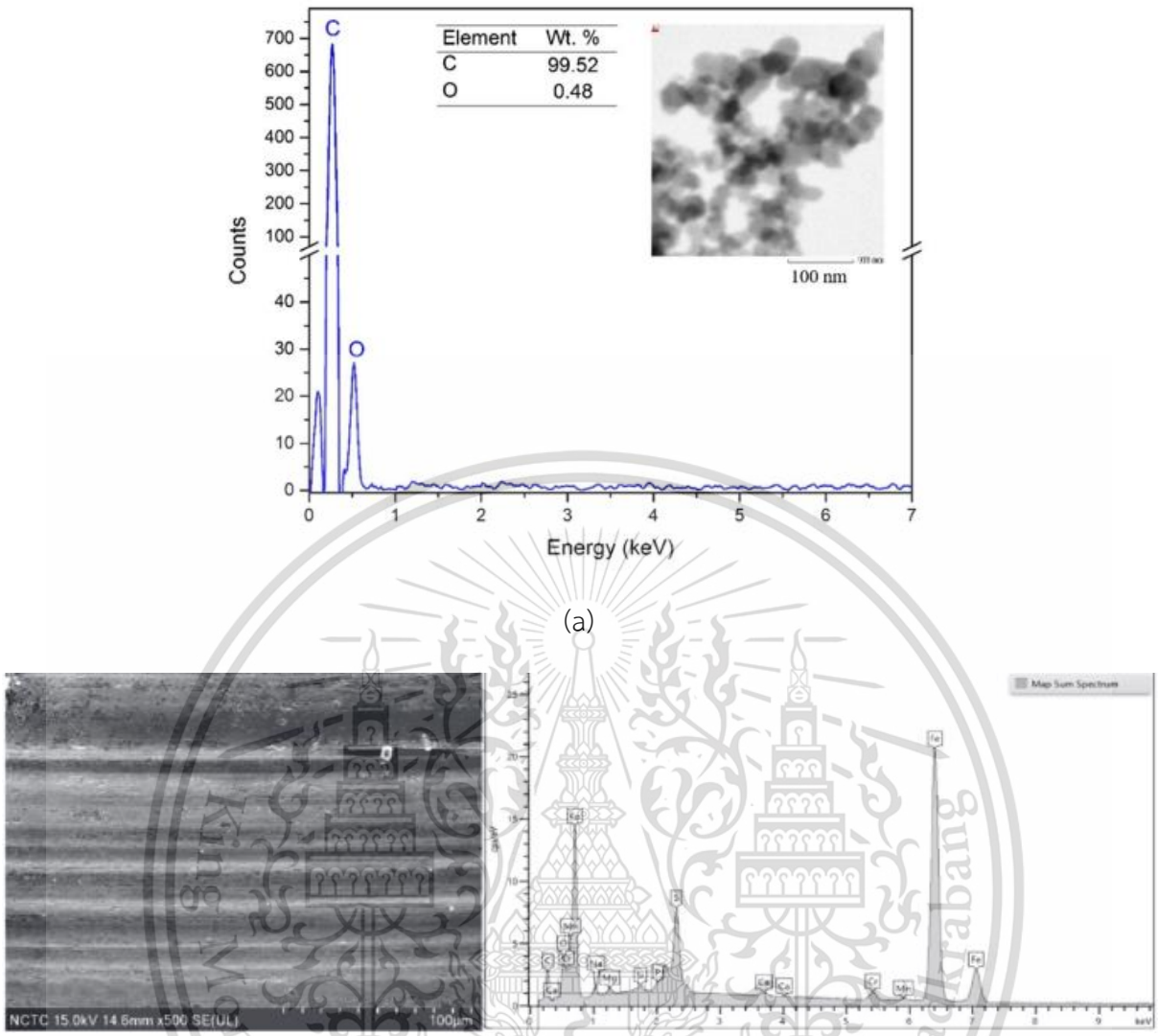

Figure 1.9 (a)TEM-EDS for the analysis of diesel PM [16] and (b) SEM-EDS for analysis of engine oil [17].

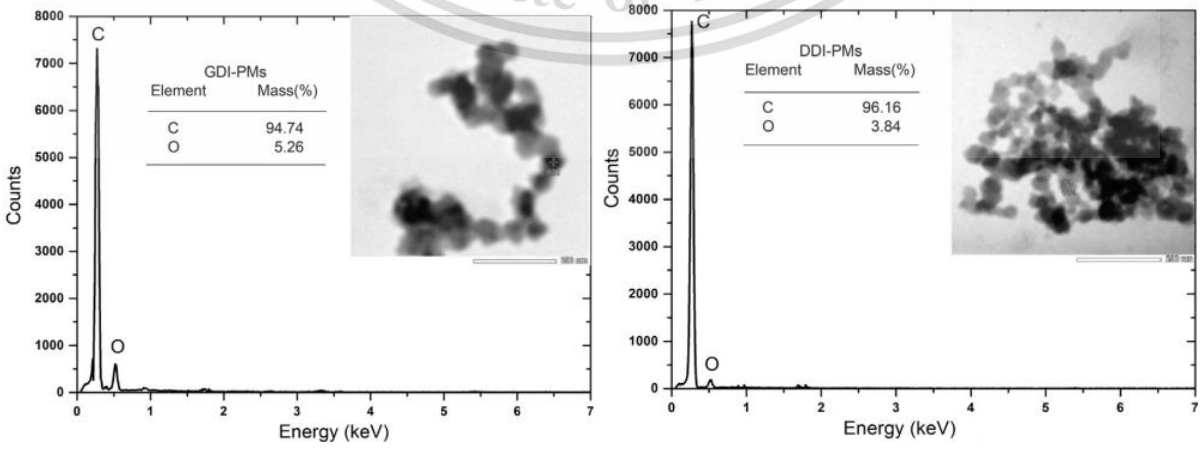

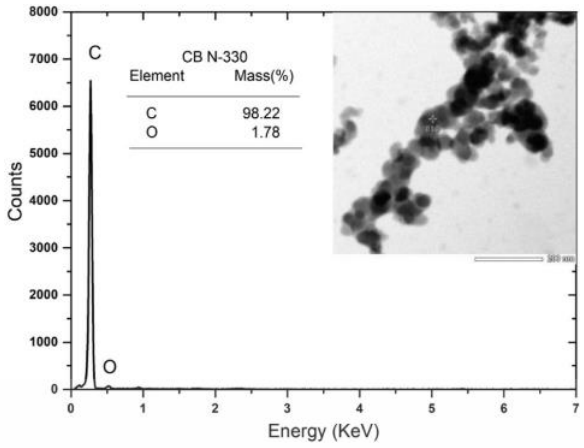

(c)

Figure 1.10 TEM-EDS elemental analysis of (a) GDI-PM, (b) DDI-PMs and (c)CB-N330 [15].

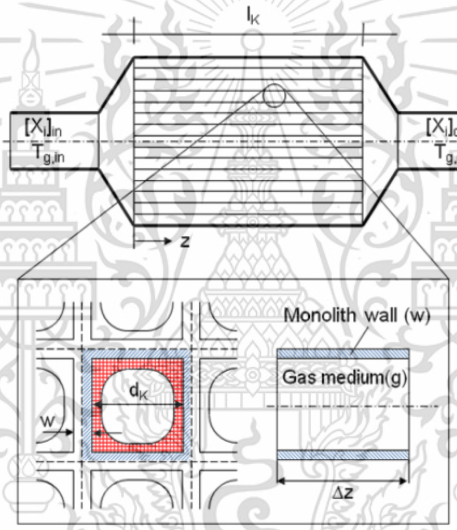

Figure 1.11 Diagram of the structure of diesel oxidation catalyst [21]

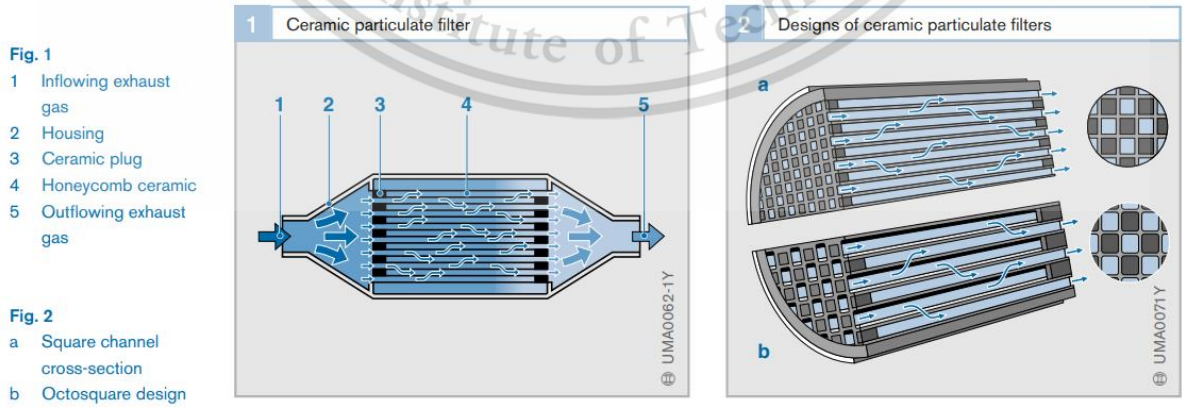

Figure 1.12 Ceramic particulate filter [22]

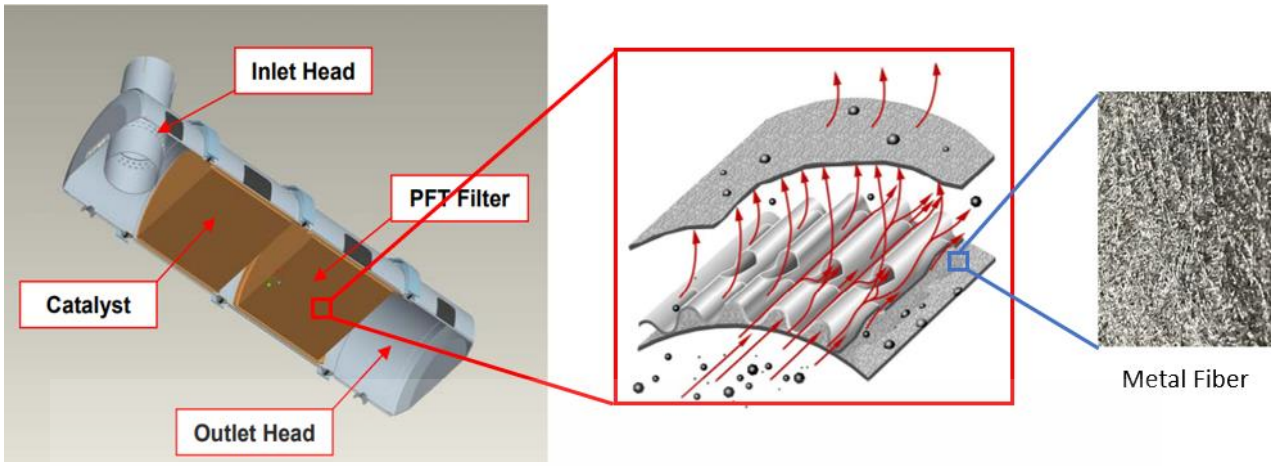

Figure 1.13 Schematic of partial-flow diesel particulate filter [23]

References

[1] C. ChooChuay, S. Pongpiachan, D. Tipmanee, O. Suttinun, W. Deelaman, Q. Wang, L. Xing, G. Li, Y. Han, J. Palakun and J. Cao, *Impacts of PM2.5 sources on variations in particulate chemical compounds in ambient air of Bangkok, Thailand*, Atmospheric Pollution Research, vol. 11, no. 9, pp. 1657-1667, 2020.

[2] Wongwatcharapaiboon, J. 2020. *Review Article: Toward Future Particulate Matter Situations in Thailand from Supporting Policy, Network and Economy*. Future Cities and Environment, 6(1): 1, 1–10. DOI: https://doi.org/10.5334/fce.79

[3] S. Steiner, C. Bisig, A. Petri-Fink and B. Rothen-Rutishauser, *Diesel exhaust: current knowledge of adverse effects and underlying cellular mechanisms*, Archives of toxicology, vol. 90, no. 7, pp. 1541-1553, 2016.

[4] N. Englert, *Fine Particles and Human Health - A Review of Epidemiological Studies*, Toxicology Letters, vol. 1, no. 3, pp. 235-242, 2004.

[5] Light-duty automotive share, *How to Use Songthaew in Bangkok by Meetrip*, 2017, https://www.thai2siam.com/news/bangkok/how-use-songthaew-bangkok-meetrip

[6] Reşitoğlu, İ.A., Altinişik, K. & Keskin, A. The pollutant emissions from diesel-engine vehicles and exhaust aftertreatment systems. *Clean Techn Environ Policy* **17**, 15–27 (2015). https://doi.org/10.1007/s10098-014-0793-9

[7] Shete, Yogesh. (2021). *Engine Emissions and Their Control: Review*. 2395-0056.

[8] Bosch. (2005). *Emissions-control technology for diesel engines*. Robert Bosch GmbH, Germany

[9] David B. Kittelson, *Engines and nanoparticles: a review*, Journal of Aerosol Science, Volume 29, Issues 5–6, 1998, Pages 575-588, ISSN 0021-8502, https://doi.org/10.1016/S0021-8502(97)10037-4.

[10] Avinash Kumar Agarwal, *Biofuels (alcohols and biodiesel) applications as fuels for internal combustion engines*, Progress in Energy and Combustion Science, Volume 33, Issue 3, 2007, Pages 233-271, ISSN 0360-1285, https://doi.org/10.1016/j.pecs.2006.08.003.

[11] H. Burtscher, *Physical characterization of particulate emissions from diesel engines: a review*, Journal of Aerosol Science, Volume 36, Issue 7, 2005, Pages 896-932, ISSN 0021-8502, https://doi.org/10.1016/j.jaerosci.2004.12.001.

[12] Bans E., Ulla M.A., Mir E., and Milt V.G., *Structured Catalysts for Soot Combustion for Diesel Engines*. Chapter 5 of the book. In Diesel Engine—Combustion, Emissions and Condition Monitoring; Saiful, B., Ed., IntechOpen: London, UK, 2013, doi: 10.5772/54516.

[13] Korres, Dimitrios & Lois, Evripidis & Karonis, Dimitrios. (2004). *Use of JP-8 Aviation Fuel and Biodiesel on a Diesel Engine*. 10.4271/2004-01-3033.

[14] Urch, R Bruce. (2023). Controlled Human Exposures to Concentrated Ambient Fine Particles and Ozone: Individual and Combined Effects on Cardiorespiratory Outcomes.

[15] Hay Mon Oo, Preechar Karin, Chinda Charoenphonphanich, Nuwong Chollacoop, Katsunori Hanamura, *Physicochemical characterization of direct injection Engines's soot using TEM, EDS, X-ray diffraction and TGA*, Journal of the Energy Institute,Volume 96,2021, Pages 181-191, ISSN 1743-9671, https://doi.org/10.1016/j.joei.2021.03.009.

[16] Karin, P., Koko, P., Charoenphonphanich, C., Chollacoop, N., & Hanamura, K. (2021). *Physicochemical Characterization of Diesel Engine's Soot and Metal Oxide Ash Nanoparticles Using Electron Microscopy*, EDS and TGA. Emission Control Science and Technology, 7, 91 - 104.

[17] Preechar Karin, Pattara Chammana, Pitchaporn Oungpakornkaew, Panyakorn Rungsritanapaisan, Warawut Amornprapa, Chinda Charoenphonphanich, Kobsak Sriprapha, *Impact of soot nanoparticle size and quantity on four-ball steel wear characteristics using EDS, XRD and electron microscopy image analysis*, Journal of Materials Research and Technology, Volume 16, 2022, Pages 1781-1791, ISSN 2238-7854, https://doi.org/10.1016/j.jmrt.2021.12.111.

[18] Karin, P., Boonsakda, J., Siricholathum, K. et al. *Morphology and oxidation kinetics of CI engine's biodiesel particulate matters on cordierite Diesel Particulate Filters using TGA*. Int.J Automot. Technol. 18, 31–40 (2017). https://doi.org/10.1007/s12239-017-0003-y

[19] K. Leistner, A. Nicolle and P. Da Costa, *Detailed kinetic analysis of soot oxidation by NO2, NO, and NO+ O2*, The Journal of Physical Chemistry C, vol. 116, no. 7, pp. 4642-4654, 2012.

[20] Banús E.D., Ulla M.A., Miró E.E. and Milt V.G., (2013), *Structured Catalysts for Soot Combustion for Diesel Engines*, InTech. doi: 10.5772/54516

[21] Kabir M. N., Alginaha Y., and Islam K., *SIMULATION OF OXIDATION CATALYST CONVERTER FOR AFTER-TREATMENT IN DIESEL ENGINES*, International Journal of Automotive Technology, Vol. 16, No. 2, pp. 193–199 (2015), doi: 10.1007/s12239–015–0021–6

[22] Reif, Konrad. (2014). *Diesel Engine Management: Systems and Components*. 10.1007/978-3-658-03981-3.

[23] Jacobs T., et., al., *Development of Partial Filter Technology for HDD Retrofit*, SAE International (SAE World Congress Detroit), 2006.

[24] Jeguirim M., Tschamber V., Brilhac J.F., and Ehrburger P., (2005). *Oxidation mechanism of carbon black by NO2: Effect of water vapour*. 84(14-15), 1949–1956. doi:10.1016/j.fuel.2005.03.026

[25] York A.P.E., Ahmadinejad M., Watling T.C., Walker A.P., Cox J.P., Gast J., Blakeman P.G., and Allansson R., (2007*), Modeling of the catalyzed continuously regenerating diesel particulate filter (CCR-DPF) system: model development and passive regeneration studies*, Society of Automotive Engineers, 2007-01-0043

CHAPTER 2

SOOT NANOSTRUCTURE ANALYSIS

2.1 Introduction

In recent years, the number of diesel engine vehicles has increased, accompanied by an increase in interest in outdoor leisure activities. Diesel engines consume less energy consumption than other internal combustion engines and emit less carbon dioxide, making them useful for environmental conservation. However, the combustion process in diesel engines generates a substantial pollutant known as soot, which is mostly composed of carbonaceous material [1].

Soot particles are a major component of exhaust emissions and contain absorbed hydrocarbons, including aromatic compounds. Carbonaceous soot is produced during high-temperature pyrolysis or burning of hydrocarbons, and it is frequently accompanied with a soluble organic fraction (SOF) comprising aromatic chemicals and other unburned hydrocarbons. Harmful substances, such as hydrocarbons (HC), carbon monoxide (CO), nitrogen oxides (NO_X), and soot particles, are emitted from diesel engines, but their levels are relatively low for HC and CO, while NO_X emissions are comparable to those of gasoline engines. The emitted soot particles are respirable and contribute significantly to air pollution. In an ideal combustion scenario, diesel fuel would produce carbon dioxide (CO_2), water (H_2O), and nitrogen (N_2) as end products. However, incomplete combustion leads to emissions of NO_X, CO, CO_2, H_2O, and unburned HC. Additionally, particulate matter (PM) is formed, consisting of unburnt carbon particles, engine oils, debris, soot, and ash particulates as shown in **Figure 2.1** a heavy-duty diesel engine's particle composition was examined in a heavy-duty transient cycle [1-3].

The formation of diesel particulate matter (PM) involves several steps: pyrolysis, nucleation, surface growth, coagulation, and aggregation. Pyrolysis occurs when fuel undergoes breakdown at high temperatures and low oxygen levels, and its occurrence is influenced by factors such as engine load and fuel characteristics. During pyrolysis, the fuel breaks down into smaller particles known as nuclei, which then intercept small hydrocarbon molecules and

combine to form aromatic compounds. As the process continues, additional hydrocarbons and carbon chains are deposited onto the nuclei, resulting in the formation of primary particles. These primary particles further aggregate with one another, forming larger agglomerate particles and are believed to consist of multilayered graphite sheets with hexagonally ordered structures [4-6].

There are two basic approaches to lowering PM from diesel engine exhaust. First, reducing during the formation process, which Oh et. al. [7] has been achieved through fuel additive by increasing biodiesel contents in the fuel and reducing after the formation process using after-treatment devices such as diesel oxidation catalyst (DOC) and diesel particulate filter (DPF). To reduce the amount of hydrocarbon (HC) and carbon monoxide (CO) emissions from engine exhaust gas, DOC are installed on diesel engine exhaust lines. DOC converts CO and HC to carbon dioxide (CO_2) and water (H_2O), and Nitric Oxide (NO) to nitrogen dioxide (NO_2) [8]. DPF is a device that physically filters particulate particles from the exhaust stream. This method of eliminating PM from the exhaust stream is well-established, efficient, and successful. After being caught, the collected PM must be handled in a safe and secure way [3].

The goal of this work is to reduce PM emitted by diesel vehicles and mainly focus by using partial-flow diesel particulate filter (P-DPF). Therefore, the soot nanostructure should be studied first. The soot collected from the position of before and after after-treatments equipment (DOC and P-DPF) that is generated from 2.5L direct injection diesel engines vehicle using biodiesel. The morphology of agglomerate structure, primary particle size, fringe length distribution, interplanar spacing and elemental analysis were measured by transmission electron microscopy (TEM) images processing method in this chapter.

2.2 Methodology

2.2.1 Collection of Particulate Matters

A 2.5L 4-cylinder common rail direct injection diesel-engine truck with a compression ratio of 18.5:1 was tested at a variety of engine speeds and loads using biodiesel fuel. **Table 2.1** displays the engine specifications. After testing at various engine speeds and loads for diesel fuel, the soot powder was collected from the exhaust pipe before entering and after

leaving the after-treatment equipment. Paper filters and a BOSCH smoke meter (DSM-240) were used to collect soot on the paper filters to analyze the agglomeration particles. On a chassis dynamometer, as shown in **Figure 2.2**, a diesel-engine truck was operated at different loads and engine speeds. For additional details of this experiment, **Figure 2.3** depicts the exhaust gas flow through the after-treatment equipment. Furthermore, **Figure 2.4** also depicts several particle sizes categorized: PM_{10}, D(diameter) < 10 μm; $PM_{2.5}$ or small particles D < 2.5 μm; $PM_{0.1}$ or ultrafine particles D < 0.10 μm; and nanoparticles, D < 0.05 μm or 50 nm [9].

2.2.2 TEM, EDS, and particle size analysis

The vehicle soot was analyzed using a Transmission Electron Microscopy and energy dispersive x-ray spectroscopy (TEM-EDS, JEM-2100Plus), as shown in **Figure 2.5** of JEM-2100Plus used in this work, at magnifications of 80K and 800K to investigate the morphology, size of vehicle soot particles, interplanar spacing, fringe length analysis, and determine the elemental composition. Furthermore, the images captured at a magnification of 80K were subjected to analysis through the software ImageJ in order to ascertain the dimensions of individual primary particles within the vehicle particulate matter (PM). Similarly, the images taken at a higher magnification of 800K were converted to grayscale and subsequently subjected to a process called skeletonization using ImageJ. This enabled a detailed examination of the nanostructure and graphite crystallite present in the particles.

2.3 Results and discussion

2.3.1 Size distribution of vehicle soot primary particles

Vehicle soot was investigated with 80K magnifications of TEM for the morphology of single primary particles. TEM micrograph image processing application ImageJ is used to measure the particle sizes and create the single primary particle size distributions. **Figure 2.6(a) and (b)** depict single primary particles that are obviously distinguishable from one another in an agglomeration comparison between before entering and after leaving after-treatment. The single primary particles size is not significantly different. The vehicle soot after after-treatment appeared in both the smallest and largest sizes and as displayed in **Figure 2.7** the primary particles sizes were in the range of 8 to 62 nm with an average primary particle size of 25.75 nm and 22.59 nm for before entering and after leaving the after-treatment

equipment, respectively. The primary particle size reduction after passing through the after-treatment system, and based on the results, it is assumed that soot surface partial oxidations took place after P-DPF treatment. Furthermore, the application of ImageJ during analysis for vehicle soot before entering and after leaving an after-treatment equipment as shown in **Figure 2.8(a) and (b)**, respectively.

2.3.2 Fringe length and Interplanar spacing of vehicle soot nanostructures

Figure 2.9(a) and (b) depicts TEM images of 800K magnifications and 10x10 nm^2 were cropped from each image for vehicle soot of before and after after-treatment. These TEM pictures were then processed with image processing tools (ImageJ). The fringes that reflect the carbon crystallite nanostructure visible in the 100 nm^2 pictures in **Figure 2.10(a) and (b)** are revealed after polarizing the TEM image into black and white. This examination is continued in **Figure 2.11(a) and (b)**, which depicts the cropped image, the black and white image after converted from cropped image, and the final skeletonized image, which were also utilized to calculate the interplanar spacing of the graphite platelets that comprise the particulate matter, that process from the black and white image. **Figure 2.12(a) and (b)** shows a skeletonized image analyzing the interplanar spacing. In more detail, **Table 2.2** shows the summary information of fringe length and interplanar spacing analysis. The average fringe length for vehicle soot before entering and after leaving after-treatment was 1.14 and 0.99 nm, respectively. The hypothesis is that the decrease in fringe length might come from some edge-site oxidation that occurs by oxygen (O_2) and nitrogen dioxide (NO_2) which was converted from DOC upstream [12]. For the interplanar spacing results of vehicle soot were 0.44 nm. before entering after-treatment equipment and 0.47 nm. for after leaving after-treatment, which increase after passing through the after-treatment. B. Oh [13] suggested that the after-treatment system reduces the average fringe length, maximum fringe length, and interplanar spacing. In additional detail, fringe length and interplanar spacing are generally inversely connected, so that decreasing one increases the other. This is because a decrease in fringe length is related with a decrease in graphitization or order, but an increase in interplanar spacing is associated with a decrease in graphitization or oxidized in surface region due to the less compact crystallite structure [14].

2.3.3 Elemental composition of vehicle soot

Energy dispersive x-ray spectroscopy (EDS) function in the JEM-2100Plus is used to analyze elemental composition in this work. **Figure 2.13(a) and (b)** shows the elemental composition of vehicle soot from before entering and after leaving after-treatment, respectively. Elements on the vehicle soot were carbon (C) and oxygen (O) for both from before entering and after leaving after-treatment. This can be able to confirm that vehicle soot is mostly carbon across all the EDS spectra tested. The carbon and oxygen content decrease after leaving the after-treatment equipment due to the after-treatment system, especially partial-flow diesel particulate filter (P-DPF) that used to trap the particulate matters (PMs). The result can be reproducible, as we can see in **Appendix B A-1 to A-3** and can also confirm that when compared with the result without an after-treatment the carbon and oxygen content decreases. Furthermore, we can clearly see that the amount of soot dramatically decreases with the installation of after-treatment equipment.

2.4 Conclusion

The vehicle soot from diesel fuel was collected from the exhaust pipe at the positions of before entering and after leaving exhaust after-treatment system and investigated the morphology of vehicle soot single primary particles, size distribution, and elemental composition by observing through TEM and TEM-EDS. An exhaust after-treatment system plays an important role in this work, as clearly seen that the average size of single primary particles decreased as the vehicle soot pass through the after-treatment system. The average primary particles diameter are 25.75 nm and 22.59 nm for before entering and after leaving after-treatment, respectively. A link between after-treatment equipment and fringes may also be noticed in the fringe analysis. The average and largest fringe lengths dropped as the vehicle soot pass through the after-treatment equipment. According to the decrease of particle size and fringe length after passing through the after-treatment system can suggest that there are some surface edge site oxidations occur by oxygen (O_2) and nitrogen dioxide (NO_2). Furthermore, the interplanar spacing was increasing after the vehicle soot passed through the after-treatment systems. Finally, the elemental composition of vehicle soot was C and O, but

EDS spectra shows that C and O contents were decreased after vehicle soot passing through the after-treatment system.

However, to further work on analysis of the after-treatment systems, the focus on the effects of partial flow diesel particulate filter (P-DPF) by installing to the exhaust pipe of light-duty diesel vehicle to investigates on vehicle thermal efficiency (such as fuel consumption, brake specific fuel consumption (BSFC), brake specific energy consumption (BSEC), and brake thermal efficiency (BTE)), diesel exhaust emission (nitric oxide (NO), carbon dioxide (CO_2), and oxygen (O_2)),and soot emission (smoke intensity).

Tables

Table 2.1 Toyota Hilux Tiger vehicle specifications

Vehicle	**Toyota Hilux Tiger**
Engine Type	2KD-FTV (Diesel)
Number of cylinders & Arrangement	4 cylinders, In-line
Valve Mechanism	16 Valve DOHC
Bore x Stroke	92.0 mm x 93.8 mm
Displacement Volume	2500 cc
Compression Ratio	18.5 : 1
Fuel System	Common-rail type Direct Injection
Maximum Power (kW at rpm)	75 kW at 3600 rpm
Maximum Torque (Nm at rpm)	260 Nm at 1600 – 2400 rpm

Table 2.2 Summary information of fringe analysis

Soot collected position	**Before entering after-treatment**	**After leaving after-treatment**
Average Fringe Length (nm)	1.14	0.99
Largest Fringe Length (nm)	6.15	6.13
Interplanar Spacing (nm)	0.44	0.47

Figures

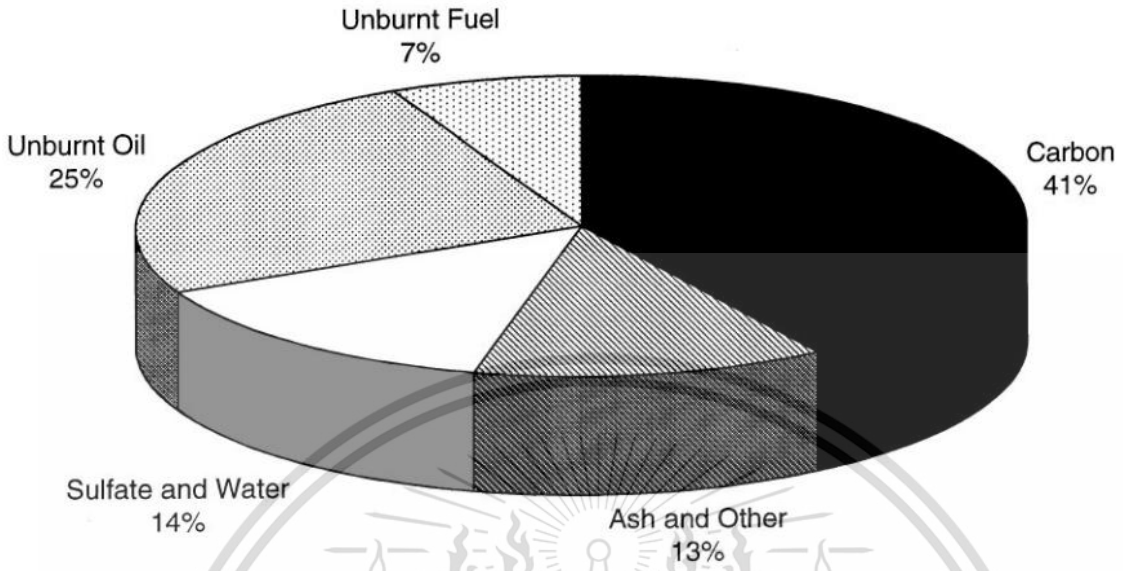

Figure 2.1 heavy-duty diesel engine's particle composition was examined in a heavy-duty transient cycle [9]

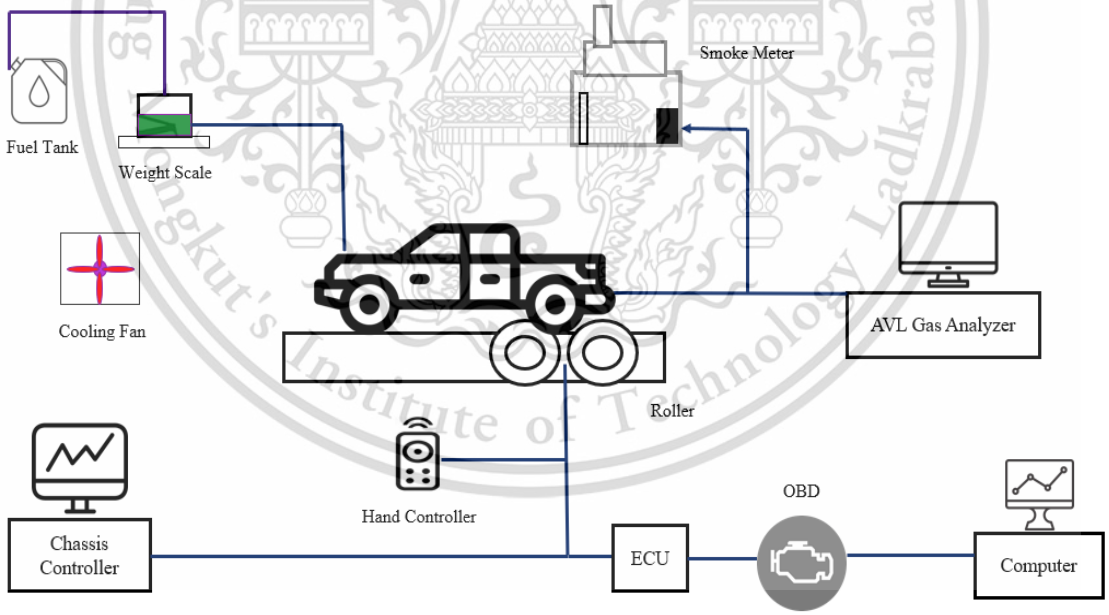

Figure 2.2 Schematic diagram of experimental setup

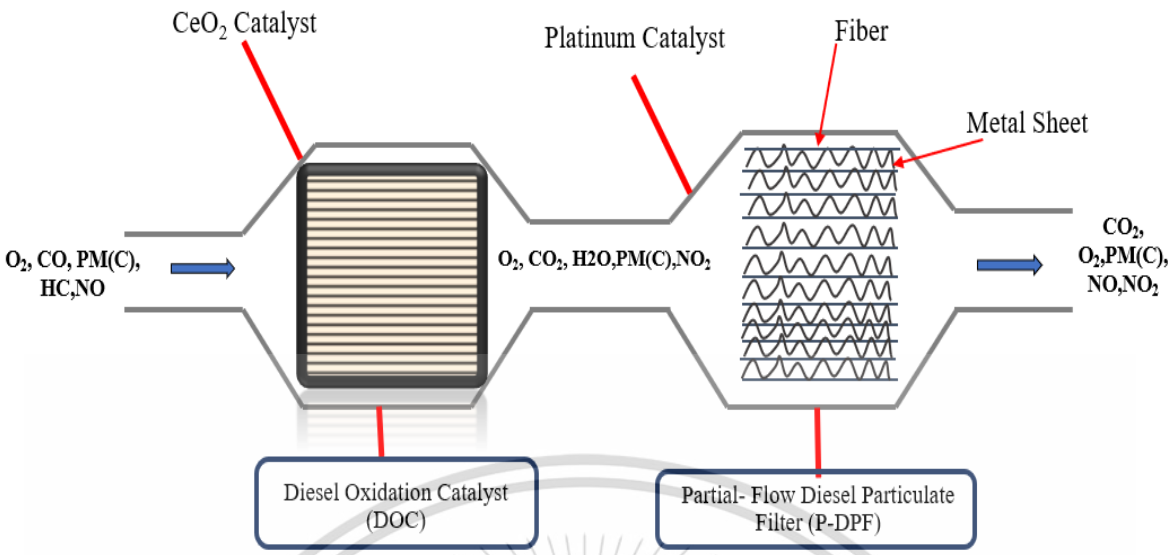

Figure 2.3 Exhaust gas flow through after-treatment equipment

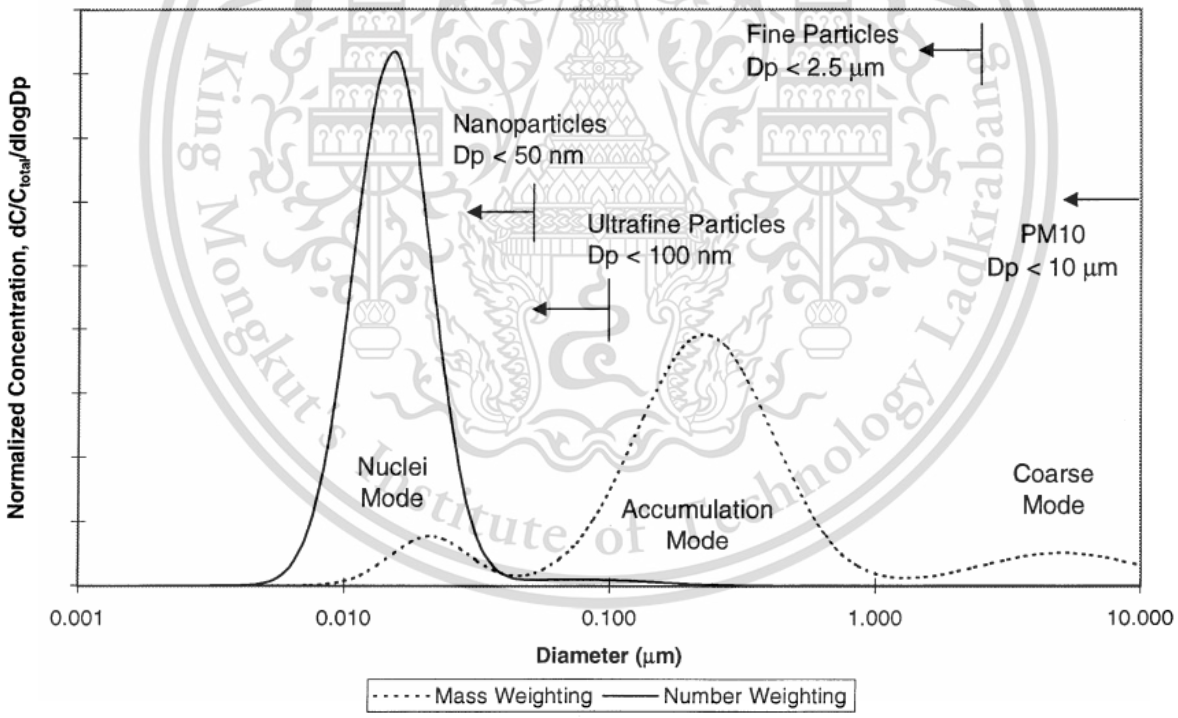

Figure 2.4 Typical engine exhaust size distribution, with weightings for both mass and number [9]

Figure 2.5 Transmission Electron Microscopy, JEM-2100Plus [11]

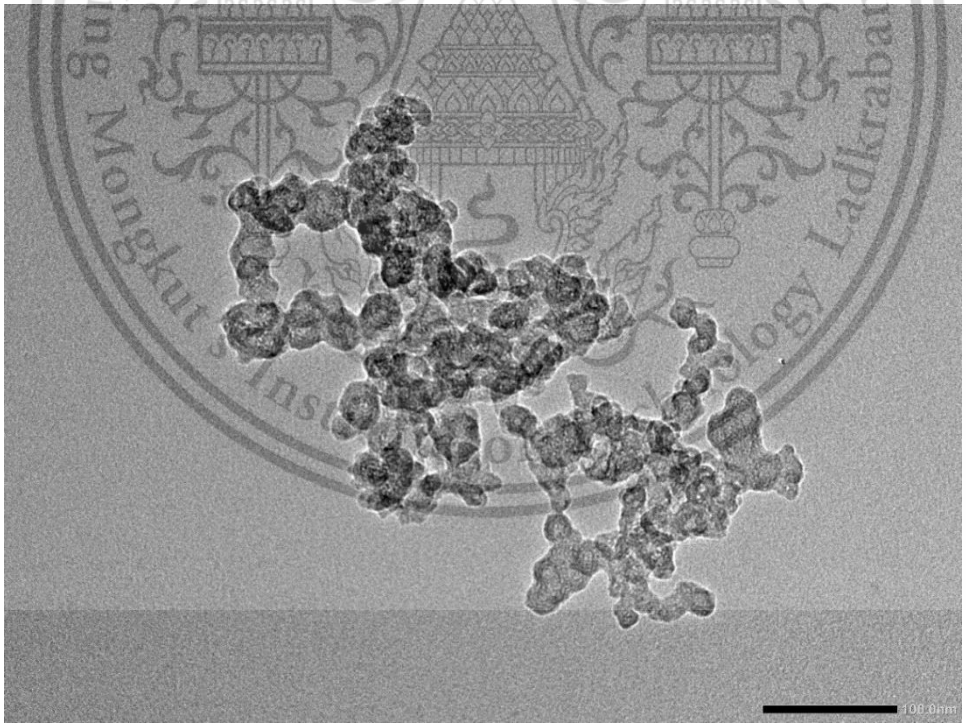

(a)

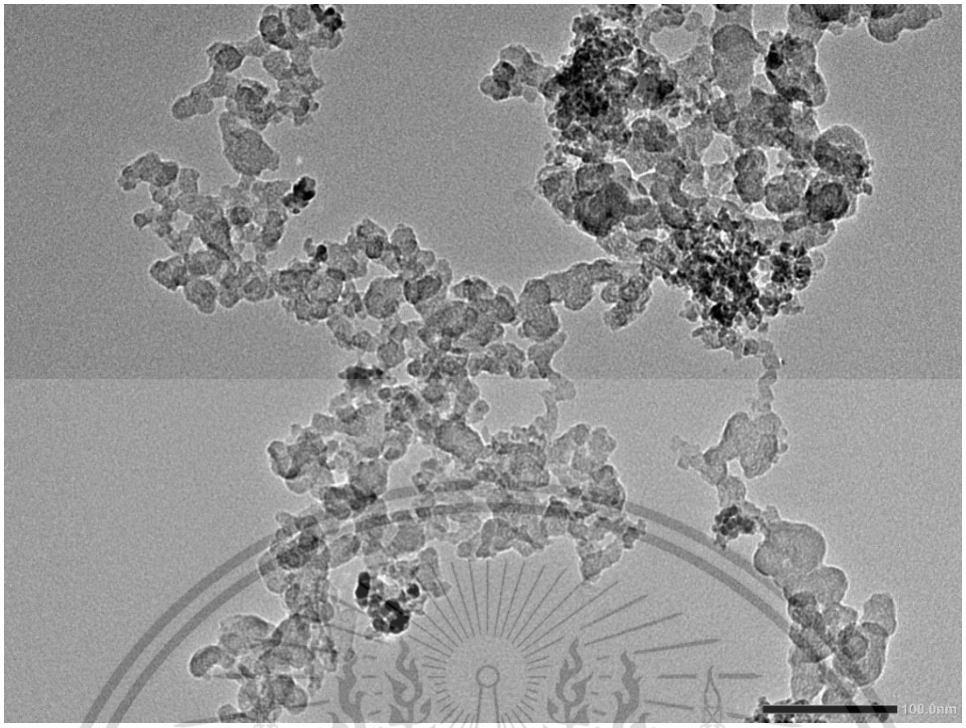

(b)

Figure 2.6 TEM images with 80K magnifications of vehicle soot (a) before entering after-treatment equipment and (b) after leaving after-treatment equipment

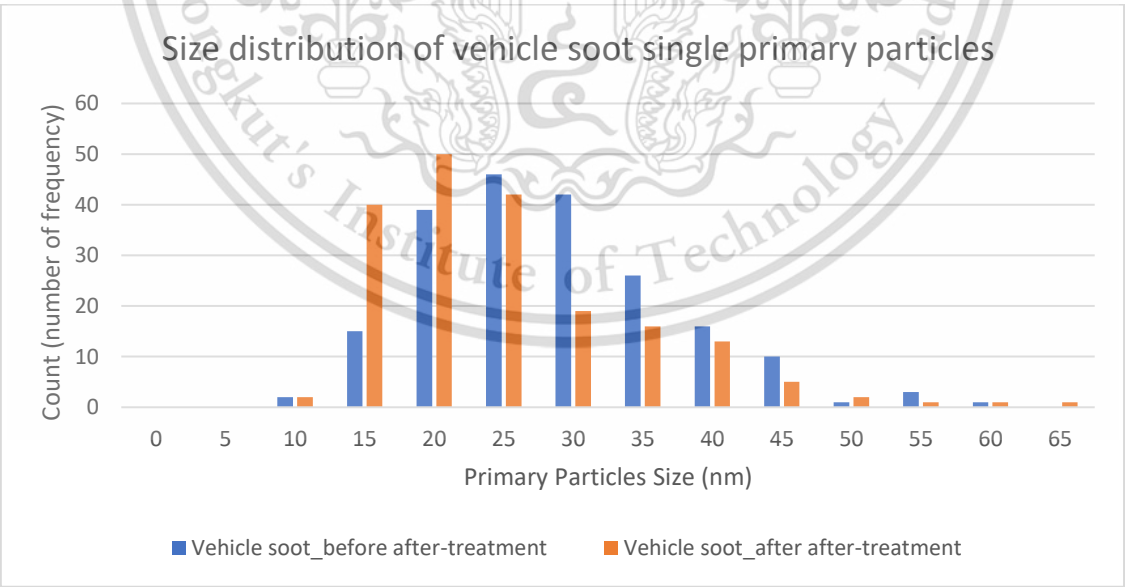

Figure 2.7 Size Distribution of vehicle soot via ImageJ with TEM analysis

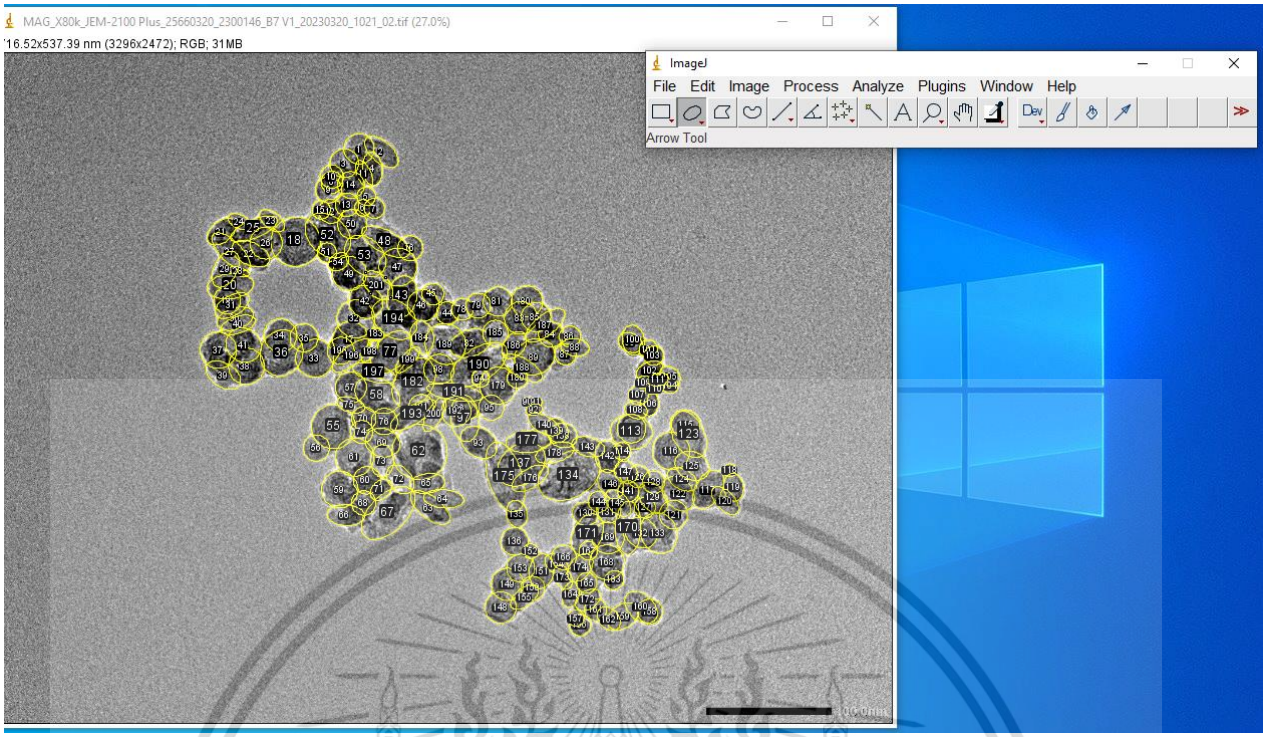

(a)

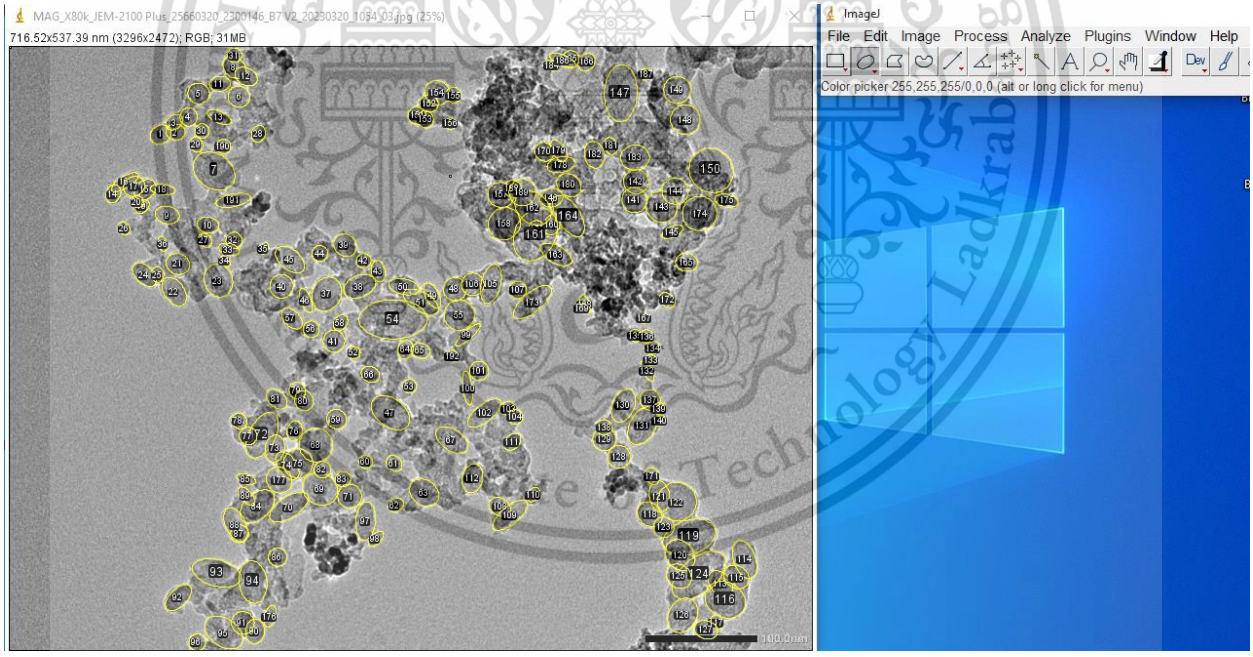

(b)

Figure 2.8 TEM images with 80K magnifications of vehicle soot using ImageJ image processing software (a) before entering after-treatment equipment and (b) after leaving after-treatment equipment

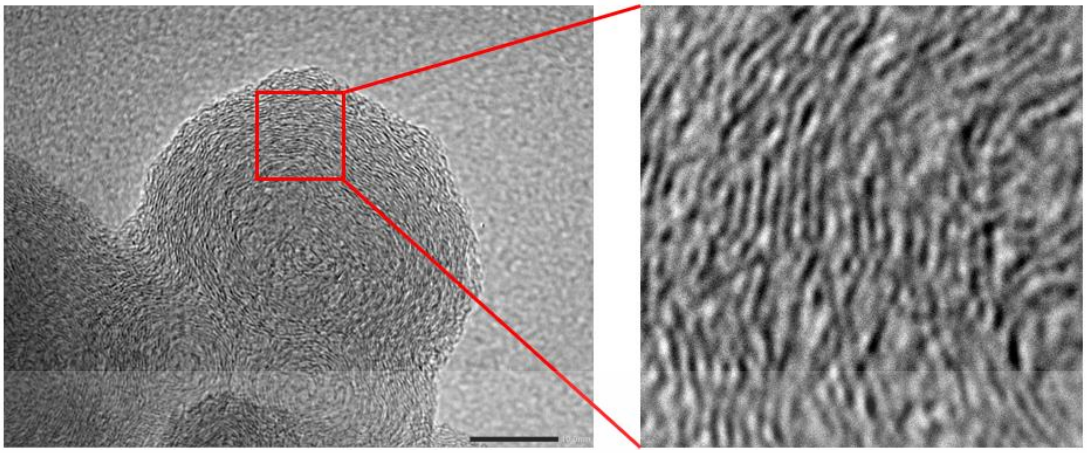

(a)

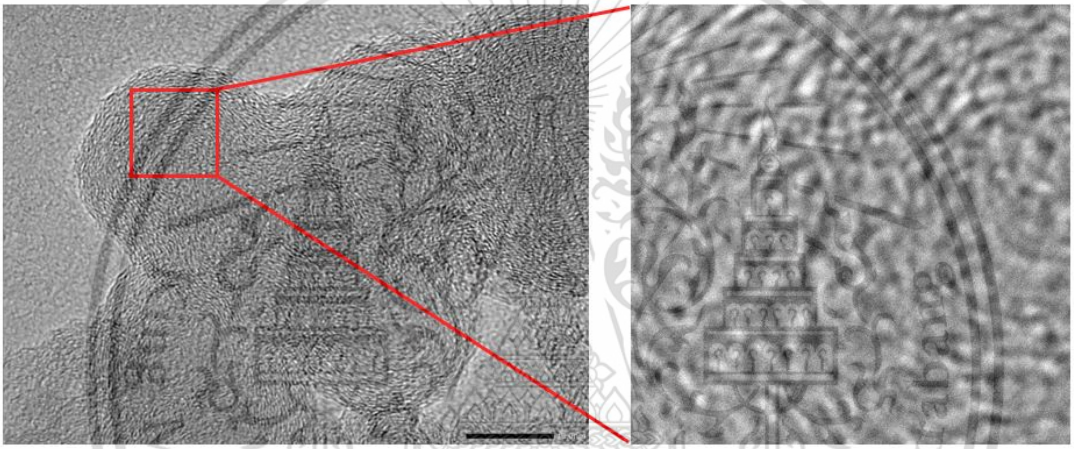

(b)

Figure 2.9 TEM images of 800K magnifications and 100 nm^2 cropped image of vehicle soot (a) before entering after-treatment equipment and (b) after leaving after-treatment equipment

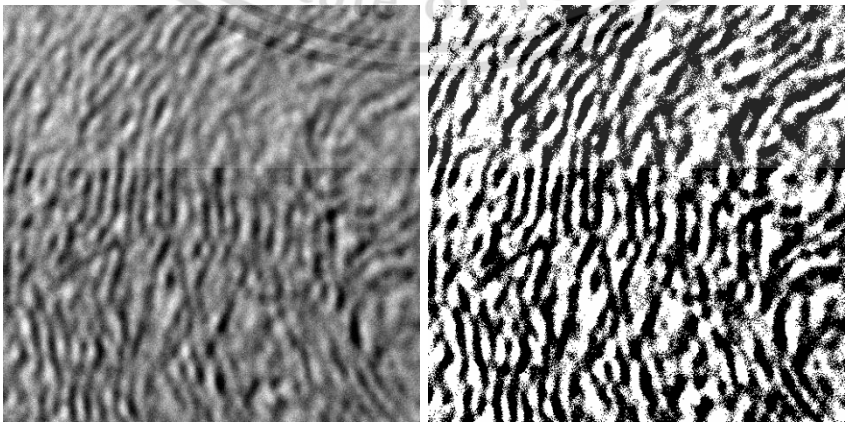

(a)

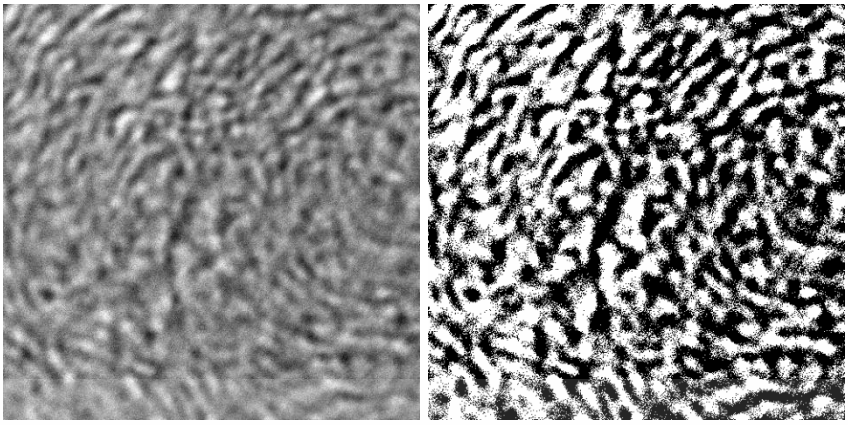

(b)

Figure 2.10 (left)100 nm^2 cropped image and (right) black and white image of vehicle soot (a) before entering after-treatment equipment and (b) after leaving after-treatment equipment

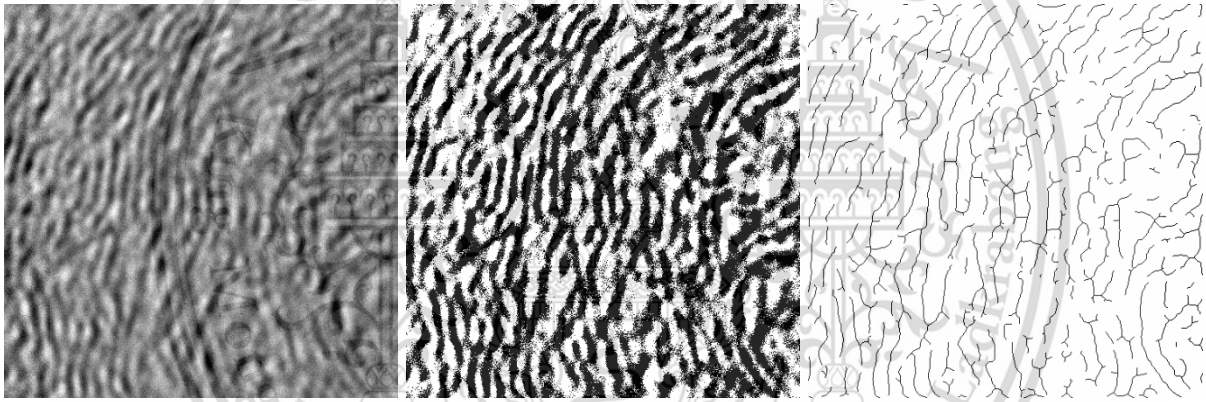

(a)

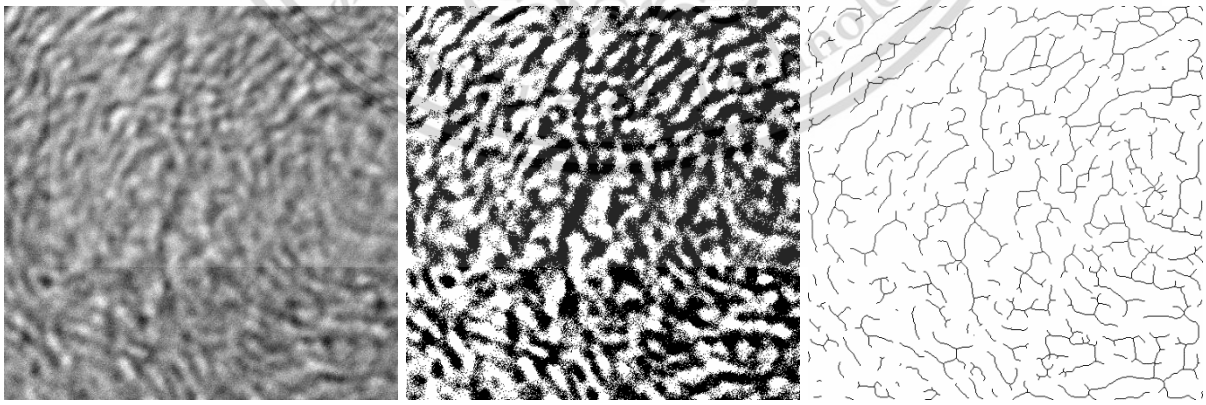

(b)

Figure 2.11 (from left) cropped image 100 nm^2, black and white image, and the final skeletonized image of vehicle soot (a) before entering after-treatment equipment and (b) after leaving after-treatment equipment

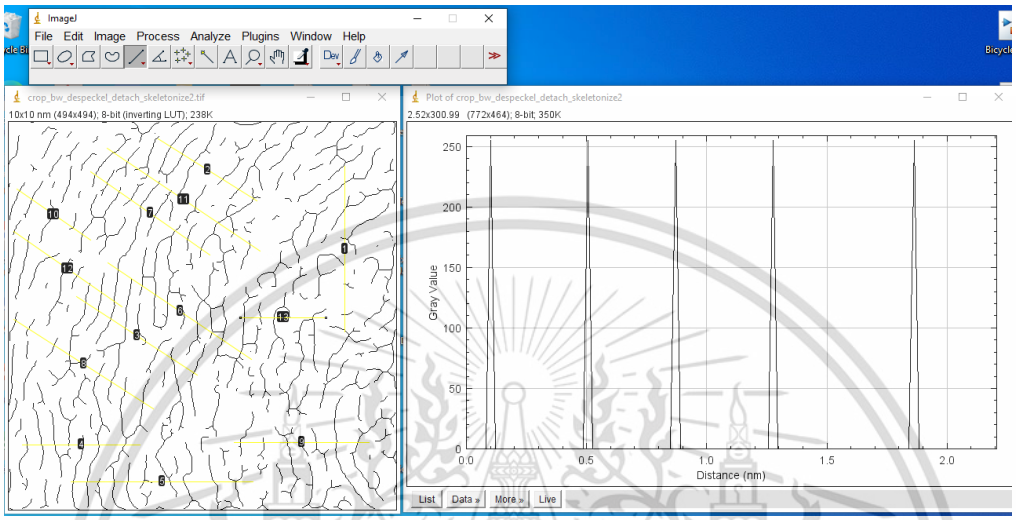

(a)

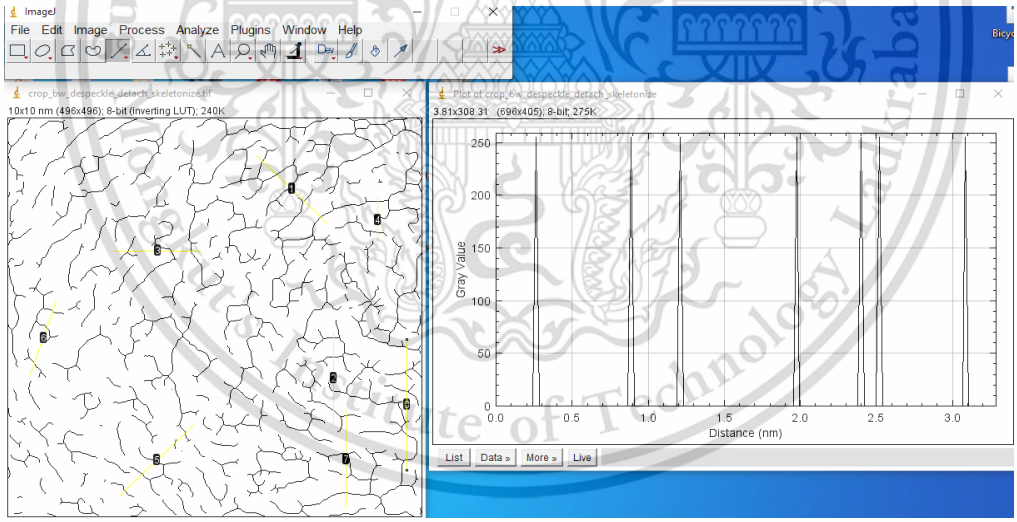

(b)

Figure 2.12 Skeletonized image analyzing the interplanar spacing (a) before entering after-treatment equipment and (b) after leaving after-treatment equipment

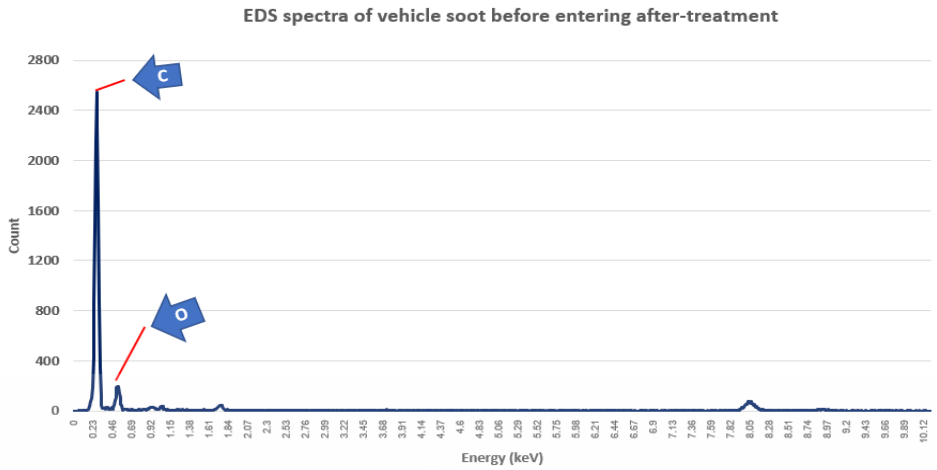

(a)

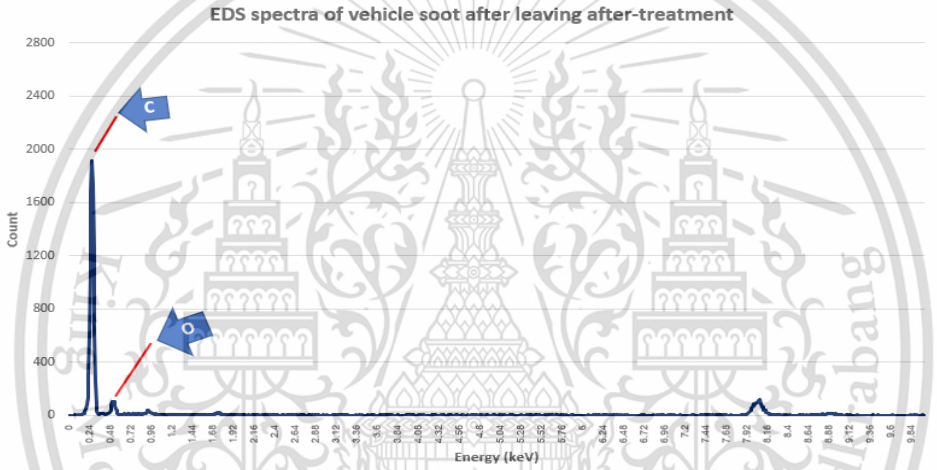

(b)

Figure 2.13 Elemental composition of vehicle soot (a) before entering after-treatment equipment and (b) after leaving after-treatment equipment

References

[1] Xi, Jinxiang & Zhong, Bei-Jing. (2006). *Soot in Diesel Combustion Systems*. Chemical Engineering & Technology. 29. 665-673. 10.1002/ceat.200600016.

[2] Liu, P., & Wang, C. (2019). *The Diesel Soot Particles Fractal Growth Model and Its Agglomeration Control*. IntechOpen. doi: 10.5772/intechopen.80851

[3] GenCat Engineering Department, How to reduce black smoke and carbon emissions from diesel engines, 2013, Diesel Particulate Filters Ver. 1.4.

[4] Mohankumar, S.; Senthilkumar, P. (2017). *Particulate matter formation and its control methodologies for diesel engine: A comprehensive review*. Renewable and Sustainable Energy Reviews, 80(), 1227–1238. doi:10.1016/j.rser.2017.05.133

[5] Karin P., Oki H., Hanamura K., and Charoenphonphanich C., *Nanostructures and oxidation kinetics of diesel particulate matters*, J Research and App in Mech Engr 2012; 2:3-8.

[6] Fernandez-Alos V, Watson J, Vander Wal R, Matthews J. *Soot and char molecular representations generated directly from HRTEM lattice fringe images using Fringe3D*. Comb and Flame 2011; 158:1807-1813. 10.1016/j.combustflame.2011.01.003

[7] Ban-seok Oh, Preechar Karin, Mek Srilomsak, Kritin Chonvasin, Watcharin Po-ngen, Sompong Srimanosaowapak, and Katsunori Hanamura, *Characterization of biodiesels and tire derived particulate matters in morphology and nanostructure*, Materials Today: Proceedings, Volume 66, Part 5,2022, Pages 2756-2761, ISSN 2214-7853,10.1016/j.matpr.2022.06.510.

[8] Kabir M.N., Alginahi Y., and Islam K., *Simulation of oxidation catalyst converter for after-treatment in diesel engines*, Int. J. of Automotive Technology, Vol. 16, No. 2, pp. 193–199 (2015).

[9] David B. Kittelson, *Engines and nanoparticles: a review*, Journal of Aerosol Science, Volume 29, Issues 5–6, 1998, Pages 575-588, ISSN 0021-8502, 10.1016/S0021-8502(97)10037-4.

[10] Hay Mon Oo, Preechar Karin, Chinda Charoenphonphanich, Nuwong Chollacoop, Katsunori Hanamura, *Physicochemical characterization of direct injection Engines's soot using TEM, EDS,*

X-ray diffraction and TGA, Journal of the Energy Institute, Volume 96, 2021, Pages 181-191, ISSN 1743-9671, 10.1016/j.joei.2021.03.009.

[11] https://www.becthai.com/en/products/435635-jeol---jem-2100plus-/-transmission-electron-microscope

[12] Singh, M., Srilomsak, M., Wang, Y., Hanamura, K., Vander Wal, R., Nanostructure Changes in Diesel Soot during NO2–O2 Oxidation under Diesel Particulate Filter-like Conditions toward Filter Regeneration. International Journal of Engine Research 20, No. 8–9, pp. 953–66, 2019, doi:10.1177/1468087418807608.

[13] Oh B., *Characterization of Soot in Trapping and Oxidation Process on Partial Flow Diesel Particulate Filter*, Chapter4, Master of Engineering Thesis Report, KING MONGKUT'S INSTITUTE OF TECHNOLOGY LADKRABANG, 2022.

[14] R. L. Vander Wal, A. J. Tomasek, K. Street, D. R. Hull and W. K. Thompson, *Carbon Nanostructure Examined by Lattice Fringe Analysis of High-Resolution Transmission Electron Microscopy Images*, Applied Spectroscopy, vol. 58, no. 2, pp. 230-237, 2004.

[15] P. Karin, P. Koko, C. Charoenphonphanich, N. Chollacoop and K. Hanamura, *Physicochemical Characterization of Diesel Engine's Soot and Metal Oxide Ash Nanoparticles Using Electron Microscopy, EDS and TGA*, Emission Control Science and Technology, vol. 7, no. 2, pp. 91-104, 2021.

[16] A. K. Neyestanaki, F. Klingstedt, T. Salmi and D. Y. Murzin, *Deactivation of postcombustion catalysts, a review*, Fuel, vol. 83, pp. 395-408, 2004.

CHAPTER 3

Effects of a Partial Flow Diesel Particulate Filter on a Vehicle's Thermal Efficiency and Exhaust Emissions

3.1 Introduction

The previous chapter was about the soot nanostructure analysis, which is harm for human health and need to reduce the particulate matters (PMs) from the exhaust gas of diesel vehicles. In this chapter, the focus on investigates the effects of partial flow diesel particulate filter (P-DPF) on a diesel vehicle's fuel consumption, brake-specific energy consumption (BSEC), brake thermal efficiency (BTE), smoke intensity, and diesel emissions.

Human activities including transportation, communication, and manufacturing typically involve the usage of internal combustion engines. Compression ignition diesel engines continue to be the primary internal combustion engine for heavy industrial, agricultural, and transportation applications. High torque and great thermal efficiency are both reflected in the diesel engine's high compression ratio. Because of the aforementioned factors, there is still a large market for diesel vehicles. Diesel use has increased along with the growth in the number of diesel cars on the road, which has significantly exacerbated the scarcity of fossil fuels. The use of automobiles is increasing in tandem with the growing human population. The increased use of autos and excessive fuel use will trigger future changes in the world ecosystem, climate, and fossil fuel sources. Automotive exhaust emissions are a major contributor to air pollution in many significant population centers across the world. The release of nitrogen oxides and smoke is another key drawback of diesel engines. Carbon monoxide (CO), nitrogen oxides (NO_x), hydrocarbons (HCs), and particulate matter (PMs) are the most common pollutants emitted by combustion engines, which come from incomplete combustion [1-2]. In any case, the fundamental disadvantage of diesel engines is that particulate matter (PMs) levels are high because fuel is delivered directly into the combustion chamber, resulting in incomplete combustion and a nonhomogeneous fuel and air mixture, which causes soot production.

As fossil fuel sources are quickly depleting, global energy consumption is growing. On the opposing side, the environmental harm caused by high amounts of greenhouse gases and

pollutants drives more research into ecofriendly alternative energy sources. Vegetable oils have been discovered to be a viable energy source that might replace fossil fuels. Additionally, it has been shown that vegetable oils have lower calorific values than regular diesel fuel. The utilization of vegetable fuels results in a nearly balanced CO_2 cycle and a reduction in greenhouse gas emissions. In comparison to liquid fossil fuels, vegetable fuels have a higher flash point (about 198 °C), making them safer to store and transport [3]. Although vegetable oils such as refined bleached and deodorized palm oil and palm stearin are used, crude palm oil (CPO) is the main component used in Thailand to create biodiesel. You may use biodiesel fuel both in pure biodiesel form (B100) and as a blend with petroleum-based diesel fuel. In the manufacturing of B100, acid-esterification and transesterification with methanol are used to transform raw materials such as crude palm oil into ethyl ester or methyl ester, which have characteristics equal to standard diesel fuel [4,5].

The emissions of PMs and NO_x from diesel engines have a significant impact on human health. Diesel vehicles release significantly more NO_x emissions in real-world driving situations than they do in the type of approval driving test cycle. A low NO_X trap (LNT), selective catalytic reduction (SCR), and SCR-catalyzed diesel particulate filter (SDPF) have all been included as after-treatment systems for emissions in numerous light-duty diesel automobiles. In this experiment, light-duty diesel vehicles were equipped with a two-stage exhaust gas recirculation (EGR), which is a mix of high-pressure (HP) and low-pressure (LP) EGR, in compliance with increased NO_x limits [6,7]. Untreated diesel engine emissions comprise hazardous gas phase pollutants as well as solid phase PMs. As a result, vehicles are equipped with after-treatment systems such as Diesel Oxidation Catalysts (DOC) and Diesel Particulate Filters (DPF), which use of DOC and DPF can greatly reduce the quantity of PM, HC, and CO released by diesel engines. DOC has no discernible effect on overall particle count. Nonetheless, a DPF is quite efficient in lowering overall PM, both in terms of mass and particle number [8]. Heavy vehicles and buses in Thailand are comparable to Euro 3, whereas passenger cars and one-ton pickup trucks are comparable to Euro 4. Consequently, no further after-treatment technology is required. Yet, stricter pollution control laws, akin to Euro 5, will be implemented soon to combat pollution [9]. This experiment and analysis will provide more data and support for the significance of implementing an after-treatment system.

The goal of this study is to determine how B20, as well as catalysts that cover DOC, P-DPF, and Long P-DPF after-treatment machinery, affect diesel emissions, soot emissions, and engine performance. To examine the vehicle thermal efficiency, this study used a 2.5-liter direct-injection diesel pickup truck. Also, a study of soot emission was carried out at constant engine speeds of 1500, 2000, and 2500 rpm with variable engine loads of 84, 112, 140, and 160 Nm since they reflect the realistic range of speed and load for diesel engines used on routes where peak performance is not always required.

3.2 Methodology

3.2.1 Fuel preparation and operational conditions

Through acid-esterification and transesterification with methanol, pure biodiesel (B100) is produced from based palm oil. B20 (20% biodiesel mixed with diesel) fuel was used to evaluate and compare vehicle thermal efficiency and exhaust emission. **Table 3.1** lists the fuel specifications. The operating circumstances for this experiment included 30 - 60% range of maximum engine loads (84, 112, 140, and 160Nm) at constant engine speeds (1500, 2000, and 2500 rpm).

3.2.2 Vehicle and testing platform

Using a chassis dynamometer, a diesel-engine pickup truck with a 2.5 Liters inline 4-cylinder common rail direct injection turbo diesel engine was operated at various engine speeds and loads. This experiment focuses on the effects of B20 fuels on vehicle thermal efficiency and exhaust pollution with three different after-treatment systems: without DOC or partial flow diesel particulate filter (P-DPF), with DOC and P-DPF, and with Long P-DPF alone. **Table 3.2** displays the vehicle specifications. The vehicle test bench was set up on the chassis dynamometer. BOSCH smoke intensity meter (DSM-240) with a measurement accuracy of 3% was used to assess smoke intensity. Also, the AVL exhaust gas analyzer (DITEST GAS 1000) was used to measure exhaust emissions of nitric oxide (NO), carbon dioxide (CO_2), and oxygen (O_2) with an accuracy of ± 5 ppm for NO, ± 0.3 %vol for CO_2, and ± 0.02 %vol for O_2. All engine conditions were recorded by the on-board diagnostic (OBD), which is also linked to the engine control unit (ECU), including emissions, mileage, and speed. During test conditions, the

computer used LabView programming software to measure engine torque, speed, and fuel consumption. **Figure 3.1** depicts a schematic representation of the equipment configuration.

3.2.3 After-treatment equipment

The after-treatment equipment in this study placed downstream of the diesel engine comprise Cerium Dioxide (CeO_2) coating DOC and Platinum (Pt) coating P-DPF. **Figure 3.2(a) and (b)** depicts the combination of DOC and P-DPF and only long P-DPF systems when they are placed in the exhaust system, respectively. The DOC is locked first, followed by the P-DPF. As stated in **Table 3.3**, DOC are fitted on diesel engine exhaust lines to minimize the level of hydrocarbon (HC) and carbon monoxide (CO) emissions from the engine exhaust gas by converting CO and HC to Carbon Dioxide (CO_2) and water (H_2O), and Nitric Oxide (NO) to Nitrogen Dioxide (NO_2) [10]. Most of the gas phase exhaust pollution may be handled at the DOC due to the reaction mechanism in the DOC, which will be employed further in the P-DPF equipment. P-DPF is made up of metal foil and fleece used to trap particulate matter (PMs) effectively, which is then combined with oxygen (O_2) and NO_2 to oxidize carbon element (soot) in the PMs to generate CO_2 and NO. Moreover, a Pt catalyst layer on a P-DPF substrate can speed up the oxidation of soot. Hence, when soot (carbon form) and NO_2 are combined in the P-DPF, NO and CO_2 levels increase (the PMs are oxidized and the P-DPF is regenerated). P-DPF and Long P-DPF were evaluated in a variety of scenarios to determine which was the best. The specifications of DOC, P-DPF, and Long P-DPF are shown in **Table 3.4**.

3.2.4 Microstructure of particulate matters

Particulate matters (PMs) were measured while the vehicle was being tested in real time using paper filters and a smoke meter. The PMs samples on the paper filters were utilized to characterize the agglomeration particles in micro-scale using an Optical Microscopy or OM (Nikon Model LV100) to magnify pictures and see the original color of the PMs as well as a Scanning Electron Microscope or SEM (FE-SEM SU5000) to analyze PMs shape and microstructure at a magnification of up to 10,000.

3.3 Calculation Equations

3.3.1 Vehicle thermal efficiency

The brake specific fuel consumption (BSFC), brake specific energy consumption (BSEC), and brake thermal efficiency (BTE) were calculated using the fuel consumption (g/s), engine speed (rev/min or rpm), and engine torque (Nm) are all findings of vehicle thermal efficiency [11].

3.3.1.1 Brake Specific Fuel Consumption (BSFC)

The rate of fuel flow to vehicle output power, which is expressed in g/kWh, is used to compute the BSFC.

$$BSFC = \frac{\boldsymbol{fuel\ flow\ rate}}{\boldsymbol{Brake\ output\ power}} = \frac{\dot{\boldsymbol{m}}\boldsymbol{f}}{\boldsymbol{4\pi\tau \cdot \frac{N}{60} \cdot \frac{1}{2}}}$$

3.3.1.2 Brake Specific Energy Consumption (BSEC)

The BSEC is the rate of energy consumption to vehicle output power, measured in kJ/kWh, and the Lower Heating Value (LHV) or Calorific Value (C.V.) used to determine in this equation were B10 LHV (43.10 kJ/g) and B20 LHV (42.42 kJ/g).

$$BSEC = BSFC \cdot C.V.$$

3.3.1.3 Brake Thermal Efficiency (BTE)

BTE is the vehicle output power generated by thermal energy provided to a system.

$$BTE = \frac{\boldsymbol{Brake\ output\ power}}{\boldsymbol{Input\ power}} = \frac{\boldsymbol{4\pi\tau \cdot \frac{N}{60} \cdot \frac{1}{2}}}{\dot{\boldsymbol{m}}\boldsymbol{f} \cdot \boldsymbol{C.V.}}$$

3.4 Results & Disscussions

The findings in terms of vehicle thermal efficiency, exhaust emission (Nitric Oxide (NO), Carbon Dioxide (CO_2), Oxygen (O_2), and smoke intensity), and soot morphology will be discussed in the next section. This experiment tested B20 fuel and results will shown as solid bar, conditions without after-treatment system, Cerium dioxide coated DOC and Pt coated P-

DPF, and Pt coated long P-DPF only will shown in blue colour, orange colour, and grey colour, respectively.

3.4.1 Vehicle Thermal Efficiency

Vehicle thermal efficiency was determined using the results of fuel consumption, BSFC, BSEC, and BTE. Fuel consumption, BSFC, BSEC, and BTE data for B20 fuels are shown in **Figure 3.3 (a) to (d)**, respectively. Fuel consumption and BTE climbed at constant engine speed as engine torque increased due to improved engine power as a result of increasing fuel injection to meet the increased workload. On the other hand, BSFC and BSEC fell significantly since the increase of fuel consumption and BTE, similar trend was also observed by An H. et al. [12] that at the constant engine speed, BSFC, also BSEC that was calculated from BSFC, drops as engine load increases to improve output power. The findings of the engine performance test are unaffected by the installation of DOC and P-DPF. The installation of after-treatment devices had no discernible influence on Fuel consumption, BSFC, BSEC, and BTE results for B20 fuel.

3.4.2 Exhaust Emissions

3.4.2.1 Nitric Oxide (NO) and Carbon Dioxide (CO_2)

Figure 3.4(a) and (b) shows the results of NO and CO_2, respectively. As a result of the increasing engine torque at each steady engine speed, NO and CO_2 levels rise. However, both of them are reduced when engine speed increases. In addition, Jung et al. found that as the engine load grows, the NO_2 part of NO_X diminishes, while the NO fraction increases, leading to the conclusion that NO_X were primarily NO at high engine loads, whereas NO_2 occurs fiercely at low engine loads [14]. The combination of nitrogen (N_2) and oxygen (O_2) in the combustion chamber causes an increase in NO. When more fuel is injected into the combustion chamber, CO_2, the main byproduct of the consumption of fuel and air, rises. As mentioned in **3.2.3**, the P-DPF mechanism raises NO and lowers CO_2 because the platinum (Pt) catalyst in P-DPF not only promotes soot oxidation with NO_2 and soot (in the form of Carbon), but also transforms CO into CO_2, resulting in increased CO_2. The outcome of NO under circumstances with DOC and P-DPF is the best because DOC first transforms NO into NO_2, and then more NO_2 reacts with soot (in Carbon form) within P-DPF. Furthermore, NO_2 and O_2 can cooperate to accelerate

soot oxidation, which is quicker than the total of the oxidation rates by only NO_2 and only O_2 [14].

3.4.2.2 Oxygen (O_2)

Figure 3.4(c) shows the result of O_2, the amount of O_2 in the exhaust gas is related to the combustion in the cylinder, specifically the air-to-fuel ratio. Furthermore, the output torque caused a modest drop in O_2. This is because additional fuel is being injected into the combustion chamber in order to boost engine torque. This conclusion holds true at all engine speeds. Yet, there are no discernible changes in the quantity of O_2 in the exhaust gas across the three distinct after-treatment system situations. O_2 falls following the installation of after-treatment systems due to the oxidation process in DOC for the treatment of HC, CO, and NO and in P-DPF for the treatment of soot.

3.4.2.3 Smoke Intensity

Figure 3.4(d) illustrates the amount of smoke intensity, which increases at low engine speeds owing to incomplete combustion. When more fuel is delivered into the combustion chamber as engine torque increases, so does the smoke intensity. As assessed by a BOSCH smoke intensity meter, the after-treatment system could very well reduce smoke intensity by up to 51% approximately. As a result of after-treatment systems, the intensity of smoke has decreased. The condition with only long P-DPF produced the largest decrease in smoke intensity due to it larger space for soot to trapped.

3.4.2.4 Microstructure of soot

Images of paper filters acquired with an optical microscope (OM, Nikon Model LV100) in Figure 3.5 and a 10,000-magnification scanning electron microscope (SEM, FE-SEM SU5000) in Figure 3.6 show the findings. The OM, SEM results of B20 without after-treatment system, CeO_2 coating DOC and Pt coating P-DPF, and Pt coating long P-DPF were shown in **Figure 3.5(a) to (c)** for B20 OM and **Figure 3.6(a) to (c)** for B20 SEM, respectively. Soot aggregation was plainly visible in the absence of an after-treatment system. Nevertheless, after installing an after-treatment system, soot aggregation decreased considerably, which was also consistent with the smoke intensity graph.

3.5 Conclusion

In conclusion, when compared to the three examples of after-treatment systems including conditions of without an after-treatment, with cerium dioxide (CeO_2) coating on diesel oxidation catalyst (DOC) and platinum (Pt) coating on partial-flow diesel particulate filter (P-DPF), and with Pt coating long P-DPF only. It was found from this experiment that the installation of Long P-DPF reduced the quantity of smoke intensity (particulate matter or PM suspended gas) by up to 51% on average, which can be clearly seen from the scanning electron microscopy (SEM) images where three distinct situations are compared that less soot is produced following installation of the after-treatment equipment. For further detail, Pt coating on P-DPF can initiate a soot oxidation process in which carbon-based soot trapped inside the material interacts with nitrogen dioxcide (NO_2) to decrease soot while boosting nitric oxide (NO). Nevertheless, the testing findings indicated that installing after-treatment equipment (DOC and P-DPF) and using B20 in the tests had no obvious influence on vehicle thermal efficiency base on the calculation from fuel consumption to brake thermal efficiency. However, to further work on the analysis of partial-flow diesel particulate filter, the determining of gas emissions level and particulate matter using the international test cycle such as the Worldwide harmonized Light vehicles Test Procedure (WLTP) or New European Driving Cycle (NEDC) should be considering to investigate.

Tables

Table 3.1 Biodiesel fuel properties [11].

Properties(units)	B100	B20
Carbon (% mass)	76.7	82.6
Hydrogen (% mass)	12.4	13.4
Oxygen (% mass)	10.9	4.0
Low heating value (kJ/g)	37.4	42.4
Cetane Number	62.1	54.5
Flash Point (°C)	184.5	66
Density at 15 °C (kg/m^3)	875	827
Viscosity at 40 °C (mm^2/s)	4.5	3.1

Table 3.2 Toyota Hilux Tiger vehicle specifications

Vehicle	Toyota Hilux Tiger
Engine Type	2KD-FTV (Diesel)
Number of cylinders & Arrangement	4 cylinders, In-line
Valve Mechanism	16 Valve DOHC
Bore x Stroke	92.0 mm x 93.8 mm
Displacement Volume	2500 cc
Compression Ratio	18.5 : 1
Fuel System	Common-rail type Direct Injection
Maximum Power (kW at rpm)	75 kW at 3600 rpm
Maximum Torque (Nm at rpm)	260 Nm at 1600 – 2400 rpm

Table 3.3 DOC Reaction Mechanism [10.]

Number of Equation	DOC Reaction Equation
1	$C_XH_Y + (X + 0.25Y)\ O_2 \rightarrow XCO_2 + YH_2O$
2	$CO + (0.5)\ O_2 \rightarrow CO_2$
3	$H_2 + (0.5)\ O_2 \rightarrow H_2O$
4	$NO + (0.5)\ O_2 \rightarrow NO_2$

Table 3.4 Specifications of DOC, P-DPF and Long P-DPF

Type of Equipment	*DOC*	*P-DPF*	*Long P-DPF*
Coating Catalyst	CeO_2 (Cerium Dioxide)	Pt (Platinum)	Pt (Platinum)
Cell Density	300	200	200
Length (mm.)	100	150	200
Diameter (mm.)	144	144	144

Figures

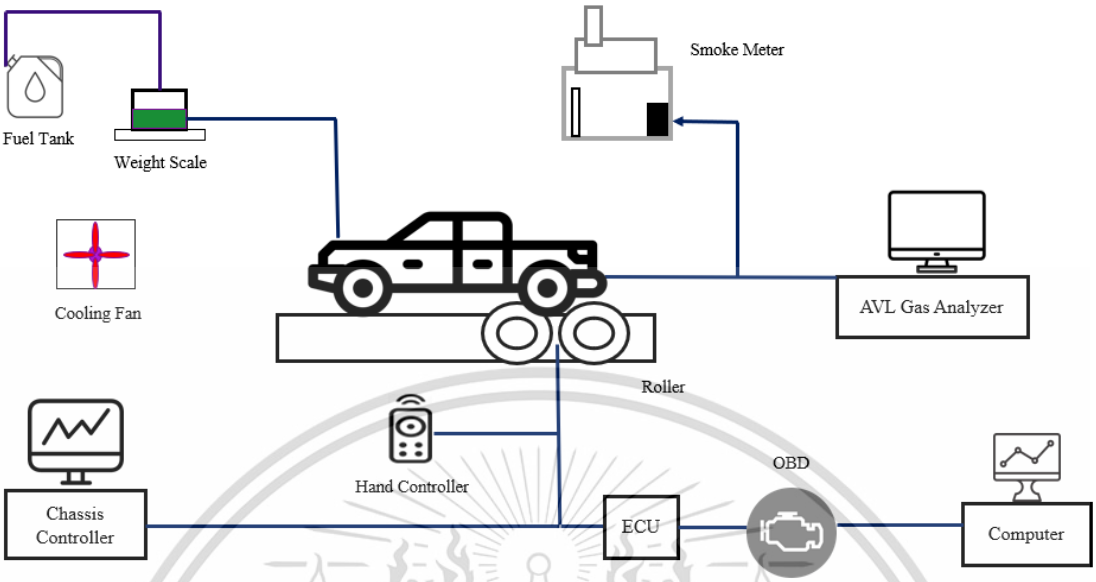

Figure 3.1. Schematic diagram of chassis dynamometer set up

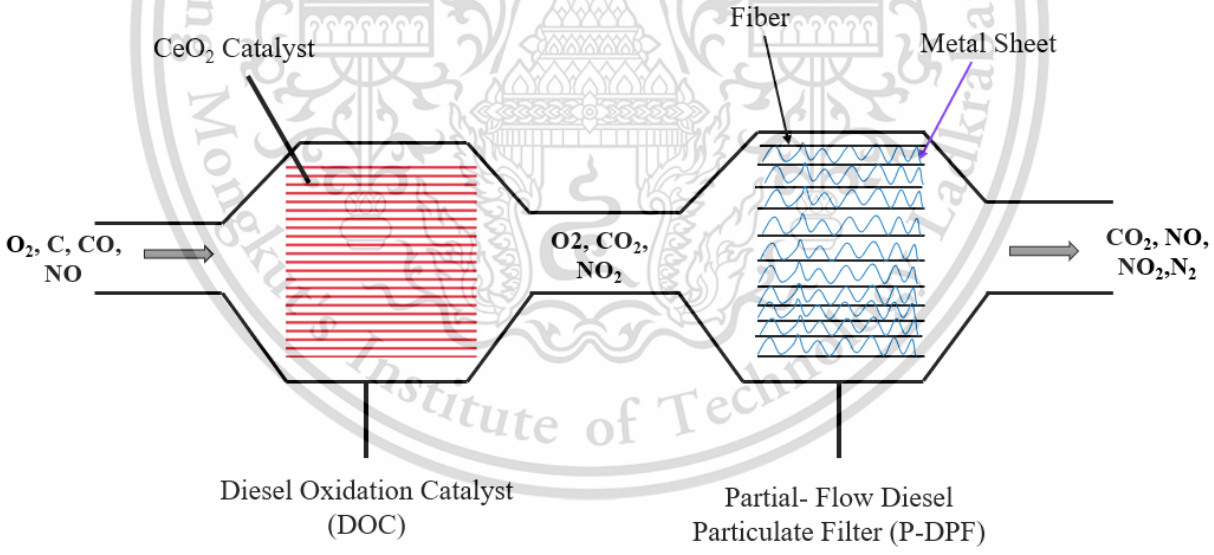

(a)

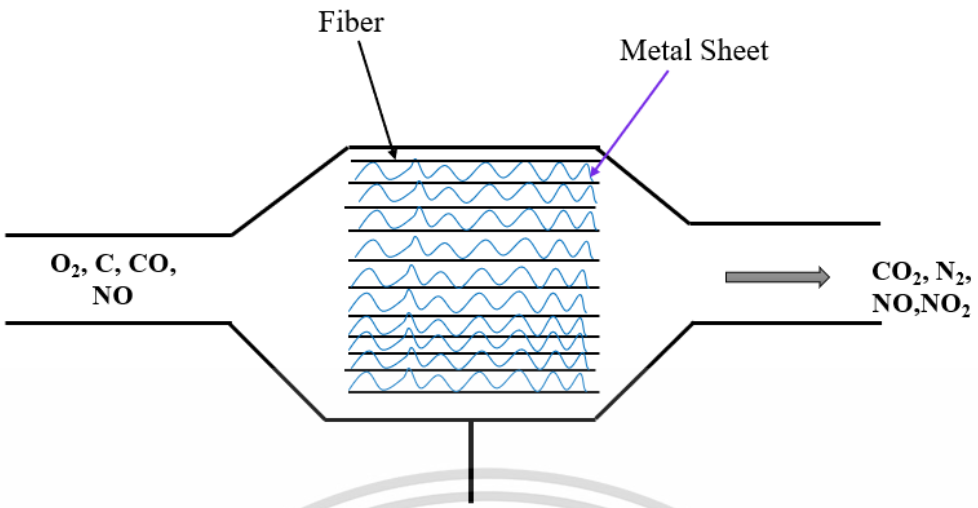

(b)

Figure 3.2 (a) Exhaust gas flow through CeO_2 coated DOC and Pt coated P-DPF, (b) Exhaust gas flow through Pt coated long P-DPF

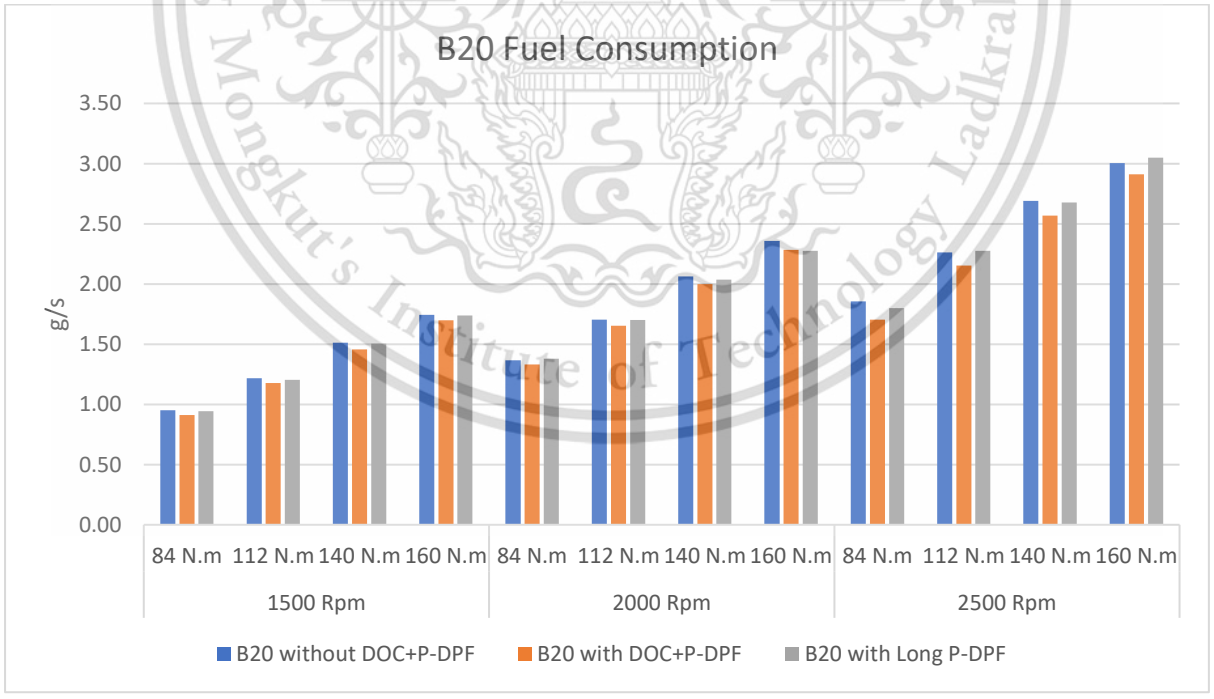

(a)

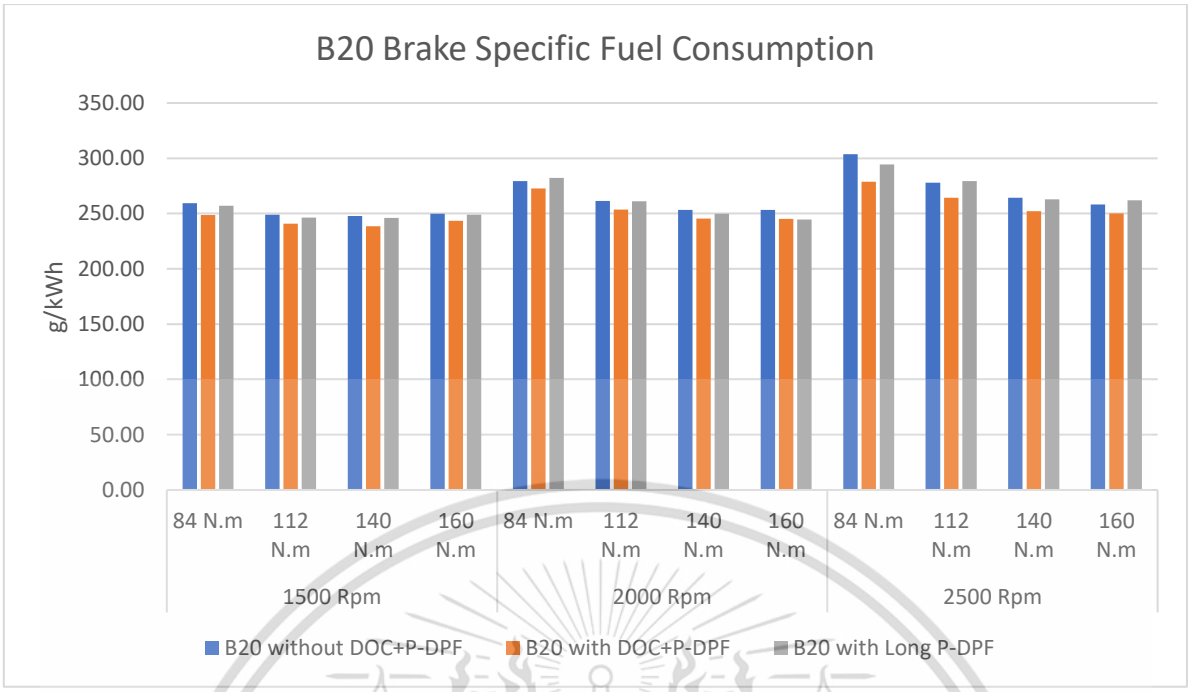

(b)

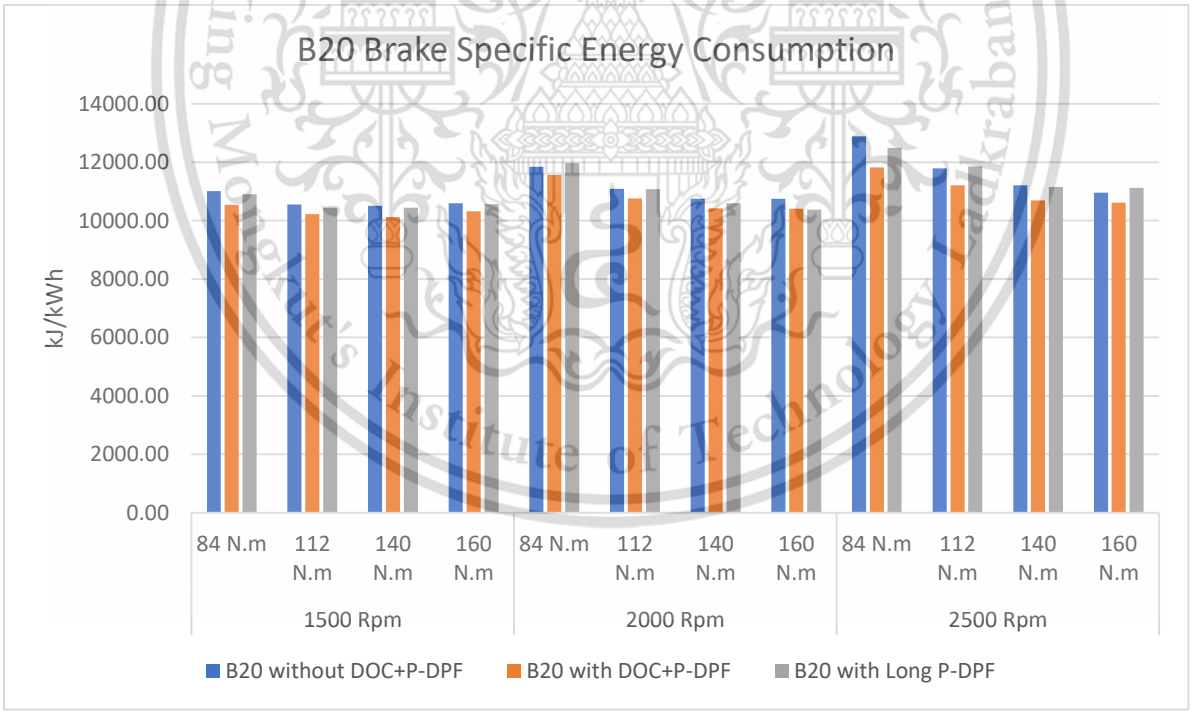

(c)

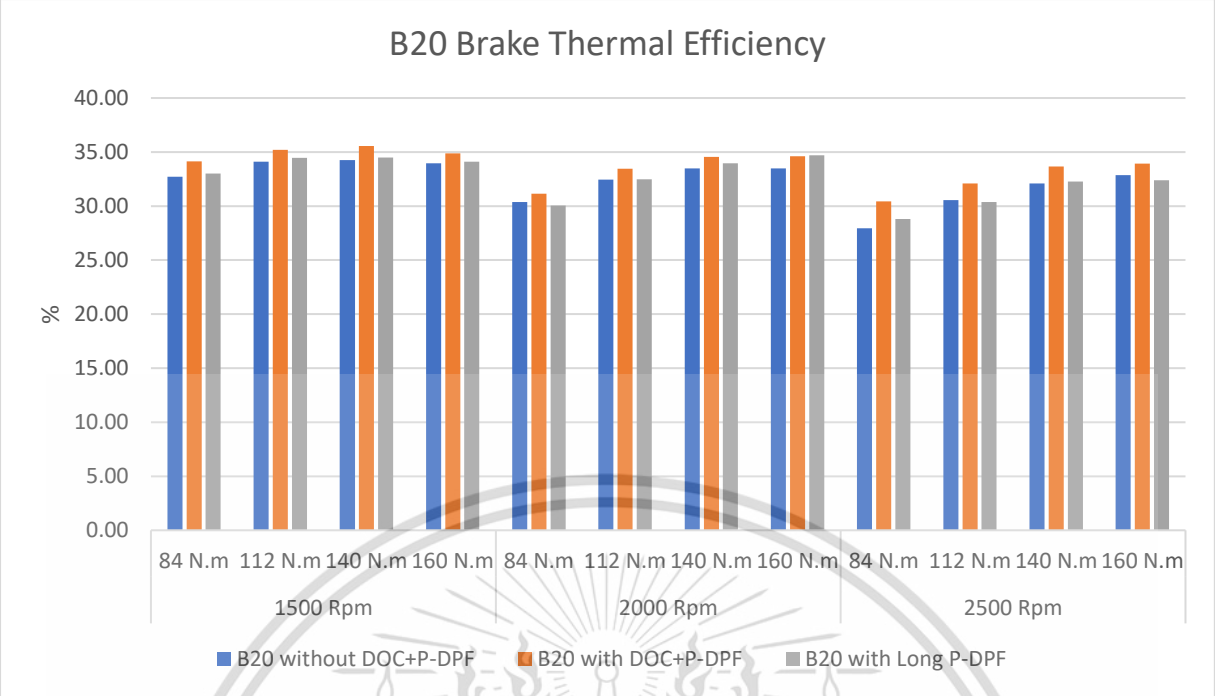

(d)

Figure 3.3 (a) Fuel Consumption, (b) Brake Specific Fuel Consumption, (c) Brake Specific Energy Consumption, and (d) Brake Thermal Efficiency

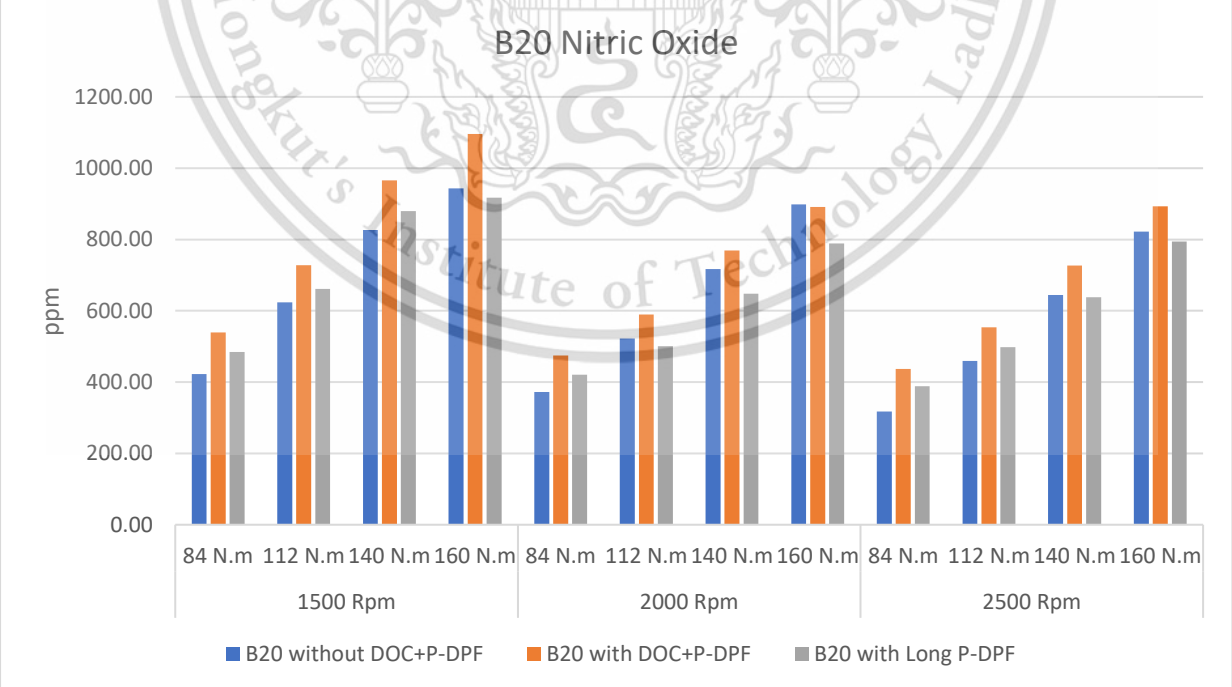

(a)

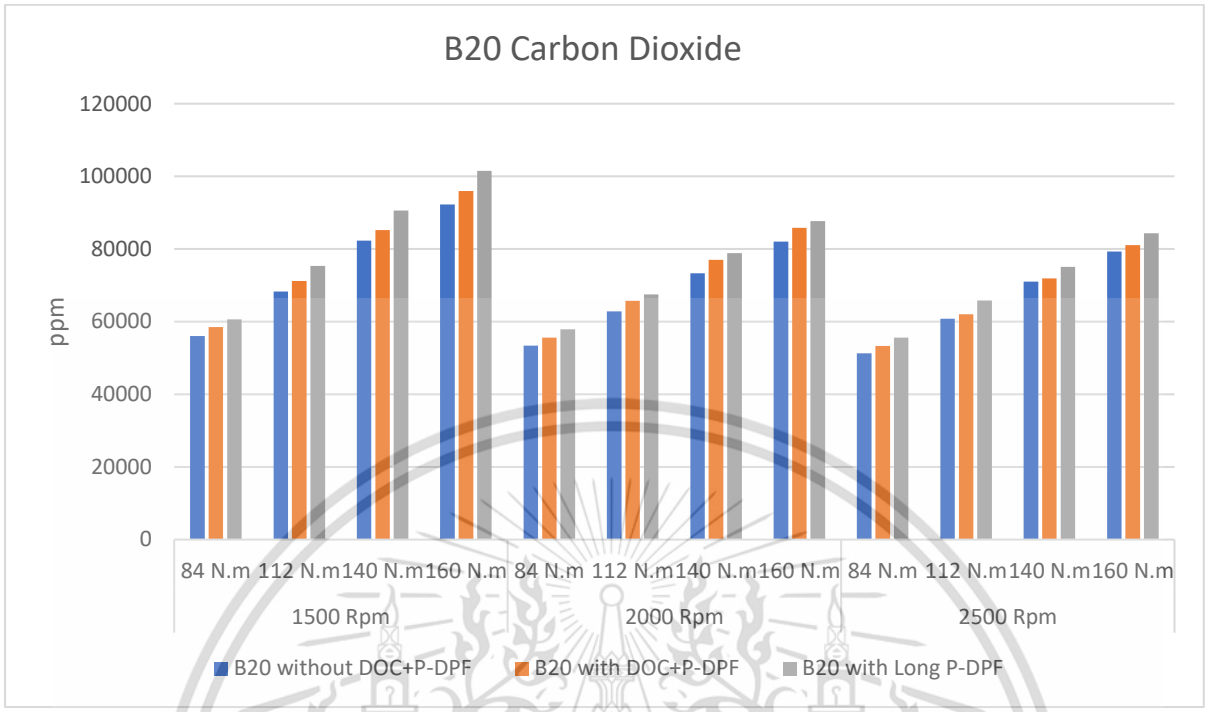

(b)

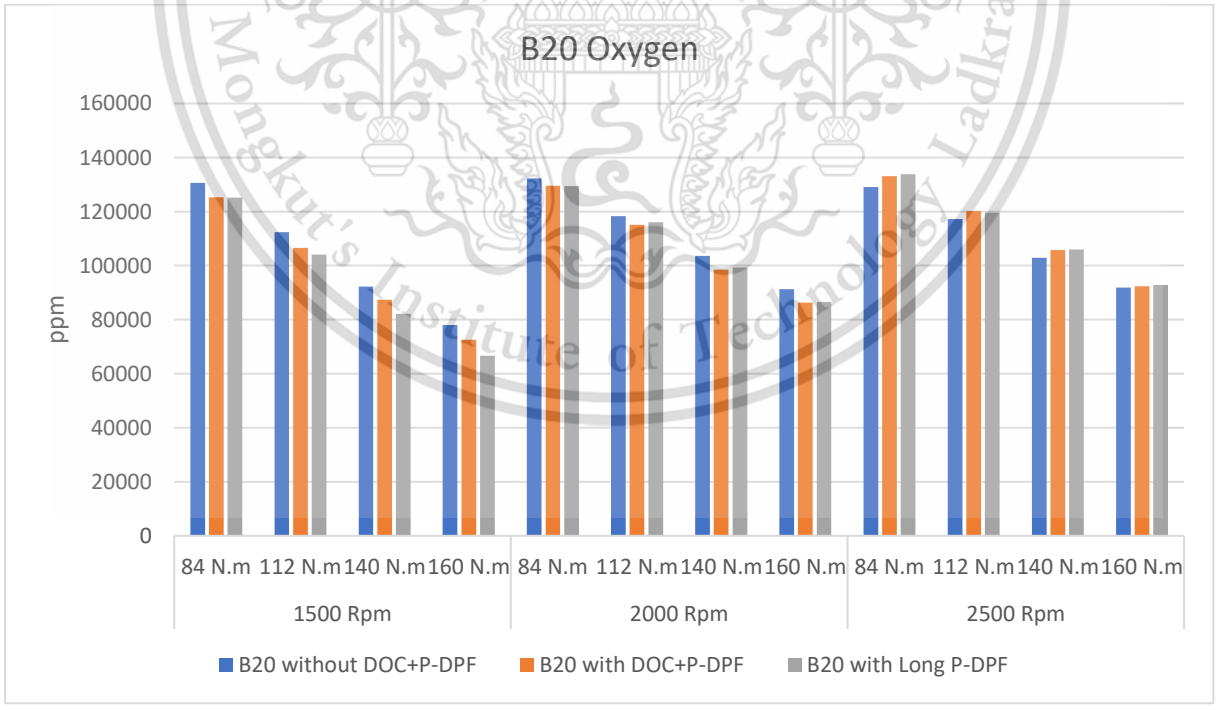

(c)

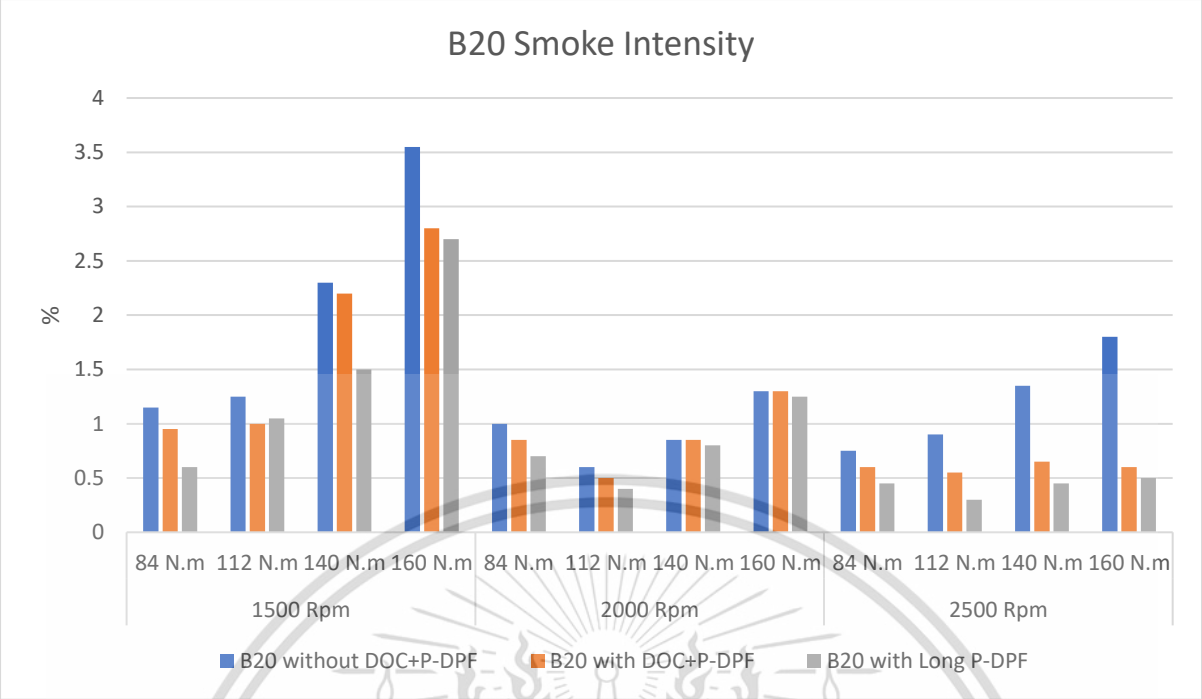

(d)

Figure 3.4 (a) Nitric Oxide, (b) Carbon Dioxide, (c) Oxygen, and (d) Smoke Intensity

(a)

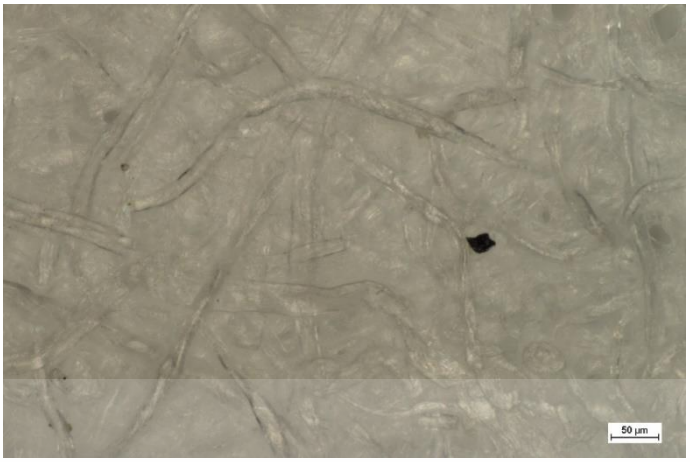

(b)

(c)

Figure 3.5 OM images (a) B20 without after-treatment, (b) B20 with CeO_2 coated DOC and Pt coated P-DPF, and (c) B20 with Pt coated long P-DPF

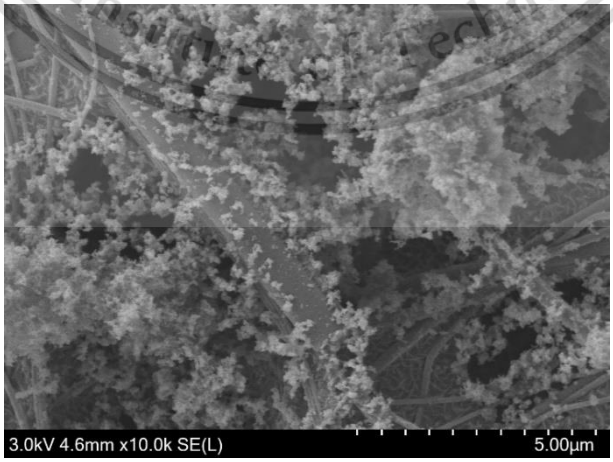

(a)

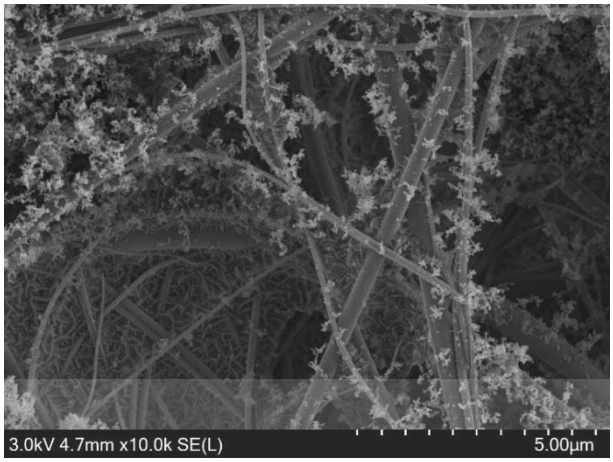

(b)

(c)

Figure 3.6 SEM images (a) B20 without after-treatment, (b) B20 with CeO_2 coated DOC and Pt coated P-DPF, and (c) B20 with Pt coated long P-DPF

References

[1] Zhu R., Cheung C.S., Huang Z., and Wang X., *Regulated and unregulated emissions from a diesel engine fueled with diesel fuel blended with diethyl adipate*, Atmos. Environ. 45 (April 2011) 2174–2181.

[2] Azimi S., Rocher V., Muller M., Moilleron R., and Thevenot D, *Sources, distribution and variability of hydrocarbons and metals in atmospheric deposition in an urban area (Paris,France)*, 2005, J. Sci. Total Environ., 337 223-239.

[3] Yusaf T.F., Yousif B.F., and Elawad M.M., 2011, *Crude palm oil fuel for diesel-engines: Experimental and ANN simulation approaches*, Energy, 36 (8) 4871–4878.

[4] Tamilselvan P., Nallusamy N., and Rajkumar S., *A comprehensive review on performance, combustion and emission characteristics of biodiesel fuelled diesel engines*, Renew. Sustain. Energy Rev. 79, 1134–1159 (2017).

[5] Salykin E.A., Kurapin A.V., Tshibanda K.E., Dygalo V.G., and Slavutskiy V.M., *Impact of diesel fuel and palm oil blend compositions on the performance of the fuel supply process in the diesel engine*, IOP Conf. Series: Materials Science and Engineering, 386 (2018) 012014.

[6] Papadopoulos G., Ntziachristos L., Tziourtzioumis C., Keramydas C., Lo T. S., Ng K. L., Wong H. L. A., and Wong C. K. L., *Real-world gaseous and particulate emissions from Euro IV to VI medium duty diesel trucks*, 2020, J. Sci. Total Environ., 731 139137.

[7] Ko J., Myung C.-L., and Park S., *Impacts of ambient temperature, DPF regeneration, and traffic congestion on NOx emissions from a Euro 6-compliant diesel vehicle equipped with an LNT under real-world driving conditions*, Atmospheric Environment (2018).

[8] Jacobs T., et., al., *Development of Partial Filter Technology for HDD Retrofit*, SAE International (SAE World Congress Detroit), 2006.

[9] Cosh P.T., et., al., *Impacts of Partial Flow Diesel Particulate Filter on Vehicle's Brake Thermal Efficiency and Exhaust Emissions Characteristics*, 2023, Proc. TSME Int. Conf. on Mechanical Engineering, p 63-69.

[10] Kabir M.N., Alginahi Y., and Islam K., *Simulation of oxidation catalyst converter for after-treatment in diesel engines*, Int. J. of Automotive Technology, Vol. 16, No. 2, pp. 193–199 (2015).

[11] Kanokkhanarat P., Karin P., Depaiwa N., Wongpattharaworakul V., Srisurangkul C. and Yamakita M., *Influence of ethanol biodiesel blends on a diesel engine's efficiency and exhaust emission characteristics*, 2022, Proc. Int. Conf. on Materials, Minerals and Polymer vol 66 p 2862-2867.

[12] An H., Yang W.M., Maghouhli A., Li J., Chou S.K., and Chua K.J., *Performance, combustion and emission characteristics of biodiesel derived from waste cooking oils*, 2013, Applied Energy, vol 112, p 493 -499.

[13] Buyukkaya E., *Effects of biodiesel on a DI diesel engine performance, emission and combustion characteristics*, 2010, Fuel, vol 89, p 3099 – 3105.

[14] Jung Y., Pyo Y.D., Jang J., Kim G.C., Cho C.P., and Yang C., *NO, NO_2 and N_2O emissions over a SCR using DOC and DPF systems with Pt reduction*, 2019, J. Chemical Engineering, vol 369, p 1059 – 1067.

[15] Sethin A. and Somnuk K., *Effect of Biodiesel B7 and B10 on Common Rail Diesel Engine Emission Characteristics at Different Engine Speeds*, 2022, IOP Conf. Ser.: Earth Environ. Sci., vol 1050, 012014

CHAPTER 4

Investigation of the characteristics of exhaust emissions and the impact of platinum-coated partial flow diesel particulate filters installed in a light-duty diesel vehicle using New European Driving Cycle (NEDC)

4.1 Introduction

Land vehicle diesel engines are one of the leading sources of air pollution in Thailand, with relatively high emission rates owing to incomplete combustion, posing health and environmental problems. Nitrogen oxides (NO_X), hydrocarbons (HCs), carbon monoxide (CO), and particulate matters (PMs) are the principal pollutants emitted by diesel engines that have a negative influence on human health. An aftertreatment system is a method or technology for removing harmful exhaust pollutants from diesel engines. In other words, it is a device that cleans exhaust gases to ensure that engines meet pollution requirements.

Although other vegetable oils such as refined bleached and deodorized palm oil and palm stearin are used, crude palm oil is the main material used to create biodiesel in Thailand. In the manufacturing of pure biodiesel (B100), acid-esterification and transesterification with methanol are used to transform raw materials such as crude palm oil into ethyl ester or methyl ester. The molecular carbon number and proportion of normal paraffins and iso-paraffins in these fuels are determined by the source material and production process utilized. Furthermore, biodiesel fuels have a high cetane number, no aromatics, no sulfur, renewable and biodegradable, same oxidation stability, and can be used in diesel engines without requiring any modifications to the engine systems since its combustion properties are making them suitable for use in diesel engines [1-3].

Particulate matter (PM) is a result of incomplete combustion in diesel engines and is often constituted of carbonaceous chemicals and adsorbed hydrocarbons. The chemical and physical properties of PM are influenced by the operating conditions of the engine (engine load and speed), the quality of the fuel, the features of fuel injection, and the lubricating oil

utilized. Soot, the insoluble organic carbon component of particulate matter, is produced by incomplete combustion of petrochemicals and consists of agglomerates ranging in size from 0.5 to 5 μm. PM are suspected of having a variety of harmful effects on human health, plant physiology, the environment, building material integrity, and regional and global climate [4-6]. Factors of the atmosphere and weather can have an immediate impact on primary pollution. Secondary pollution will accumulate because of atmospheric oxidants and dilution oxidizing initial contamination in the air. Secondary pollutants such as particulate matter (PM) and volatile organic compounds (VOCs) are formed when oxidized VOCs condense on particles, because of the creation of semi-volatiles or the oxidation of primary PM. $PM_{0.1}$, PM_1, $PM_{2.5}$, and PM_{10} are particles with diameters smaller than 0.1, 1, 2.5, and 10 μm, respectively, as defined by regulations and the general public. These four size classes are often employed in public health studies and in air quality regulations [7]. This study looks into a variety of methods for decreasing PM and managing emissions by blending biodiesel fuels with various after-treatment systems.

In the future, the aftertreatment system will be one of the most significant elements for internal combustion engines (ICEs). Since European emission standards for CO, HC, NO_X, and PM have become even more stringent. After-treatment technologies are the most cost-effective way to reduce exhaust emissions to permissible levels since they have little to no influence on engine performance. Diesel particulate filters (DPF), diesel oxidation catalysts (DOC), low NOx traps (LNT), selective catalytic reduction (SCR), or a combination of these are the principal after-treatment methods used to reduce emissions from Combustion Ignition engines [8]. DOC are installed on the exhaust line of a diesel engine to reduce the amount of HC and CO emissions from the engine exhaust gas. The exit temperature is enhanced by oxidizing HC and CO, which is frequently done with a platinum-based catalyst. This temperature increase aids the DPF's active regeneration. As a result, a DOC is usually installed in the diesel vehicle exhaust pipe prior to a DPF [9]. To capture some, but not all, of the soot from engine exhaust and lower PM without clogging the filter, partial-flow diesel particulate filter (P-DPF), which will be used with DOC in this study, combines the features of a flow through substrate with a wall flow filter. Nonetheless, a one-of-a-kind foil and metal fleece filter substrate is used, which combines the advantages of a flow through design with the

ability to collect soot particles [10]. The P-DPF project aimed to develop a low-cost PM reduction system that could reduce PM by over 50% and HC/CO by over 60% in a modular, simple-to-maintain package without additional electronic control system.

Light-duty vehicle (LDV) emissions are certified all around the world utilizing a range of driving cycles and type approval test procedures. The New European Driving Cycle (NEDC), for example, is used throughout Europe for certification. The NEDC, a cold start driving cycle, has been chastised for failing to adequately simulate actual vehicle performance. This method for emission type approval is required for all Euro 3 and later LDVs in Europe [11]. Thus, in this experiment, under the NEDC, to monitor in-use qualities in terms of quantities of pollutants emitted from used vehicle, evaluate the success of each countermeasure to control, and reduce gas and soot emissions emitted from vehicles as much as we can.

Nonetheless, several studies on fuel economy, exhaust emissions, and particulate matter have been conducted. Regardless, the goal of this study will be to investigate the effects of gas emissions, soot emissions, soot nanostructure, and soot morphology on B20 and combinations of catalyst coated DOC and P-DPF. This research used an actual pickup truck with a 2.5-liter direct injection diesel engine operating on the NEDC to investigate the real-time driving situations of urban driving cycles (UDCs) and extra-urban driving cycle (EUDC).

4.2 Methodology

4.2.1 Experiment procedures and fuel preparation

This study used the New European Driving Cycle (NEDC) that was carried out in accordance with the prevailing Regulation No.83 of the Economic Commission for Europe of the United Nations (UN/ECE) [12] to examine how B20 affected gas emissions and soot emissions. Also known as the MVEG cycle (Motor Vehicle Emissions Group), it begins with a warm-up phase lasting about 400 seconds, then includes four urban driving cycles (UDCs) or phase 1 with low vehicle speed, low engine load, and low exhaust gas temperature, and followed by one extra-urban driving cycle (EUDC) or phase 2 with more aggressive and higher speed driving. Together, these phases last a combined 1,180 seconds and cover 11.03 kilometers [11], which will only show the phase 1 and phase 2 target velocity profiles in **Figure**

4.1. Furthermore, the maximum speeds for phases 1 and 2 are 50 km/h and 120 km/h, respectively.

Following each test, the after-treatment equipment in the exhaust pipe of the vehicle was replaced. If we needed to change the testing fuel, the fuel line was emptied and refilled with new test fuel. After that, the injection system was purged, and the engine was operated at high speed to eliminate any remaining residues of previously tested fuel.

For fuel preparation, the process of creating pure biodiesel in Thailand comprises the acid-esterification and transesterification of palm oil with methanol. This biodiesel, also known as B100, is blended in various ratios with diesel fuel to produce commercial varieties B7 (7% biodiesel blend), B10 (10% biodiesel blend), and B20 (20% biodiesel blend). In this study, B20 fuel was utilized to test and compare exhaust pollution. It was determined that biodiesel had a higher boiling point than diesel but a lower distillation temperature, whereby the parameters of biodiesel utilized in this experiment are shown in **Table 4.1**. Furthermore, its viscosity is higher, which improves fuel lubricity. The calorific values of B20, as shown in **Table 4.2**, were determined using an Isoperibol Bomb Calorimeter from LECO Analytical Instruments (AC500 Isoperibol Calorimeter), and the findings indicate that the heat of combustion reduces as the amount of biodiesel in the fuel increases [13].

4.2.2 Vehicle specifications and experiment setup

The NEDC driving cycles were performed on a chassis dynamometer using a used vehicle with 2.5L 4-cylinder common rail direct injection diesel-engine truck, the same vehicle utilized in **Chapter 3**. This study evaluates the impact of B20 fuel on fuel economy and exhaust emissions between with and without using after-treatment equipment. **Table 4.3** shows the vehicle specifications.

The Automotive Emission Laboratory (AEL), which was created by The International Organization for Standardization / The Inter-national Electrotechnical Commission 17025 (ISO/IEC 17025) to assess laboratory quality systems, investigated the operational circumstances of this experiment. Furthermore, accreditation agencies can be used as global standards to assess laboratory competency. **Figure 4.2** shows that all AEL light duty test cell equipment complies with European emissions standards 4. First, the vehicle was placed on

the chassis dynamometer system, which includes a roller and a cooling fan that provides variable air speed in tandem with the roller's speed. The fuel tank was isolated from the main fuel tank to avoid contamination and maintain the weight steady during the experiment, in which the vehicle's fuel economy was assessed using the carbon balance method.

The vehicle's exhaust gas, which contains exhaust emissions such as Carbon Monoxide (CO), Carbon Dioxide (CO_2), Total Hydrocarbon (THC), Methane (CH_4), and Nitrogen Oxide (NO_x), will be combined with air from the air filter in the dilution tunnel. The exhaust gas will then separate and pass through particulate filters, a Constant Volume Sampler (CVS), an exhaust gas sampling system, a gas analyzer system with dilute measurement, an AVL Opacimeter, and a particle counting system. Lastly, the control room includes the chassis dyno controller, iGEM vehicle, driver aid, emissions bench remote desktop, and Fourier Transform Infrared (FTIR) emissions bench remote desktop. **Figure 4.3** will also depict the real test diagram at the AEL. On top of that, AEL has analyzed the quantity of pollution that vehicles emit to further allow efficiency development and energy conservation to certify vehicle quality and avoid air pollution.

4.2.3 After-treatment system

4.2.3.1 Diesel Oxidation Catalyst (DOC)

Diesel oxidation catalysts (DOC) are used in diesel engine exhaust pipes to reduce hydrocarbon (HC) and carbon monoxide (CO) emissions by converting them to carbon dioxide (CO_2) and water (H_2O), as well as nitric oxide (NO) to nitrogen dioxide (NO_2). DOC is frequently fitted upstream of a partial-flow diesel particulate filter (P-DPF) in the vehicle exhaust pipe. To initiate DOC's operations, exhaust gas will pass through the monolith's multiple narrow channels, each with a porous wall coated with catalyst. Some gas will diffuse to the porous channel wall, where the reactions will take place. The reactions produce new chemicals, which then enter the channels. As a result, diffusions and reactions in the porous wall continuously reduce HC and CO at the DOC outflow [9]. Cerium dioxide (CeO_2) DOC was employed in this experiment. When compared to without the CeO_2 catalyst coated on DOC, the catalyst lowers more HC and CO to generate more H_2O and CO_2 due to the oxygen (O_2) species of the catalyst [14].

4.2.3.2 Partial-flow Diesel Particulate Filters (P-DPF)

Trapping soot particles generated by the engine is the main purpose of the Diesel Particulate Filter (DPF). A wall-flow filter is a typical type of filter that captures soot particles by forcing exhaust gas through the walls of a monolith [15].

P-DPF is used to trap particulate matter (PMs), which is then combined with oxygen (O_2) and nitrogen dioxide (NO_2) to oxidize carbon element (soot) in the PMs, resulting in CO_2 and NO. Moreover, partial flow filters have already been explored as a retrofit option for heavy duty vehicles or as a prospective installation in gasoline direct injection (GDI) engine exhaust as a possible solution to future laws imposing particle mass and number limitations [16]. The exhaust passes via a metallic foil (channel) with a ramp or "shovel" etched along its length, causing the exhaust to follow a complex course. The wall between the channels is formed by a porous sintered metal fleece material crushed between metal foils. **Figure 4.4** shows how the shovels in the channels send part of the exhaust into this metallic fleece material, which absorbs some of the soot. Like a flow through a substrate, the residual exhaust leaves the tube at the opposite end. The NO_2 created by the upstream catalyst combusts the soot trapped in the fleece material, renewing the filter, and allowing for fresh soot collection [10]. In this experiment, two varieties of P-DPF were used: platinum (Pt) coating P-DPF and platinum (Pt) coating long P-DPF. Initially, P-DPF was utilized to capture PM, and then O_2 and NO_2 from DOC were employed to oxidize soot to generate CO_2 and NO. Meanwhile, the Pt catalysts on the monolith started catalyzing the oxidation of NO to NO_2. The NO_2 then reacted with the fuel additive-catalyzed soot. As seen in **Figure 4.5(a)**, the considerable rise may be explained by assuming that each NO_x molecule is burned many times. **Figure 4.5(b)** displays a reaction scheme for the proposed soot oxidation process using a containing of platinum and cerium fuel additive [14].

4.2.3.3 After-treatment system combination in this experiment

In this experiment, DOC and P-DPF are used in combination to minimize exhaust emissions and PMs, which are separated into two conditions on B20 to compare with the circumstances without an after-treatment system. Pt-coated P-DPF (Cell density: 200) was used to study the effects of B20 fuel on exhaust and soot emissions. The effects of B20 fuel

on exhaust emissions and soot emissions were investigated using cerium or CeO_2 coated on DOC in conjunction with Pt coated P-DPF (Cell density: 200) and Pt coated long P-DPF (Cell density: 200). **Table 4.4** indicates the after-treatment equipment specifications utilized in this experiment, and **Figure 4.6(a) and (b)** depicts the mechanism of diesel exhaust flow via the CeO_2 coated DOC coupled with Pt coated P-DPF and Pt coated long P-DPF, respectively.

4.3 Calculation Method

4.3.1 Calculation of Fuel Economy and Emissions

Fuel efficiency and emissions were compared to the two NEDC stages known as UDC and EUDC. Also, the total phase will be shown as the average of UDC and EUDC. Carbon balancing is a well-established and widely accepted way of measuring fuel efficiency that requires no changes to engines or fuel lines. Rather than measuring the volume or weight of fuel entering the engine, the products of combustion that depart the engine are measured. To put it another way, the amount of carbon in the exhaust is measured. Equation 1 shows how to calculate fuel economy [17].

Vehicles with compression ignition engines fueled with diesel (B5),

$$FC = \left(\frac{0.116}{D}\right) \cdot [(0.861\,HC) + (0.429\,CO) + (0.273\,CO_2)] \quad \text{Equation 1.}$$

While:

FC = fuel consumption in liters per 100km

D = density of the test fuel

HC = measured emission of hydrocarbon

CO = measured emission of carbon monoxide

CO_2 = measured emission of carbon dioxide

The mass M of each pollutant produced by the vehicle during the test should be calculated by multiplying the volumetric concentration by the volume of the gas in question, adjusting for the following densities under the reference circumstances given above:

In the case of carbon monoxide (CO): d = 1.25 g/l

In the case of hydrocarbons:

For petrol (E5) ($C_1H_{1.89}O_{0.016}$) d = 0.631 g/l

For diesel (B5) ($C_1H_{1.86}O_{0.005}$) d = 0.622 g/l

For LPG ($CH_{2.525}$) d = 0.649 g/l

For NG/biomethane (C_1H_4) d = 0.714 g/l

For ethanol (E85) ($C_1H_{2.74}O_{0.385}$) d = 0.932 g/l

In the case of nitrogen oxides (NO_x): d = 2.05 g/l

The following formula must be used to determine mass emissions of gaseous pollutants as shown in equation 2:

$$M_i = \frac{V_{mix} \cdot Q_i \cdot k_h \cdot C_i \cdot 10^{-6}}{d}$$ Equation 2.

Where:

M_i = mass emission of the pollutant i in grams per kilometer,

V_{mix} = volume of the diluted exhaust gas expressed in liters per test and corrected to standard conditions (273.2 K and 101.33 kPa),

Q_i = density of the pollutant i in grams per liter at normal temperature and pressure (273.2 K and 101.33 kPa),

k_h = humidity correction factor used for the calculation of the mass emissions of oxides of nitrogen. There is no humidity correction for HC and CO,

C_i = concentration of the pollutant i in the diluted exhaust gas expressed in ppm and corrected by the amount of the pollutant i contained in the dilution air,

d = distance corresponding to the operating cycle in kilometers.

4.4 Result and discussion

4.4.1 Fuel Economy and exhaust emissions over the New European Driving Cycle

The controlled emissions are reported in mass values (mg/km) to analyze the effects of employing B20 fuel and catalyst coating on various components, such as partial flow diesel particulate filters (P-DPF), long P-DPF, and diesel oxidation catalysts (DOC) using the New European Driving Cycle (NEDC). Also known as the Motor Vehicle Emissions Group (MVEG) cycle consists of a warm-up phase, four cycles of urban driving (phase 1), one cycle of extra-urban driving (phase 2), and two driving cycles' mean value (total phase), all of which adhere to Euro emission standards.

Figure 4.7(a) depicts the fuel economy of B20 fuel in terms of kilometers per liter (km/l) for phase 1, phase 2, and total phase. The fuel economy fluctuated between 11 km/l in phase one, 16 km/l in phase two, and 14 km/l overall. Given that it used the carbon balancing method to measure the vehicle's fuel economy, a similar evaluation of the CO_2 emissions of B20 fuel data supplied in the unit of milligram per kilometer (mg/km) for all stages was produced, as shown in **Figure 4.7(b)**. Emissions of CO_2 were in the 226-240 g/km (226,000-240,000 mg/km) range for phase 1, 154-166 g/km (154,000 - 166,000 mg/km) range for phase 2, and 181-193 g/km (181,000-193,000 mg/km) range for the total phase. CO_2 emissions are lower in phase 2 than in phase 1 due to less time of EUDC compared to UDC (cycle time in phase 1 and phase 2 are 780 s. and 400 s., respectively) and a reduction in the amount of fuel fed into the combustion chamber due to lower cycle time. Despite this, installing an after-treatment system (DOC, P-DPF, or Long P-DPF) did not appear to have a substantial influence on either fuel economy or CO_2 emissions.

Figure 4.7(c) and (d) depicts the total hydrocarbon (THC) and carbon monoxide (CO) emissions of B20 fuel in mg/km for phase 1, phase 2, and entire phase. Because of the incomplete combustion under low load settings, THC and CO emissions from phase 1 were found to be substantially higher than those from phase 2. In contrary, THC and CO emissions from phase 2 have higher load circumstances that result in higher vehicle speed and higher exhaust temperatures, which can contribute to more complete combustion. THC emissions were decreased by the DOC and P-DPF up to 58% and by the long P-DPF up to 64% following

the installation of the after-treatment system. Whereas employing Cerium dioxide catalyst coating on DOC pairings with platinum coating P-DPF and platinum coating long P-DPF can lower CO emissions by up to 81% and 89%, respectively.

Figure 4.7(e) displays the Nitrogen Oxides (NO_x) emissions of B20 fuel in mg/km for phase 1, phase 2, and whole phase. The maximum concentration of NO_x emissions was found in regions with low speed (10.0-30.0 km/h) and quick acceleration (1.0-2.0 m/s^2). As the acceleration rate increased from the comparably slow deceleration rate (0 m/s^2), the NO_x production increased [19]. Therefore, NO_x emissions from phase 1 were found to be substantially greater than those from phase 2. Because of the mechanism of P-DPF, which was mentioned in the **4.2.3.2** section, NO_x emissions increased while using DOC, P-DPF, and Long P-DPF in contrast to the fuel scenario without the after-treatment system. Nonetheless, more research on the effect of catalyst coating on NO_x emissions is required.

Particulate matter (PM) emissions are worrisome for a variety of reasons, including health, environmental, governmental, and national problems. PM, often known as smoke, is composed of ash, water, a trace of metallic compounds, carbon soot particles, and volatile organic compounds [20]. As seen in **Figure 4.7(f)**, PM is measured in milligrams per kilometer (mg/km). PM emissions ranged from 13.76 to 41.65 mg/km in phase 1 and 7.62 to 26.48 mg/km in phase 2. According to the NEDC, PM levels are greater in phase 1 due to low engine speed, which results in incomplete combustion. Finally, after installing an after-treatment system, the combination of Ceria catalyst coated DOC and Platinum coated P-DPF reduced PM up to 59% and 62% in phases 1 and 2, respectively. In phases 1 and 2, platinum coated on Long P-DPF can lower PM by up to 65% and 69%, respectively. **Figure 4.7(g)** shows the average particulate number (PN), which after the installation of after-treatment system PN are reduced by around 42% with DOC and P-DPF and reduced up to 45% with Long P-DPF.

4.4.2 Exhaust emissions evolve throughout time

THC, NO_X, CO, CO_2, and PN emissions real-time measurement continuous data of B20 fuel, with and without after-treatment systems of the testing vehicle operated by utilizing the NEDC, provided the unit in part per million (PPM), were displayed in **Figures 4.8(a) to (e)** in accordance with their corresponding emissions levels. THC emission rose with vehicle

acceleration and decreased with vehicle deceleration. NO_X emissions were quite low during the deceleration period but rose as acceleration increased. This was due mostly to the acceleration-induced rapid increase in fuel injection mass, which enriched the fuel-air mixture inside the cylinder and increased the combustion temperature [19]. Furthermore, during the acceleration phase, the engine control unit (ECU) closes the exhaust gas recirculation (EGR) to allow more oxygen into the intake side, resulting in an increase in NO_X. In contrast, NO_X reduced during vehicle slowing to maintain constant speed because the EGR valve was opened. CO and CO_2 emissions fell throughout the deceleration phase and rose as acceleration increased. At high speeds, the rate of CO and CO_2 emissions rose fast because the car engine was in a rich combustible state and required more fuel to generate the proper amount of power. PN is higher at the beginning because the vehicle ran at idle speed for the warm-up period before the recording and emits higher when pushing the acceleration until a steady paddle and lower with deceleration.

After the installation of after-treatment equipment, THC, NO_x, CO, CO_2, and PN emissions exhibit the same pattern as before the installation of after-treatment equipment. PN is lower up to 45% when installed the after-treatment system. THC and CO emissions were reduced as a result of the diesel oxidation catalyst (DOC) mechanism, which transformed CO and THC into CO_2 and H_2O (water), respectively. However, NO_X levels increased somewhat due to the DOC process, which not only transformed CO and THC into CO_2 and H_2O (water), but also changed Nitric Oxide (NO) to Nitrogen Dioxide (NO_2). Nonetheless, CO_2 emissions increase as a result of the partial-flow diesel particulate filter (P-DPF) mechanism, which traps particulate matter (PMs) and uses oxygen (O_2) and NO_2 to oxidize soot in the PMs to generate CO_2.

4.4.3 The effect of an after-treatment system on diesel particulate matter

Images of paper filters taken at 10,000-magnifications using scanning electron microscopy (SEM, FE-SEM SU5000) to investigate the influence of an after-treatment equipment on the microstructure of particulate matter collected on the paper filter serve as examples of the findings. SEM images of PMs obtained from B20, B20 with Ceria coated DOC and platinum coated P-DPF, and B20 with long P-DPF are shown in Figures **4.9(a) to (c)**,

respectively. Soot aggregation decreased dramatically after the installation of an after-treatment system, and it was discovered that under the condition of Long P-DPF, soot fell the most because the space for soot to trap is greater.

4.5 Conclusion

This study aimed to evaluate the impact of ceria and platinum coated diesel oxidation catalysts (DOCs) and partial-flow diesel particulate filters (P-DPFs) on the emissions of a 2.5-liter light-duty diesel engine pick-up truck under the New European Driving Cycle (NEDC). The vehicle was tested with and without an exhaust after-treatment system, using B20. The focus was on the influence of the after-treatment system on total hydrocarbons (THC), carbon monoxide (CO), particulate matter (PMs), and carbon dioxide (CO_2) emissions. The results of this study demonstrate that the emission criteria for THC, CO, PN, and PM were reduced, while nitrogen oxides (NO_x) were increased after installing after-treatment systems. The utilization of DOCs and P-DPFs led to significant reductions in THC levels, with reductions of up to 58% observed. Furthermore, when combining the ceria DOC with platinum P-DPF and the long P-DPF, CO emissions were reduced by 81% and 89%, respectively. Nevertheless, the installation of DOC and P-DPF reduced PN by up to 42% and with long P-DPF reduced PN up to 45%.

Analyzing PM data under three different settings, it was observed that the use of ceria DOC and platinum P-DPF resulted in PM reductions of up to 62% and the long P-DPF PM emissions were reduced by 69% as can clearly see from Scanning Electron Microscopy (SEM) images that soot aggregation dramatically decreases after installation of after-treatment equipment. However, the installation of the after-treatment system did not have a noticeable impact on carbon dioxide (CO_2) emissions. Considering the limited time constraints of the experiment for each scenario, it is plausible to infer from the CO_2 emissions data that the passive regeneration of PM within the filter occurs slowly or may not occur at all.

However, to further investigate the passive regeneration process within the P-DPF, future studies should focus on real-time monitoring of exhaust temperature, CO_2 emissions, and PM emissions. This will help determine whether the passive regeneration of PM is taking place within the P-DPF and provide deeper insights into the performance of the after-treatment system.

Tables

Table 4.1 Parameters of B20 biodiesel.

Parameters (Units)	B20
Carbon (% mass)	82.6
Hydrogen (% mass)	13.4
Oxygen (% mass)	4.0
Low heating value (J/g)	42,400
Cetane Number	54.5
Flash Point (°C)	66
Density at 15 °C (g/m^3)	827,000
Viscosity at 40 °C (mm^2/s)	3.1

Table 4.2 Calorific value of tested fuels.

TESTED FUELS	CALORIFIC VALUES (KJ/KG)
B20	44,950

Table 4.3 Vehicle Specification.

VEHICLE	TOYOTA HILUX TIGER
ENGINE TYPE	2KD-FTV (Diesel)
MODEL OF VEHICLE	TOYOTA D4D
MASS OF VEHICLE	1590 kg.
NUMBER OF CYLINDERS & ARRANGEMENT	4 cylinders, In-line
MECHANISM OF THE VALVE	16 Valve DOHC
BORE X STROKE	92.0 mm x 93.8 mm
DISPLACEMENT VOLUME	2500 cc
COMPRESSION RATIO	18.5 : 1
FUEL SYSTEM	Common rail type Direct Injection
MAXIMUM POWER (KW AT RPM)	75 kW at 3600 rpm
MAXIMUM TORQUE (NM AT RPM)	260 Nm at 1600 – 2400 rpm

Table 4.4 After-treatment equipment that used in this experiment specifications.

Equipment	DOC	P-DPF	Long P-DPF
Element	CeO_2 (Cerium Dioxide)	Pt (Platinum)	Pt (Platinum)
Cell Density	300	200	200
Length (mm)	100	150	200
Diameter (mm)	144	144	144

Figures

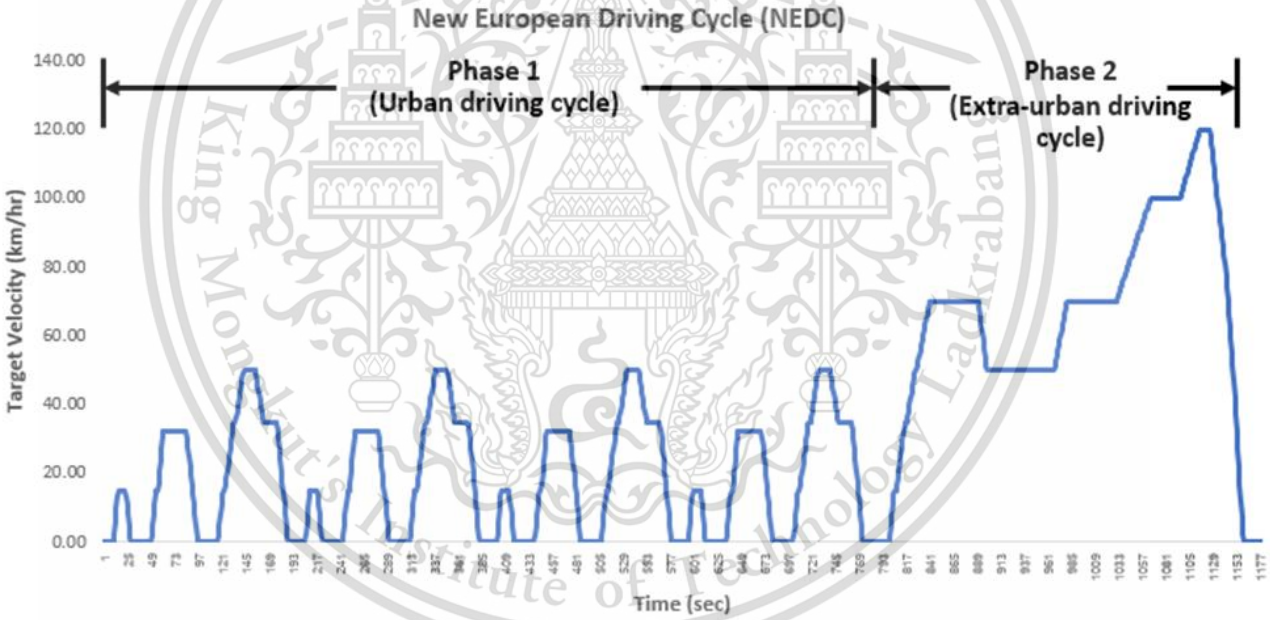

Figure 4.1 MVEG Driving Cycles

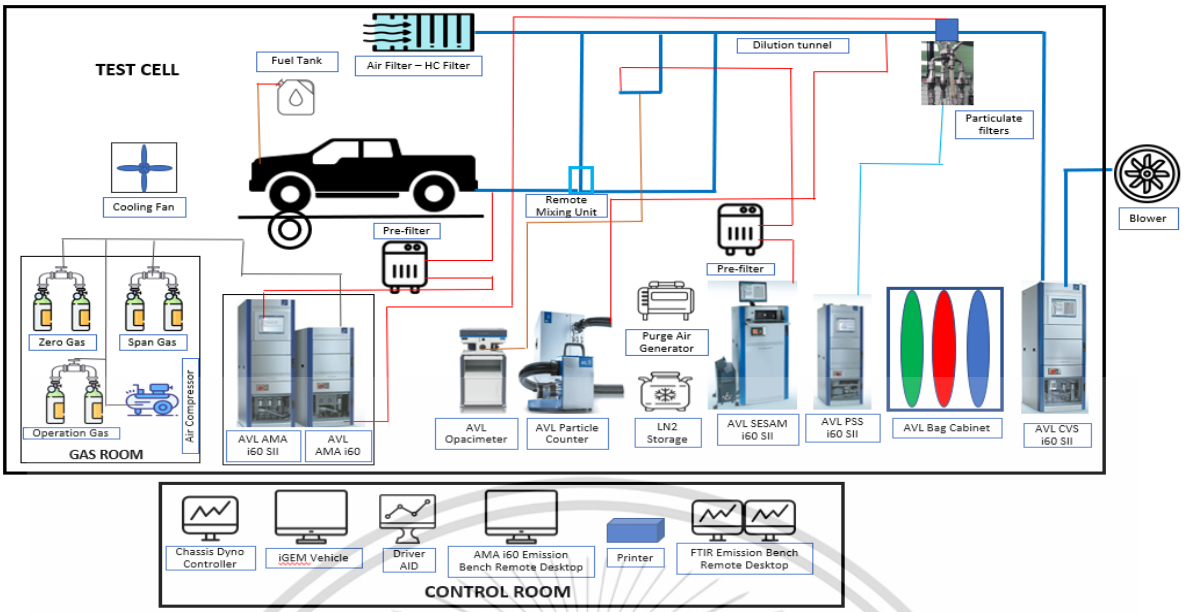

Figure 4.2 AEL Light duty vehicle setup

(a)

(b)

Figure 4.3 Actual Test Diagram at Automotive Emissions Laboratory (a) Test Cell Room and (b) Control Room

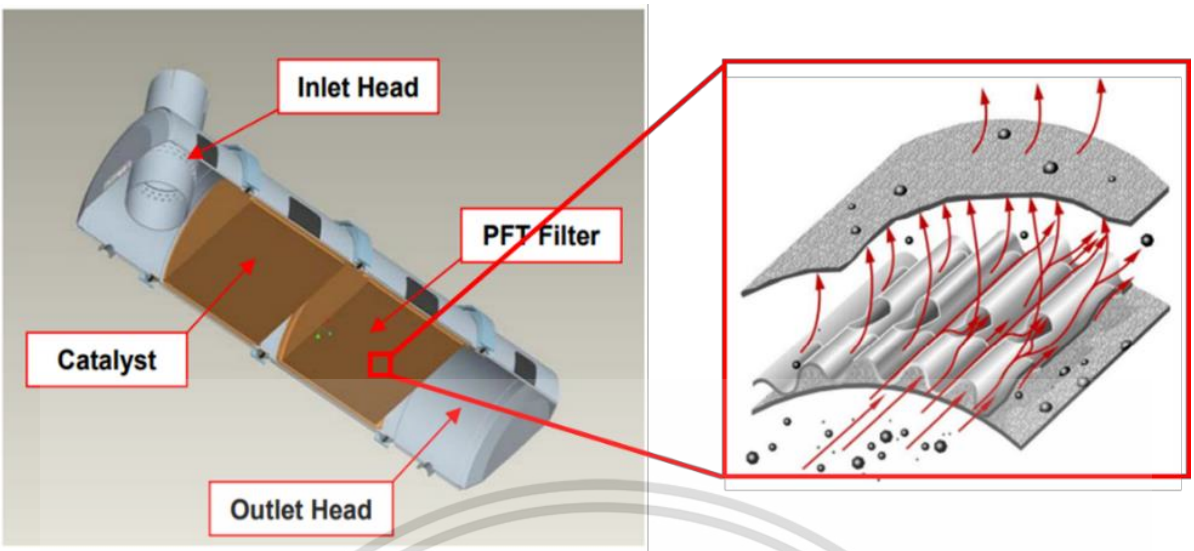

Figure 4.4 "Shovels" forcing soot into the sintered metal fleece material [10]

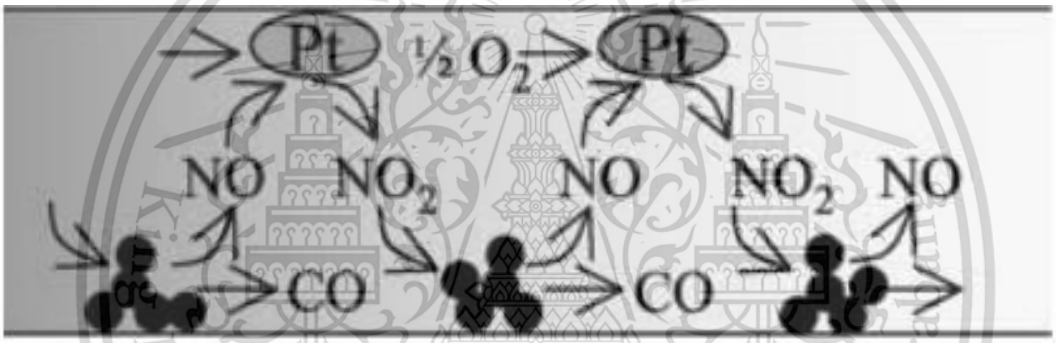

Figure 4.5(a) Illustration of a soot-oxidation mechanism in which one NOx molecule subsequently reacts with three consecutive soot particles [14].

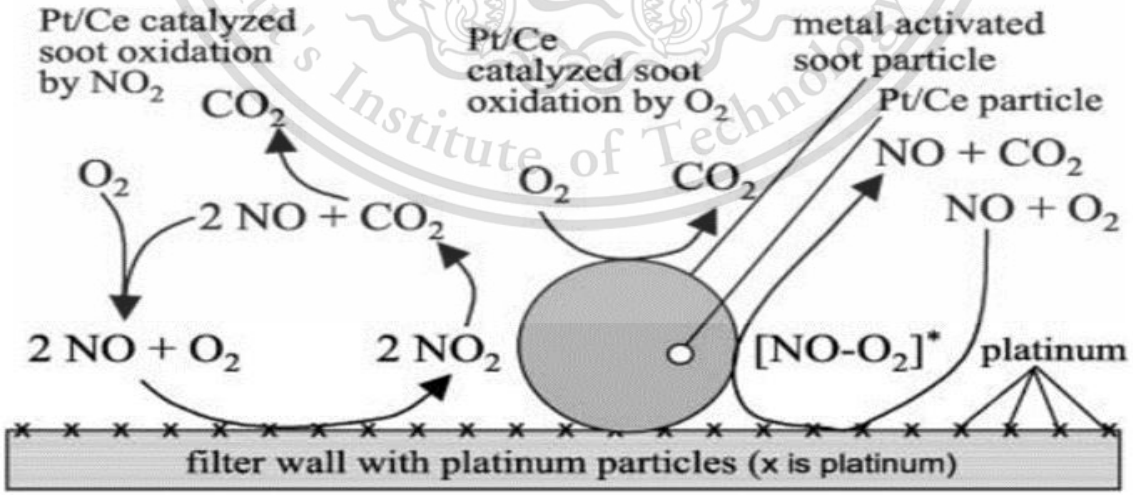

Figure 4.5(b) Mechanism of the oxidation of soot with NO_x and O_2 catalyzed by platinum and cerium fuel additives [14].

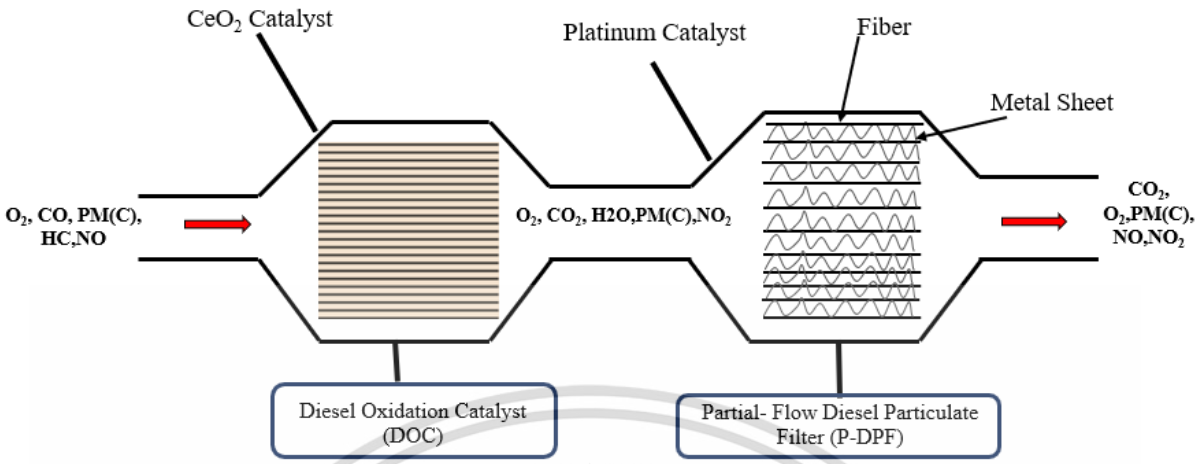

Figure 4.6(a) Exhaust gas flow through the conditions of Ce coated DOC and Pt coated P-DPF

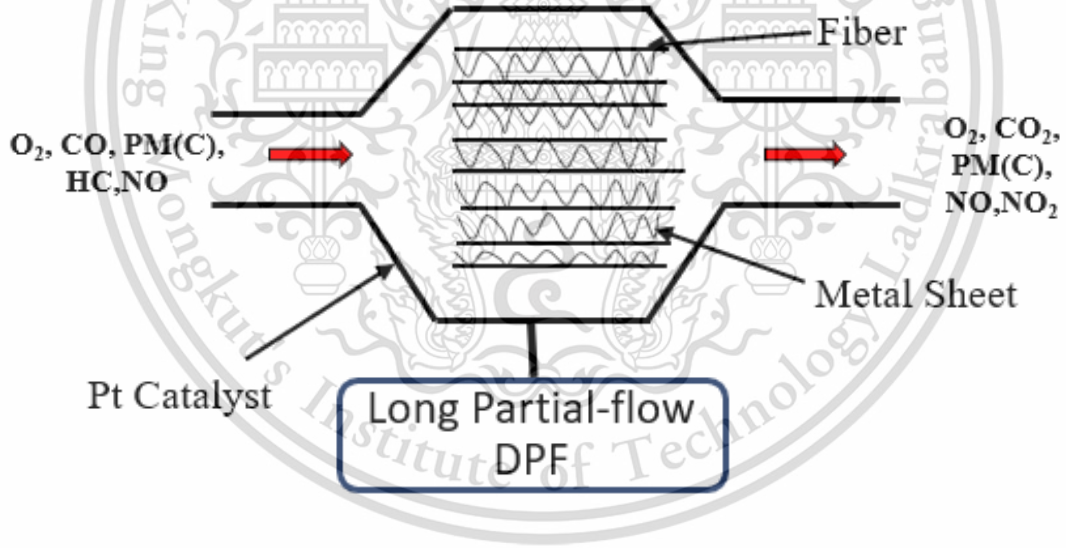

Figure 4.6(b) Exhaust gas flow through the conditions of Pt coated long P-DPF

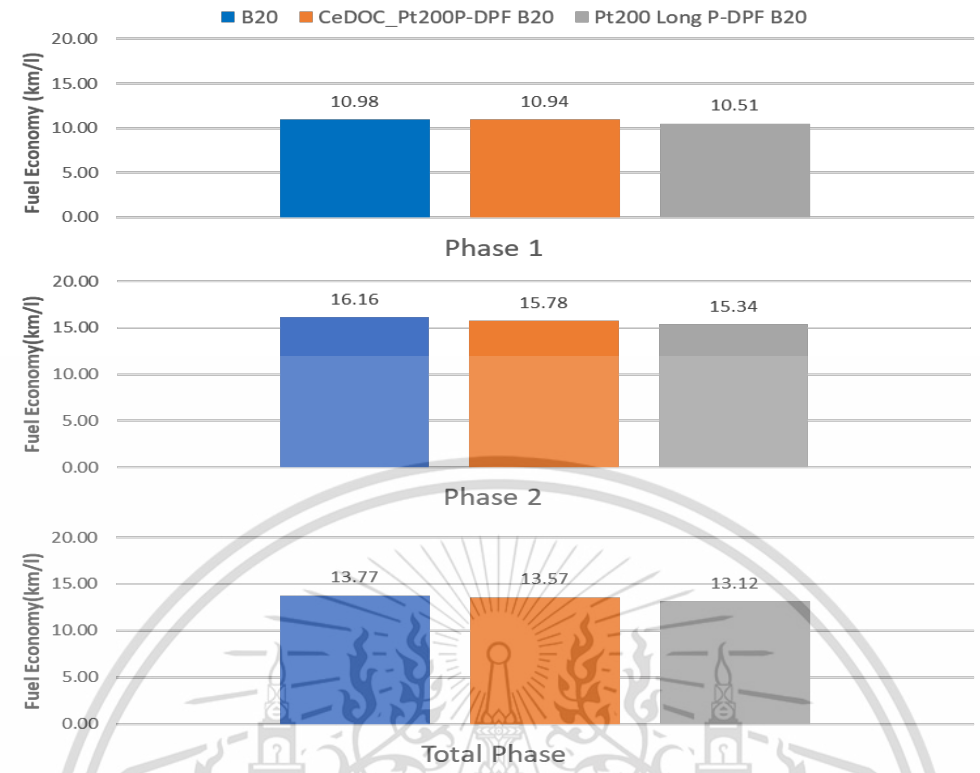

Figure 4.7(a) Fuel Economy results of phase 1, phase 2, and total phase

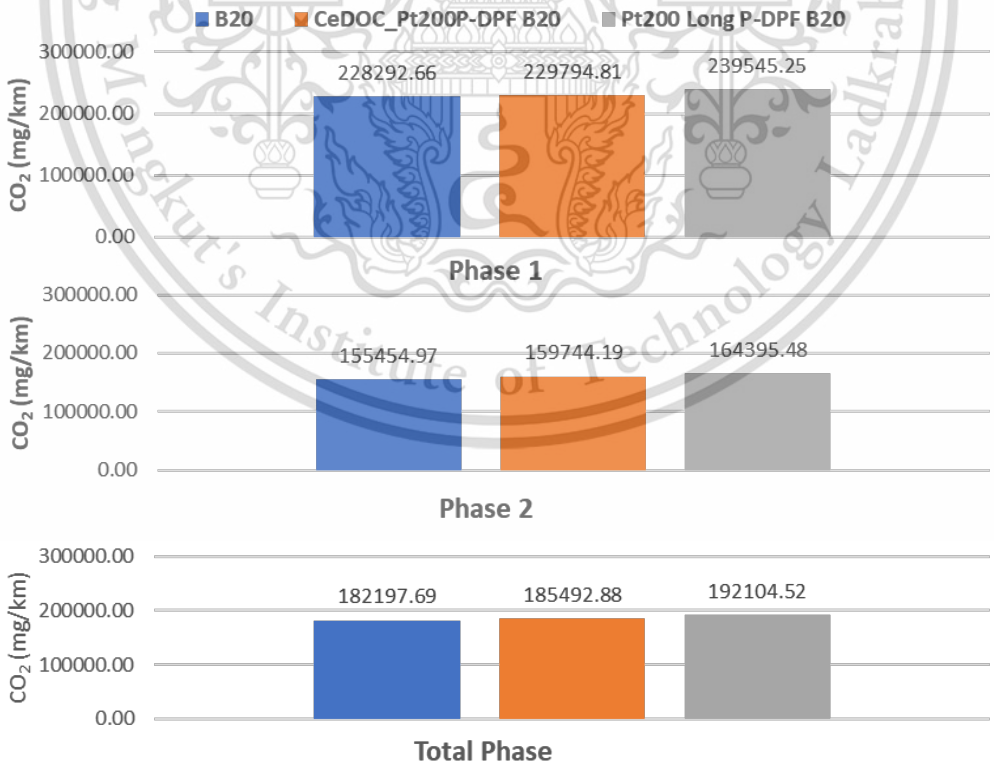

Figure 4.7(b) CO_2 emissions results of phase 1, phase 2, and total phase

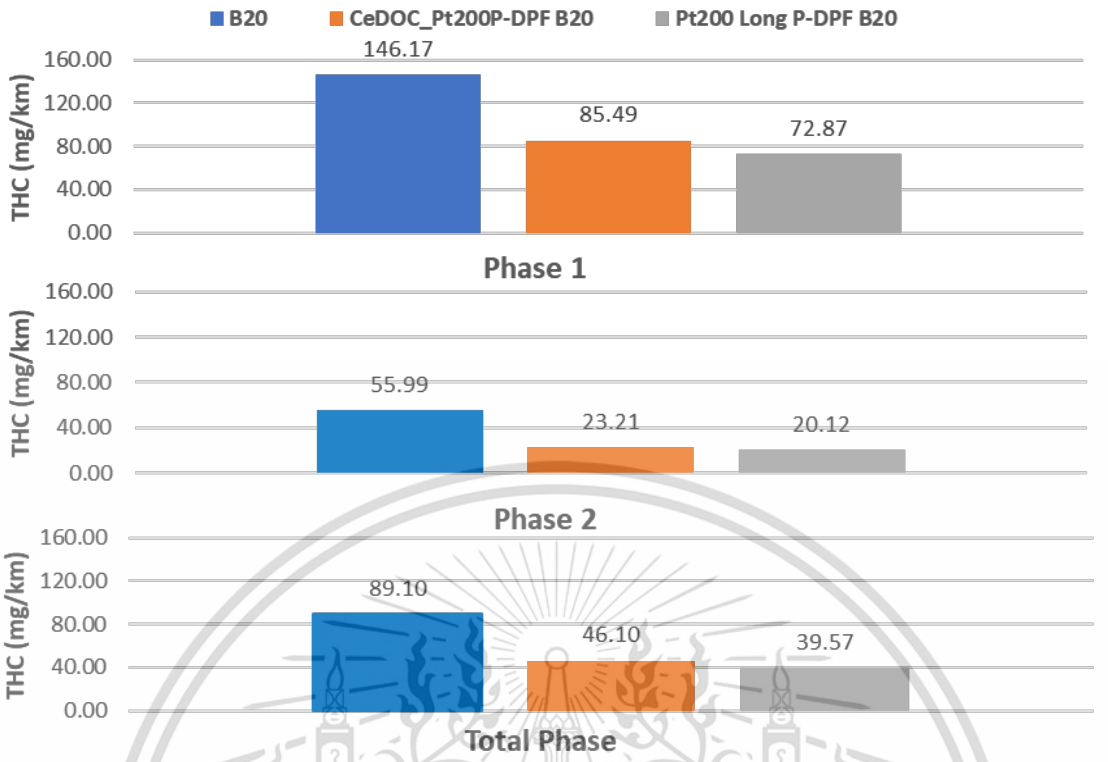

Figure 4.7(c) THC emissions results of phase 1, phase 2, and total phase

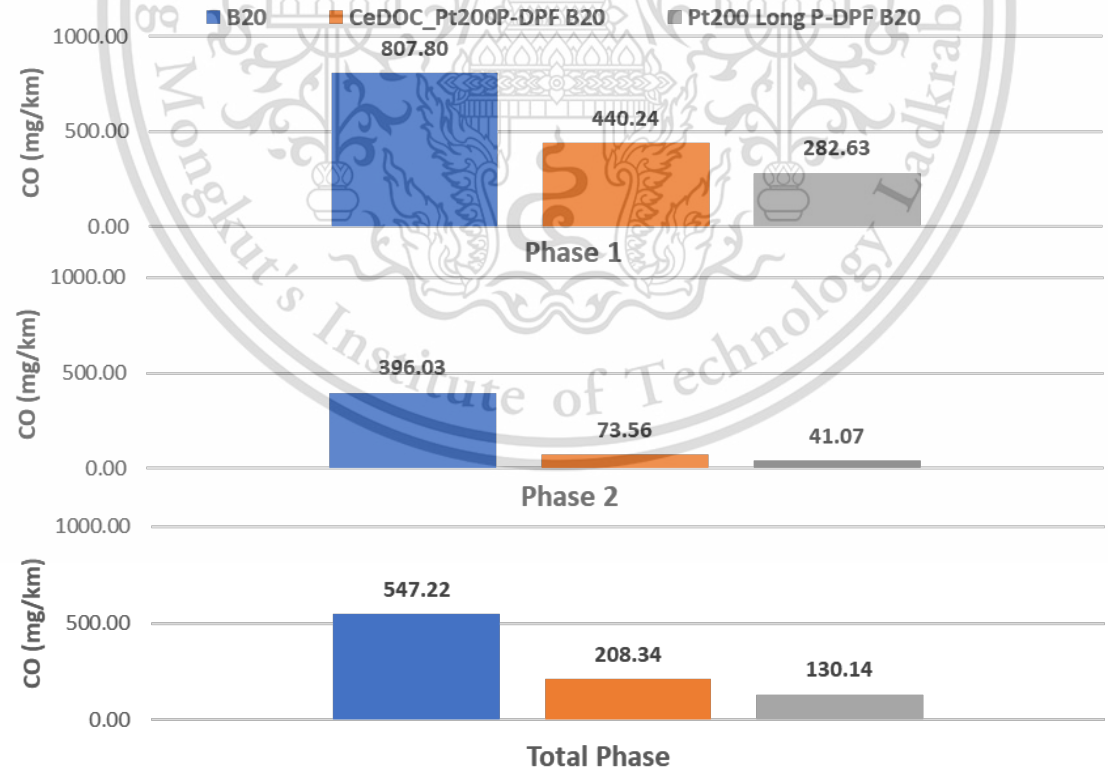

Figure 4.7(d) CO emissions results of phase 1, phase 2, and total phase

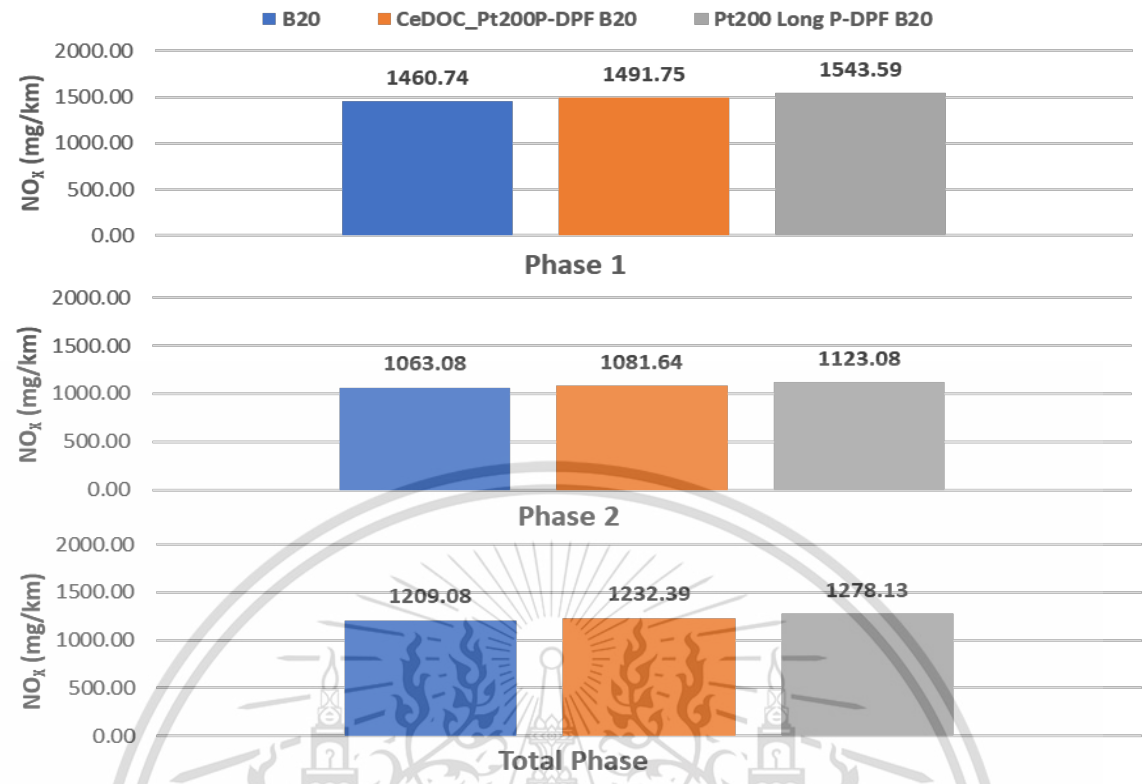

Figure 4.7(e) NO_X emissions results of phase 1, phase 2, and total phase

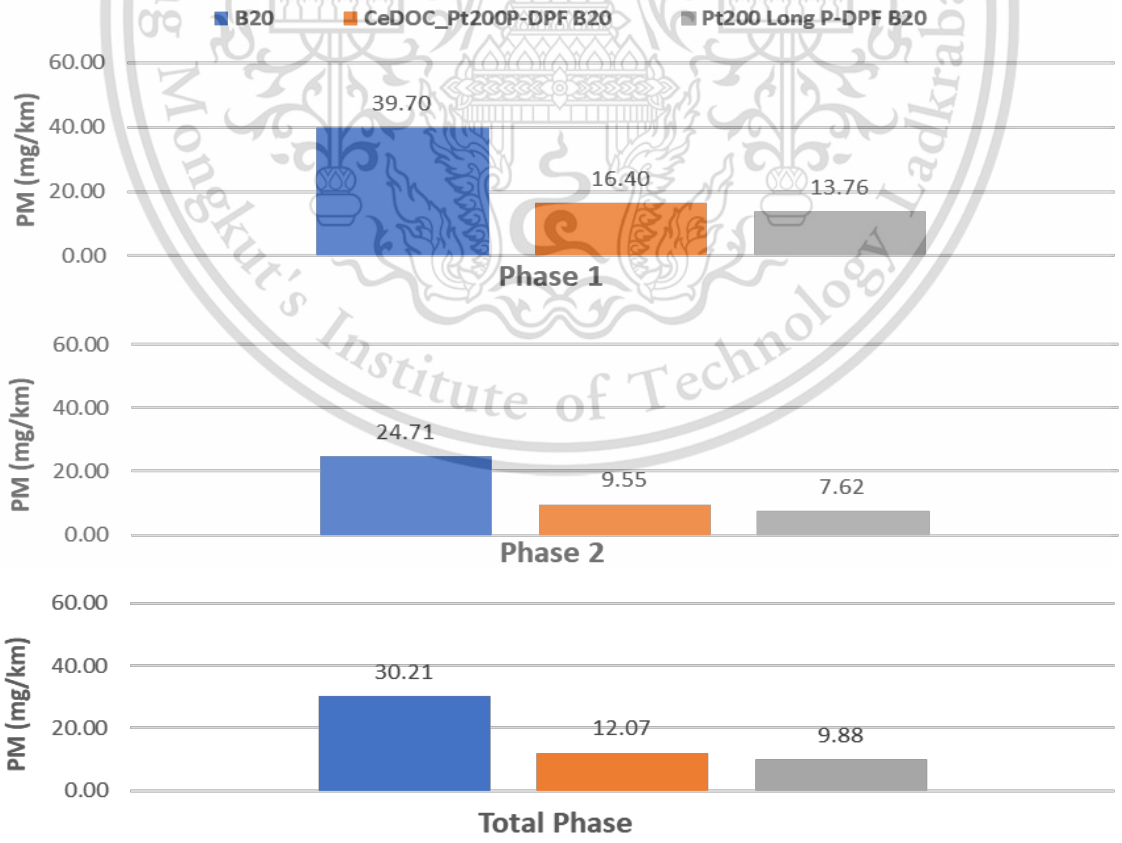

Figure 4.7(f) PM emissions results of phase 1, phase 2, and total phase

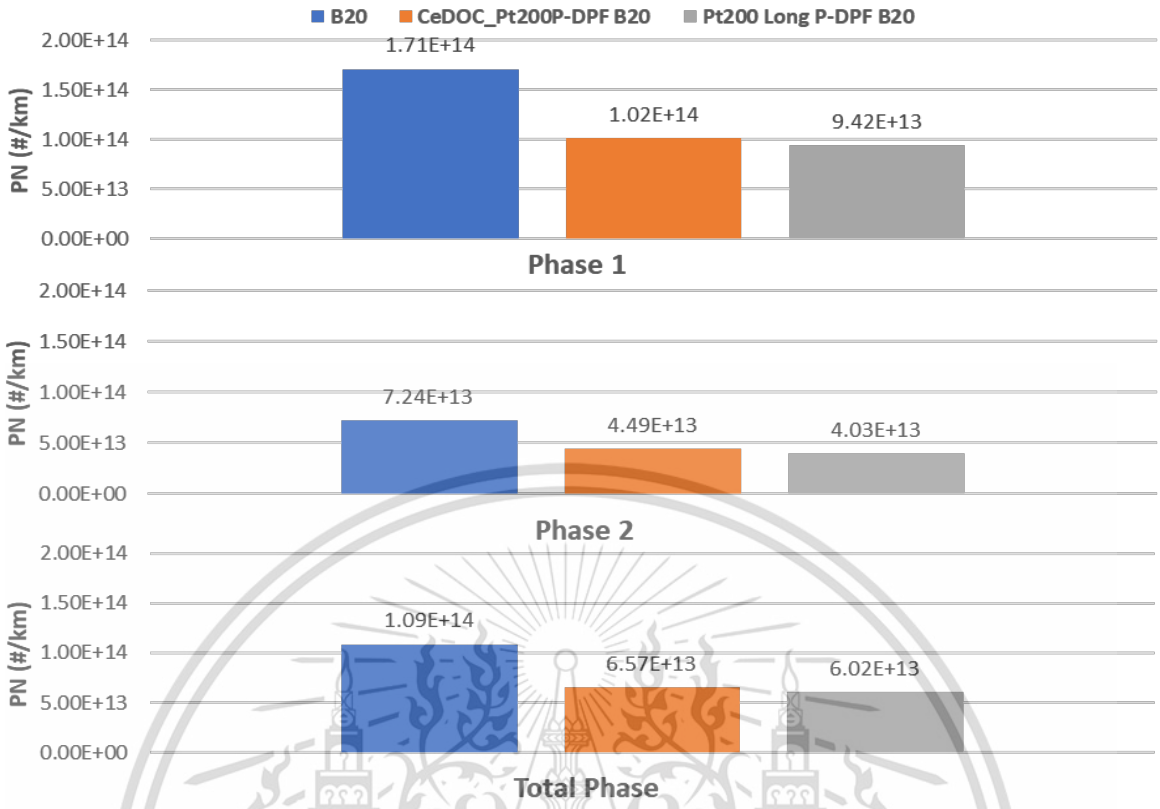

Figure 4.7(g) PN emissions results of phase 1, phase 2, and total phase

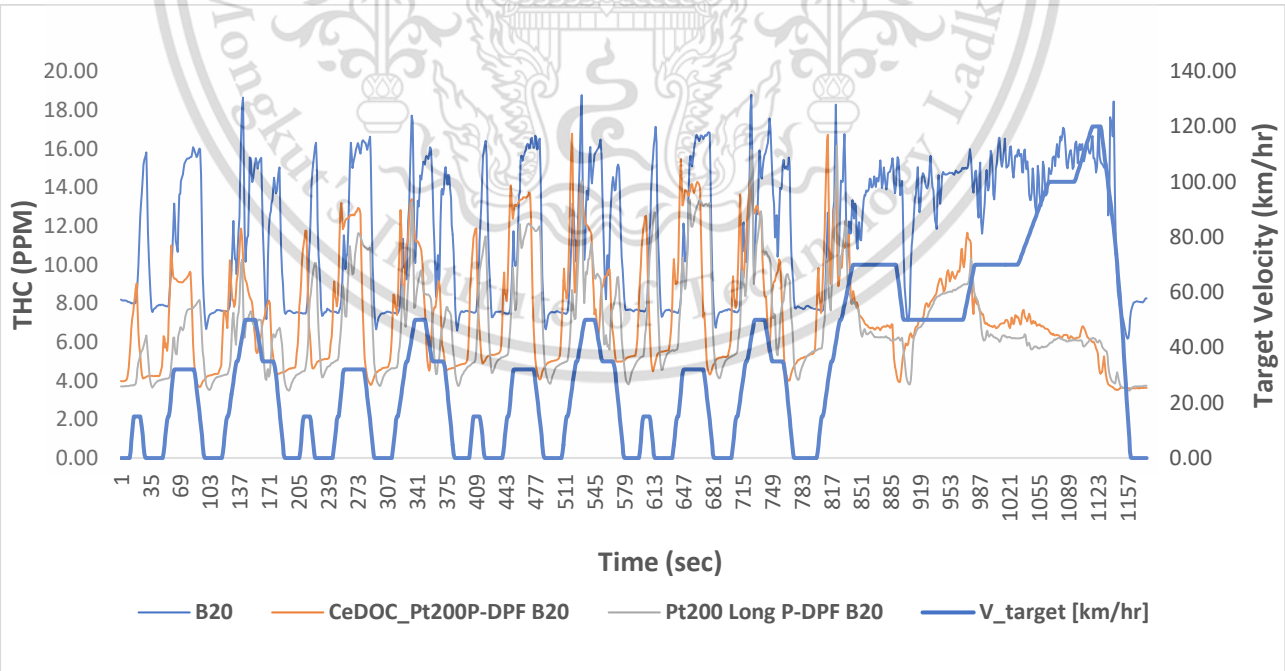

Figure 4.8(a) THC emissions real-time measurement

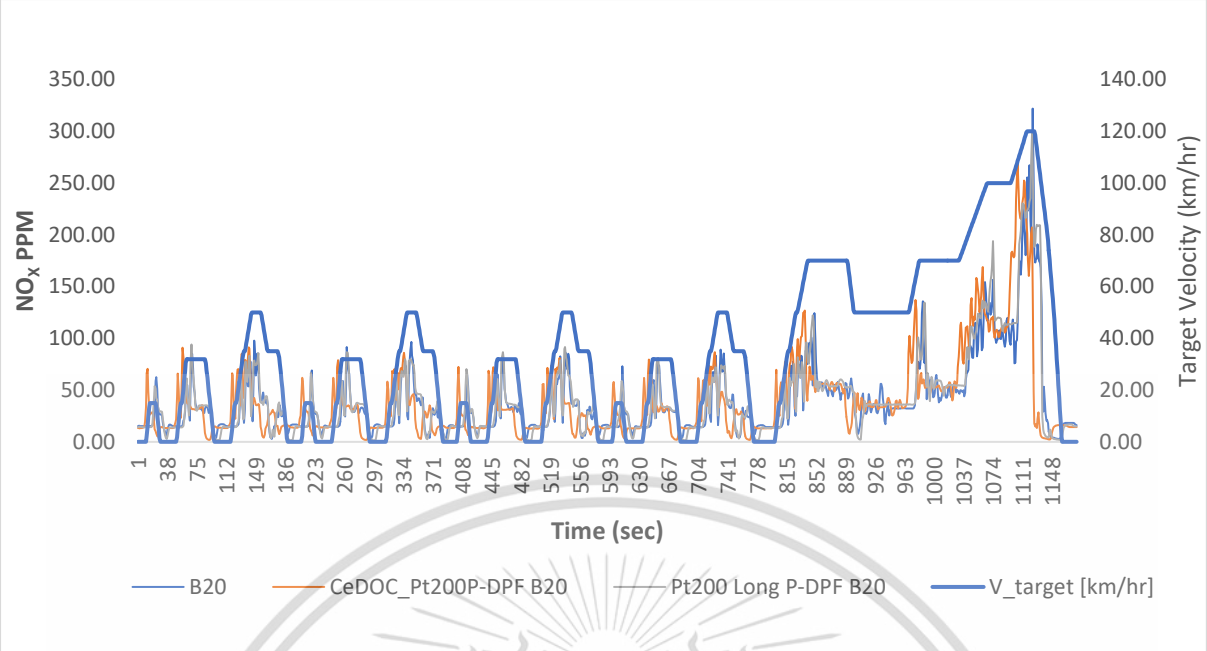

Figure 4.8(b) NO_X emissions real-time measurement

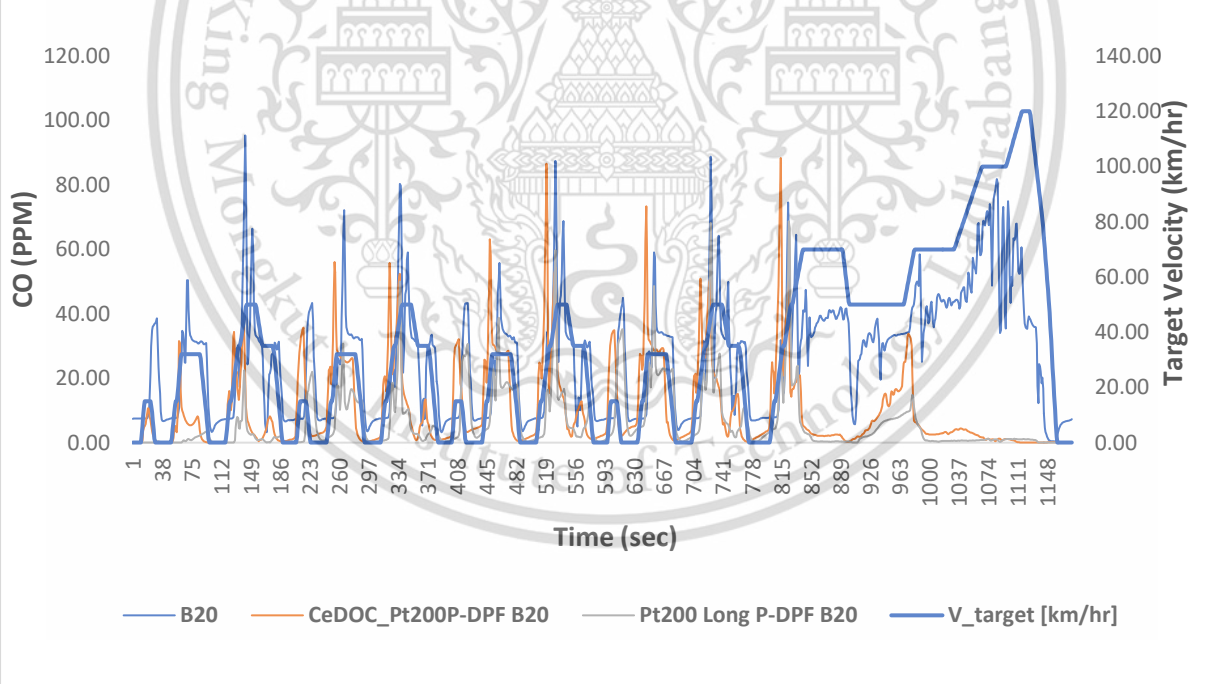

Figure 4.8(c) CO emissions real-time measurement

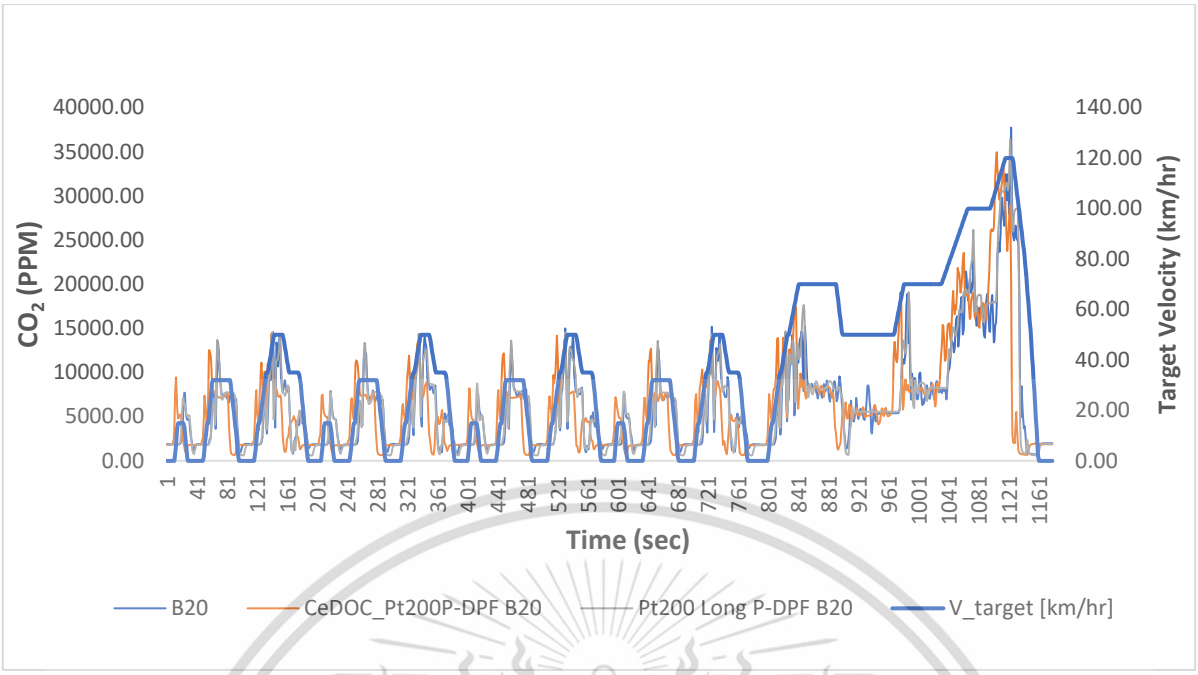

Figure 4.8(d) CO_2 emissions real-time measurement

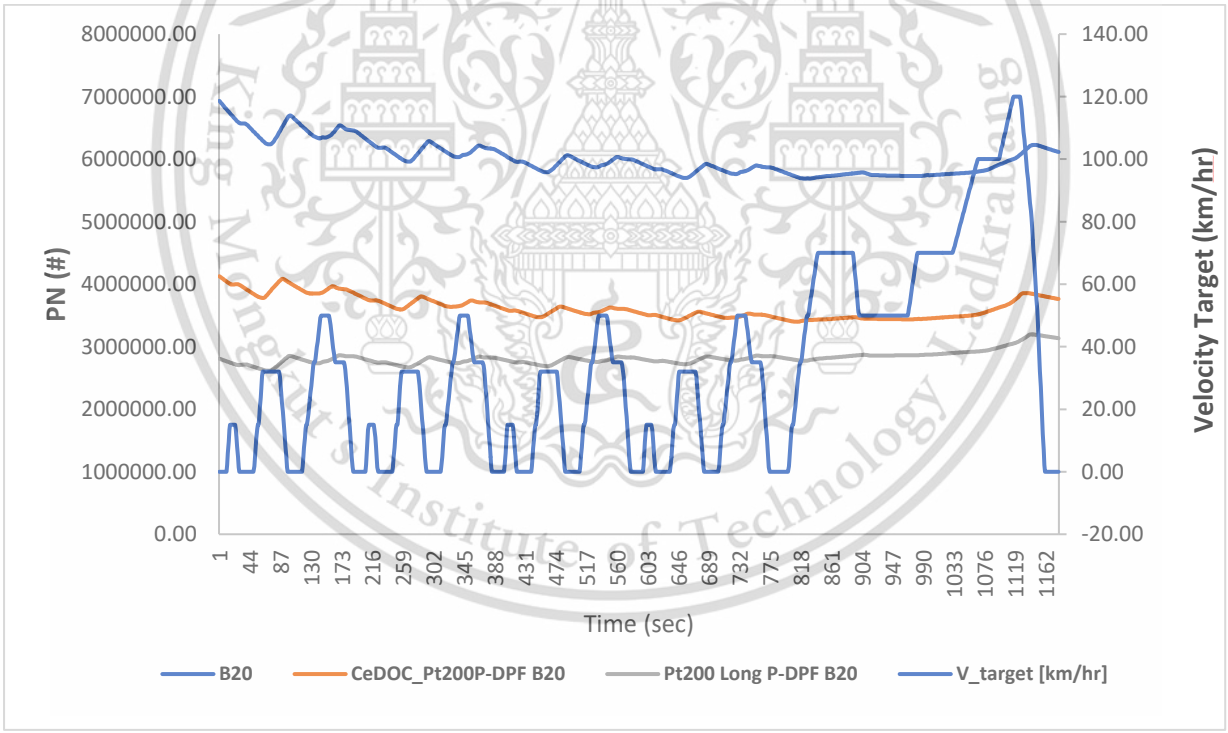

Figure 4.8(e) PN emissions real-time measurement

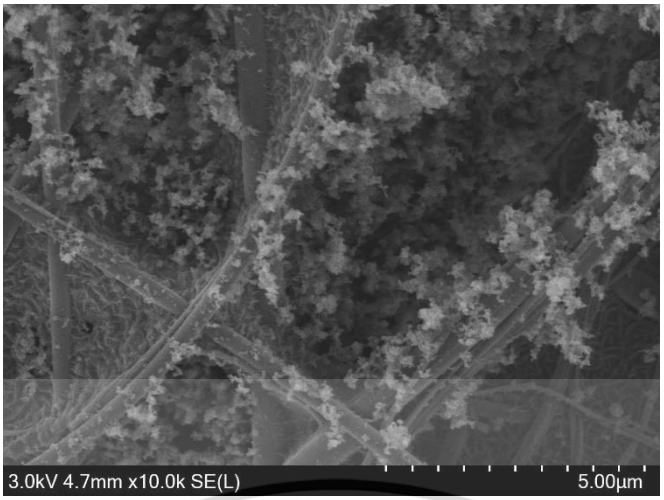

Figure 4.9(a) SEM images of B20 PM without after-treatment equipment

Figure 4.9(b) SEM images of B20 PM with DOC and P-DPF

Figure 4.9(c) SEM images of B20 PM with Long P-DPF

References

[1] Nakajima T., Kitano K., and Mogi K., *Effects of Next-Generation Bio Diesel Fuel on the Engine Performance*, 2015, SAE Technical Paper 2015-01-1928

[2] Tamilselvan P., Nallusamy N., and Rajkumar S., *A comprehensive review on performance, combustion and emission characteristics of biodiesel fuelled diesel engines*, Renew. Sustain. Energy Rev. 79, 1134–1159 (2017).

[3] Mohd Noor C.W., Noor M.M., and Mamat R*., Biodiesel as alternative fuel for marine diesel engine applications: A review*, Renew. Sustain. Energy Rev. 94, 127–142 (2018).

[4] Agarwal A.K., Shrivastava A., and Prasad R.K., *Evaluation of toxic potential of particulates emitted from Jatropha biodiesel fuelled engine.* Renew. Energy 2016, 99, 564–572.

[5] Yang, K., Fox, J.T. & Hunsicker, R. *Characterizing Diesel Particulate Filter Failure During Commercial Fleet Use due to Pinholes, Melting, Cracking, and Fouling*. Emiss. Control Sci. Technol. 2, 145–155 (2016).

[6] Prasad R. and Bella V.R., (2010). *A Review on Diesel Soot Emission, its Effect and Control*. Bulletin of Chemical Reaction Engineering & Catalysis. 5. 10.9767/bcrec.5.2.794.69-86.

[7] Verma P., et., al., *An Overview of the Influence of Biodiesel, Alcohols, and Various Oxygenated Additives on the Particulate Matter Emissions from Diesel Engines*, Energies 2019, 12, 1987, doi:10.3390/en12101987

[8] Ayodhya A. S. and Narayanappa K. G., *An overview of after-treatment systems for diesel engines*, Environmental Science and Pollution Research (2018) 25:35034–35047

[9] Kabir M. N., Alginahi Y., and Islam K., *SIMULATION OF OXIDATION CATALYST CONVERTER FOR AFTER-TREATMENT IN DIESEL ENGINES*, International Journal of Automotive Technology, Vol. 16, No. 2, pp. 193–199 (2015)

[10] Jacobs T., et., al., *Development of Partial Filter Technology for HDD Retrofit*, SAE International (SAE World Congress Detroit), 2006.

[11] Marotta A., Pavlovic J., Ciuffo B., Serra S., and Fontaras G., *Gaseous Emissions from Light-Duty Vehicles: Moving from NEDC to the New WLTP Test Procedure*, Environ. Sci. Technol. 2015, 49, 8315−8322

[12] *Regulation No 83 of the Economic Commission for Europe of the United Nations (UN/ECE) – Uniform provisions concerning the approval of vehicles with regard to the emission of pollutants according to engine fuel requirements*, Official Journal of the European Union, 2006

[13] Wai P., et., al., *Experimental investigation of the influence of ethanol and biodiesel on common rail direct injection diesel Engine's combustion and emission characteristics*, Case Studies in Thermal Engineering 39 (2022) 102430

[14] Barry A. A. L. van Setten, Michiel Makkee & Jacob A. Moulijn, 2001, *Science and technology of catalytic diesel particulate filters*, Catalysis Reviews: Science and Engineering, 43:4, 489-564, DOI: 10.1081/CR-120001810

[15] Hansen T. K., et., al., *The Effect of Pt Particle Size on the Oxidation of CO, C3H6, and NO Over Pt/Al2O3 for Diesel Exhaust Aftertreatment*, Top Catal (2017) 60:1333–1344, DOI 10.1007/s11244-017-0818-9

[16] Lefort I., Herreros J., and Tsolakis A., *The Use of a Partial Flow Filter to Assist the Diesel Particulate Filter and Reduce Active Regeneration Events*, SAE Int. J. Engines 7(4):2014, doi:10.4271/2014-01-2806.

[17] *Regulation No 83 of the Economic Commission for Europe of the United Nations (UN/ECE) – Uniform provisions concerning the approval of vehicles with regard to the emission of pollutants according to engine fuel requirements*, Official Journal of the European Union, 2006

[18] Pinzi S., Rounce P., Herreros J.M., Tsolakis A., and Dorado M.P., *The effect of biodiesel fatty acid composition on combustion and diesel engine exhaust emissions*, Fuel, 104, 170–182 (2013).

[19] Hanzhengnan Y., Megliang L., Jingyuan L., Liu Y., He L., and Kunqi M., *Real-road NOx emission and fuel characteristics of China IV public transit busses*, Energy, Procedia ,158, (2019) 4623–4628

[20] Rounce P., Tsolakis A., Leung P., and York A.P.E., *A comparison of diesel and biodiesel emissions using dimethyl carbonate as an oxygenated additive.*, Energy Fuels, 2010.

[21] De Serio D., De Oliveira A., and Sodré J. R., *Application of an EGR system in a direct injection diesel engine to reduce NOX emissions*, 2016, J. Phys.: Conf. Ser., 745 032001

CHAPTER 5

SOOT OXIDATION IN PASSIVE REGENERATION PROCESS OF PARTIAL-FLOW DIESEL PARTICULATE FILTER

5.1 Introduction

The increasing number of vehicles powered by diesel has forced the development of sophisticated after-treatment systems to reduce the negative environmental impact of diesel exhaust emissions. The main pollutants released by diesel engines that are harmful to human health are nitrogen oxides (NO_X), hydrocarbons (HCs), carbon monoxide (CO), and particulate matter (PMs), which PM and NO_x in exhaust gas have been mandated to be reduced globally [1]. In this chapter, the focus is on soot oxidation in passive regeneration process by using the partial-flow diesel particulate filter (P-DPF).

Many researchers have used thermogravimetric analysis (TGA) to examine the oxidation kinetics of soot's alone under circumstances typical of DPF active and passive regeneration operations [2-4]. Although the soot oxidation by using the P-DPF on real-engine real-vehicle have not been widely discussed. In real-engine real-vehicle, the diesel oxidation catalyst (DOC), usually positioned upstream of the partial-flow diesel particulate filter (P-DPF), has the ability to convert all nitric oxide (NO) present in diesel exhaust gas into nitrogen dioxide (NO_2). This conversion process plays a crucial role in facilitating soot oxidation at lower temperatures. In order to achieve effective soot oxidation, practical strategies often incorporate the use of a soot oxidation catalyst, which relies on the oxidation potential of NO_2 [5].

The mechanisms of NO_2-soot oxidation at low temperatures have received a lot of attention. Increasing the NO_2 concentration increased soot oxidation in the 200-580 °C temperature range. These O_2 and NO_2 impacts were discovered to be considerable and temperature dependent. There are two oxidizing gases present in diesel exhaust emissions that are ideal for soot oxidation: O_2 and NO_2. Both are essential for DPF regeneration. Diesel exhaust emissions include far more O_2 than NO_2, yet NO_2 is far more active than O_2 [6-7]. Furthermore, **Figure 5.1** shows the temperature profile that O_2 and NO_2 start to combust the soot.

The catalyst plays a critical role in lowering the ignition temperature of particulate matter (PM) that has accumulated within the filter. Its presence reduces the oxidation temperature of the PM by approximately 300-400 °C. Specifically, a platinum (Pt)-based catalyst facilitates the conversion of nitric oxide (NO) into nitrogen dioxide (NO_2), thereby initiating the combustion process of the soot that has been collected within the downstream Diesel Particulate Filter (DPF). This catalytic action of Pt enables the effective regeneration of the DPF and the removal of trapped soot particles from the exhaust system [8-9]. Furthermore, the pressure drop profile is another confirmation that soot oxidation occurred inside the particulate filter as shown in **Figure 5.2** [10]. Okawara et. al. found that if the pressure drop was a saturation tendency it can be considered that the trapped soot was oxidized inside the particulate filter by NO_2 [1].

The primary objective of this thesis is to investigate the phenomenon of soot oxidation in the passive regeneration of diesel particulate filters. Specifically, the research aims to analyze the influence of various catalyst coatings, such as cerium dioxide (CeO_2) and platinum (Pt), on the characteristics of soot oxidation. By monitoring exhaust temperatures, pressure drop profiles, and emissions of carbon dioxide (CO_2), oxygen (O_2), and nitric oxides (NO), a comprehensive understanding of the passive regeneration process and its associated effects can be achieved.

5.2 Methodology

5.2.1 Procedures for experiments and vehicle specifications

This study used the same vehicle as previous chapter, a 2.5L 4-cylinder common rail direct injection diesel-engine truck, with a compression ratio of 18.5:1, maximum power of 75 kW at engine speed of 3600 rpm, and maximum torque of 260 Nm at engine speed between 1600 – 2400 rpm as the specification of tested vehicle shown in **Table 5.1**. The vehicle exhaust pipe was installed with an after-treatment equipment with the upstream of cerium dioxide (CeO_2) coated diesel oxidation catalyst (DOC) and followed by platinum (Pt) coated partial-flow diesel particulate filter (P-DPF) to examine that the soot oxidation occurs inside the P-DPF by using B20 fuels. Furthermore, the vehicle was run continuously with constant vehicle speed and constant engine load at 140 Nm. (About 54% of vehicle maximum engine load),

which test was divided into two different vehicle speed consist of 90 kilometers per hour (kph) according to speed limit of open roads and 120 kph according to the speed limit of motorways in Thailand [11].

This experiment focuses on the continuously regeneration trap (passive regeneration system) includes CeO_2 catalyst coated DOC and Pt catalyst coated P-DPF while monitoring the real time data of temperature and pressure drop, and gas emissions includes carbon dioxide (CO_2) emissions, oxygen (O_2) emissions and nitric oxide (NO) emissions were measured randomly.

5.2.2 Experimental Setup

Toyota Hilux Tiger with the after-treatment equipment installation in the exhaust pipe was placed on a chassis dynamometer at two different vehicle speeds (90 and 120 kph) and constant load (140 Nm.) by using B20 fuel. **Figure 5.3** shows the schematic diagram of the experimental setup and **Figure 5.4** depicts the actual setup of vehicle on chassis dynamometer. First, the vehicle was placed on chassis dynamometer, which includes roller and cooling fan that used to cool down the cooling system of the vehicle. Next, to minimize contamination and keep the weight constant during the experiment, the B20 fuel tank was segregated from the main fuel tank. In addition, with an accuracy of 0.001, the AVL exhaust gas analyzer (DITEST GAS 1000) was utilized to detect the real time exhaust emissions (NO, CO_2, and O_2) from the vehicle. The on-board diagnostic (OBD), which is also connected to the engine control unit (ECU), recorded the real time data of the vehicle, including coolant temperature, fuel temperature, engine speed, and vehicle speed to monitor the data to prevent the danger that might happened during the experiment.

This experiment used a combination of CeO_2 coated DOC and Pt coated P-DPF as the specification of after-treatment equipment shown in **Table 5.1**. Thermocouple type K and plastic tube were installed in the position of before entering the DOC and after leaving the P-DPF at the center of the equipment to measure the real time temperature and pressure continuously, as shown in **Figure 5.5**. The temperature and pressure sensors were linked to the Arduino board then converted the data on software in the computer to get the real time

temperature and pressure results, as shown as schematic diagram in **Figure 5.6**. Furthermore, **Figure 5.7** shows the actual position of Arduino board on the vehicle.

5.3 Result and discussion

5.3.1 Temperature and exhaust emissions

5.3.1.1 Temperature VS CO_2 and O_2 emission

The temperature at the position of before entering DOC and after leaving P-DPF are reported in degree Celsius (℃), which T1_C represent the temperature of exhaust gas before entering the DOC and T2_C represent the temperature of exhaust gas after leaving the P-DPF. CO_2, O_2, and NO emissions at the position of before entering DOC and after leaving P-DPF are reported in unit of parts-per million (ppm). Due to the limitations of AVL DITEST 1000, the data emissions result of both CO_2 and O_2 can be measured only one position at a time. Furthermore, during the experiment the engine load has been taken out and keeps the vehicle running at speed constant, while that the AVL also does not record the emissions, to cool down the coolant temperature which lasts about 120 - 240 seconds. The engine speed for 90 kph with/without engine load (140Nm.) were about 2,510 and 2,450 rpm and for conditions at 120 kph were about 3,335 and 3,250 rpm.

Figure 5.8 (a) depicts the temperature and emissions at the condition of vehicle speed at 90 kph and engine load of 140 Nm. The total time of this condition is 2,880 seconds or 48 minutes, which cool down time takes 240 seconds or 4 minutes after the AVL measures the emissions for 240 seconds. Furthermore, there are 6 times of measurement from AVL, the 1,3, 5 is the emission result from before entering the DOC and 2,4,6 are the emissions data after leaving P-DPF. The temperature increases from 400 – 450 ℃ and 220 - 360 ℃ for conditions of before entering DOC and after leaving P-DPF, respectively. During the stop process the temperature at the position of before entering DOC and after leaving P-DPF dramatically drops about 200 ℃ and 85 ℃ due to the engine load that has been taking out and the vehicle speed contains constant. For CO_2 and O_2 emissions, yield in the opposite direction, results are constant during 90 kph and 140 Nm. CO_2 rises and O_2 drops at the position of before entering DOC is due to more fuel injection. For the soot oxidation, CO_2 rises and O_2 drops at the position after leaving P-DPF, with the range of temperature at position of after leaving P-DPF is 220 –

360 °C can lead to nitrogen dioxide (NO_2) passive regeneration approach that the exhaust temperatures must be consistently above 250 °C as shown in equation (1). Because Nitrogen (N_2) is present in high concentrations in diesel exhaust, a hypothetical NO_x reduction to N_2 would be imperceptible under engine conditions and cannot be ruled out, so equation (2) - (5) will represent the possible reaction of NO_x, soot (in form of carbon (C)), and also O_2 [6].

$$NO_2 + C \rightarrow CO_2 + 0.5\ N_2 \quad (1)$$

$$NO_2 + 2\ C \rightarrow 2\ CO + 0.5\ N_2 \quad (2)$$

$$2\ NO + C \rightarrow CO_2 + N_2 \quad (3)$$

$$NO + C \rightarrow CO + 0.5\ N_2 \quad (4)$$

$$NO + 0.5\ O_2 \rightarrow NO_2 \quad (5)$$

Figure 5.8(b) depicts the temperature and emissions at the condition of vehicle speed at 120 kph and engine load of 140 Nm. The total time of this condition is 2,160 seconds or 36 minutes, which the emission data were randomly measured for 120 seconds or 2 minutes each, so in this experiment the emissions at before entering DOC ('before' in the graph) will be measured first and emissions after leaving P-DPF ('after' in the graph) will continue after finish measured the emission at before entering DOC. The stop time (take out the load but keep the vehicle speed constant at 120kph) decreases to 120 seconds or 2 minutes to cool down the coolant temperature and meanwhile trying not to decrease too much temperature of the exhaust gas. After done with the cool down, the engine load will be added back up to 140 Nm for 360 seconds which during that there will not be any emission data record from AVL. The temperature increases from 450 -550 °C and 270 -375 °C at the position of before entering the DOC and after leaving the P-DPF, respectively. During the stop process the temperature before entering DOC and after leaving P-DPF drops about 220 °C and 100 °C due to the engine load that has been taking out to cooldown the coolant temperature for 120 seconds. CO_2 and O_2 emissions yield in the opposite direction, results are constant during 120 kph and 140 Nm. but the concentration of CO_2 in these conditions is higher, O_2 is lower, than 90 kph and 140 Nm. that due to more fuel is injected into the combustion chamber when increasing the vehicle speed. The study reveals that after passing through the P-DPF, there is

an increase in CO_2 levels and a decrease in O_2 levels. This can be attributed to the process of soot oxidation through NO_2 passive regeneration, which is supported by temperature data analysis (T2_C temperatures). The findings align with previous research conducted by M. Singh et al. [4], who concluded that NO_2 acts as an accelerator for edge-site carbon atoms, modifying the combustion behavior of diesel soot. Their research demonstrated that the addition of NO_2 to O_2 significantly enhances the absolute oxidation rate. These results highlight the effectiveness of NO_2 as a catalyst in the P-DPF system, facilitating efficient and accelerated soot oxidation. Moreover, Pt catalyst plays the role of reducing ignition temperature of the particulate matter (PM) deposited in the filter, which the catalyst reduces the oxidation temperature of the PM by around 300-400 °C [8]. Catalyst is there to increase the regeneration efficiency and the temperature at after leaving the P-DPF in 120 kph conditions is higher than 90 kph, so the amount of CO_2 is higher because there is higher soot conversion at higher temperatures [9].

5.3.1.2 Temperature VS NO emission

Figure 5.9(a) and (b) shows the results of NO emission for 90 kph and 120 kph at 140Nm, respectively. NO emission for condition 90 kph at 140Nm were in the range of 560 – 750 ppm and for condition of 120 kph at 140Nm were in the range of 700 – 900 ppm, so higher vehicle speed higher NO emission. Furthermore, NO emission increases consistent with the increase in exhaust temperature (T1_C and T2_C). NO emission at the position before entering the DOC undergo oxidation and reduction when went pass through the after-treatment equipment as clearly seen at **Figure 5.9(b)** that when record the NO data at after leaving after-treatment equipment. The DOC is designed to exclusively oxidize hydrocarbon (HC) and carbon monoxide (CO) emissions, but NO is oxidized into NO_2 in the DOC by the following equation (5). Finally, the results of NO after leaving P-DPF suggest that the soot oxidation is occurring inside the P-DPF due to the decreases in NO after leaving P-DPF, which the chemical reaction in equation (3)-(4) can explain the decrease of NO at temperature ranging from 270 – 375 °C and can clearly see in **Figure 5.9(b)**.

In addition to the unwanted oxidation in the DOC, further oxidation occurred in the P-DPF. Finally, the conversion of NO to NO_2 lets NO drop while NO_2 increases in both DOC and

P-DPF [12]. The higher quantity of NO_2 behind the DOC (before entering the DPF) can aid in the oxidation of soot and PM in the DPF at temperatures ranging from 300 to 400 ℃, which is typical of diesel exhaust. Furthermore, NO_2 in collaboration with O_2 can accelerate oxidation, which is quicker than the total of only NO_2 and only O_2 oxidation rates [13-15]. The oxidation reactions by NO_2 in collaboration with O_2 is shown in equation (6).

$$C + 0.5\ O_2 + NO_2 \rightarrow NO + CO_2 \qquad (6)$$

5.3.2 Pressure VS Temperature

The pressure drop was measured in kilo Pascal (kPa) different in between before entering DOC and after leaving P-DPF as shown in figure 5.5. The pressure drop was unstable due to the vibration of the vehicle that run on the chassis dynamometer. The minimum and maximum pressure drop is 5.98 kPa and 1.31 kPa for 90 kph and 140 Nm., 8.15 kPa and 4.08 kPa for 120 kph and 140Nm. **Figure 5.10(a) and (b)**, shows the real-time data between pressure vs temperature. The pressure at the condition of 120 kph and 140 Nm is higher than 90 kph and 140 Nm due to higher vehicle speed. Due to the vibration of the vehicle while doing the actual run-on chassis dynamometer the pressure data is not easy to see the trend. The pressure drops correlate with the accumulation of soot within the P-DPF [16]. An elevated pressure drop indicates a higher level of soot trapped in the P-DPF, whereas a decrease in pressure drop suggests the possibility of soot oxidation taking place within the P-DPF. Additionally, the average pressure drop ranged from 4.0 to 7.2 kPa. This led to increased friction loss and exhaust temperature, but it did not significantly impact on vehicle thermal efficiency.

Furthermore, **Table 5.2 and 5.3** will represent the average result of temperatures before and after leaving after-treatment T_1 and T_2, pressure drop, CO_2 emissions, O_2 emissions, and NO emissions for the conditions of 90 kph and 120 kph with constant engine load of 140 Nm, respectively. From this result, CO_2 slightly increases, O_2 and NO decrease after leaving the P-DPF due to the CeO_2 coated DOC that generate more CO_2 and converting NO to NO_2 as explained in **Chapter 4 4.2.3.1**, along with the average T2 is > 250 ℃ suggest that NO_2 passive regeneration is occurred for both conditions of 90 kph and 120 kph with constant engine load of 140 Nm.

5.4 Conclusion

The present study investigated the influence of diesel oxidation catalyst (DOC) and partial-flow diesel particulate filter (P-DPF) on the passive regeneration of the P-DPF, with the aim of reducing soot emissions from diesel-engine applications. The research was conducted on a 2.5L 4-cylinder common rail direct injection diesel-engine truck, which was tested using B20 fuel at two different vehicle speeds (90 and 120 kph), while keeping a constant engine load of 140 Nm. Various parameters such as exhaust temperatures, pressure drop, and diesel emissions (carbon dioxide (CO_2), oxygen (O_2), and nitric oxide (NO)) were monitored to investigate the characteristics of soot oxidation.

The findings of this work shed light on the effects of DOCs and P-DPFs on soot oxidation characteristics. When the vehicle was run at speeds of 90 and 120 kph with no engine load, the exhaust temperature did not regularly surpass 250 °C, notably at the location immediately after exiting the P-DPF. As a result, under these conditions, passive regeneration through nitrogen dioxide (NO_2) could not occur.

Analyzing the emissions of CO_2, O_2, and NO, it was not possible to clearly determine whether soot oxidation had occurred, with the exception of a decrease in NO emissions after passing through the after-treatment systems. However, based on the exhaust temperature observations, it can be concluded that soot oxidation occurred owing to temperatures surpassing 250 °C after exiting the P-DPF at speeds of 90 and 120 kph with an engine load of 140 Nm. This can be attributed to the aid of the Pt catalyst, which reduces the soot oxidation temperature. These findings collectively suggest that the soot trapped inside the P-DPF has been oxidized by NO_2 according to the inlet and outlet maximum temperature were 550 °C and 375 °C, respectively.

Overall, the findings of this study shed light on the potential of DOCs and P-DPFs for passive regeneration and reducing soot emissions from diesel-engine applications. The impacts on exhaust temperatures, pressure drop, and emissions reported give useful information for the development and improvement of exhaust after-treatment systems in diesel cars, adding to the overall objective of lowering dangerous pollutants and improving air quality.

Tables

Table 5.1 Specifications of DOC and P-DPF used in this work

Type of Equipment	DOC	P-DPF
Type of Coating Catalyst	CeO_2 (Cerium Dioxide)	Pt (Platinum)
Cell Density	300	200
Length (mm.)	100	150
Diameter (mm.)	144	144

Table 5.2 Average result of temperature, pressure drop, and emission at 90 kph_140Nm.

	T_1 (°C)	T_2 (°C)	Pressure Drop (kPa)	CO_2 [ppm]	O_2 [ppm]	NO [ppm]
Before entering DOC	-	-	-	74456	97066	619
After leaving P-DPF	-	-	-	74620	96587	571
Overall	407.25	254.75	3.97	-	-	-

Table 5.3 Average result of temperature, pressure drop, and emission at 120 kph_140Nm.

	T_1 (°C)	T_2 (°C)	Pressure Drop (kPa)	CO_2 [ppm]	O_2 [ppm]	NO [ppm]
Before entering DOC	-	-	-	81110	88856	828
After leaving P-DPF	-	-	-	82512	83610	775
Overall	530.78	370.32	7.24	-	-	-

Figures

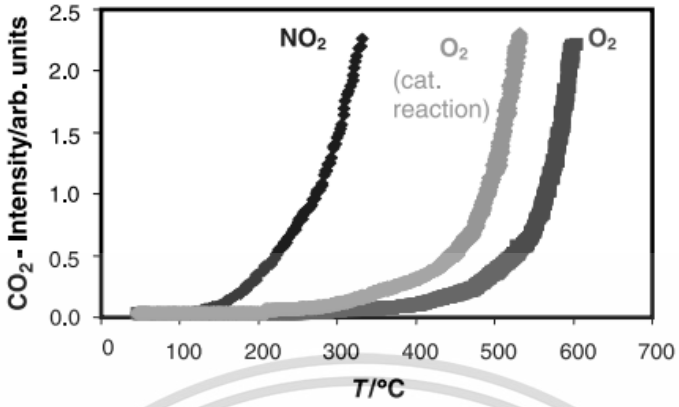

Figure 5.1 Temperature profile when O_2 and NO_2 start to combust soot [6]

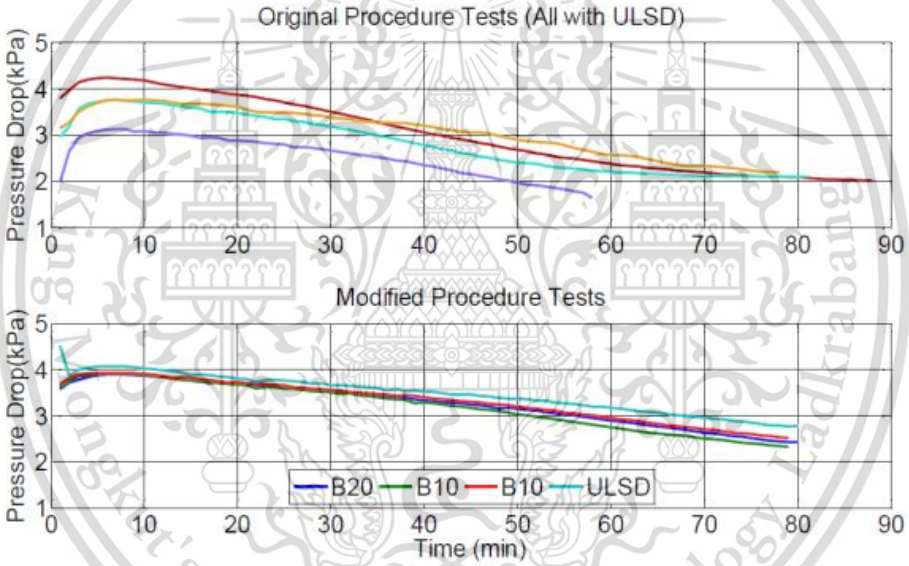

Figure 5.2 Pressure drop profile [10]

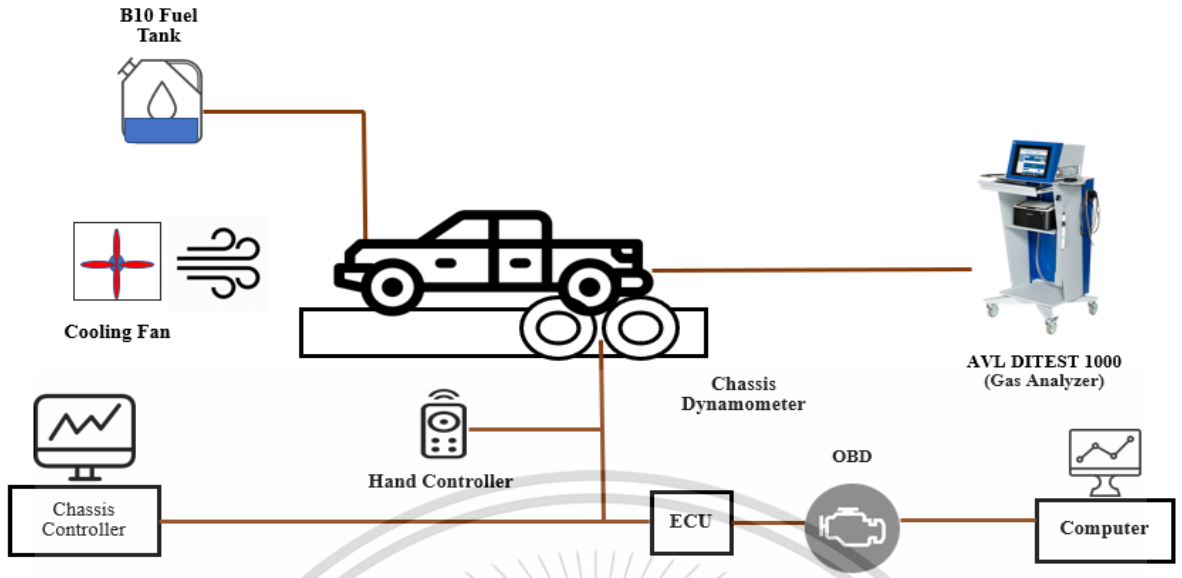

Figure 5.3 Schematic diagram of the experimental setup

Figure 5.4 Actual setup of this experiment

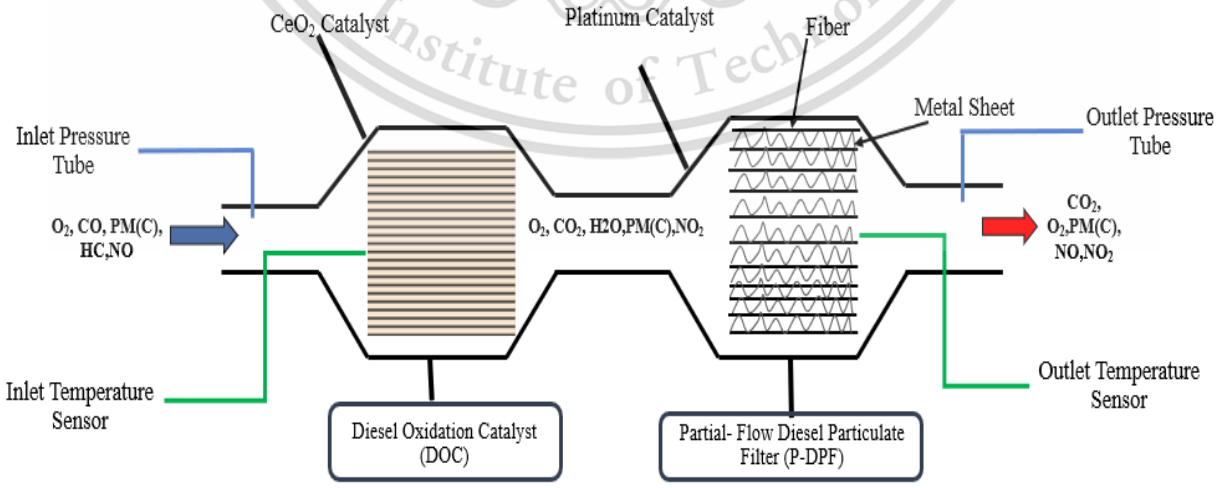

Figure 5.5 Schematic diagram of after-treatment equipment used in this work

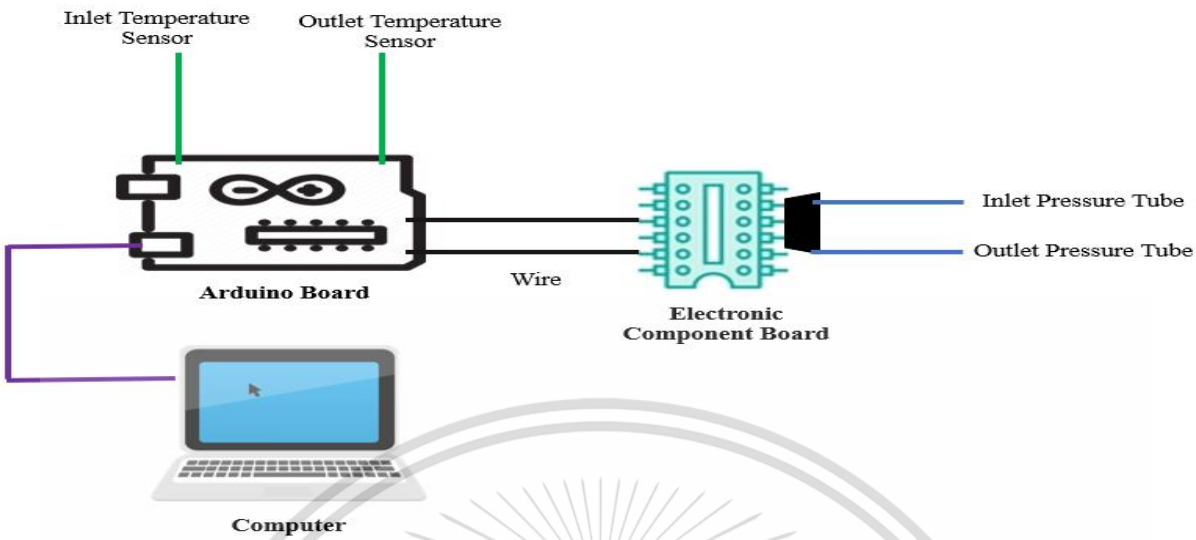

Figure 5.6 Schematic diagram of Arduino for measured real time temperature and pressure

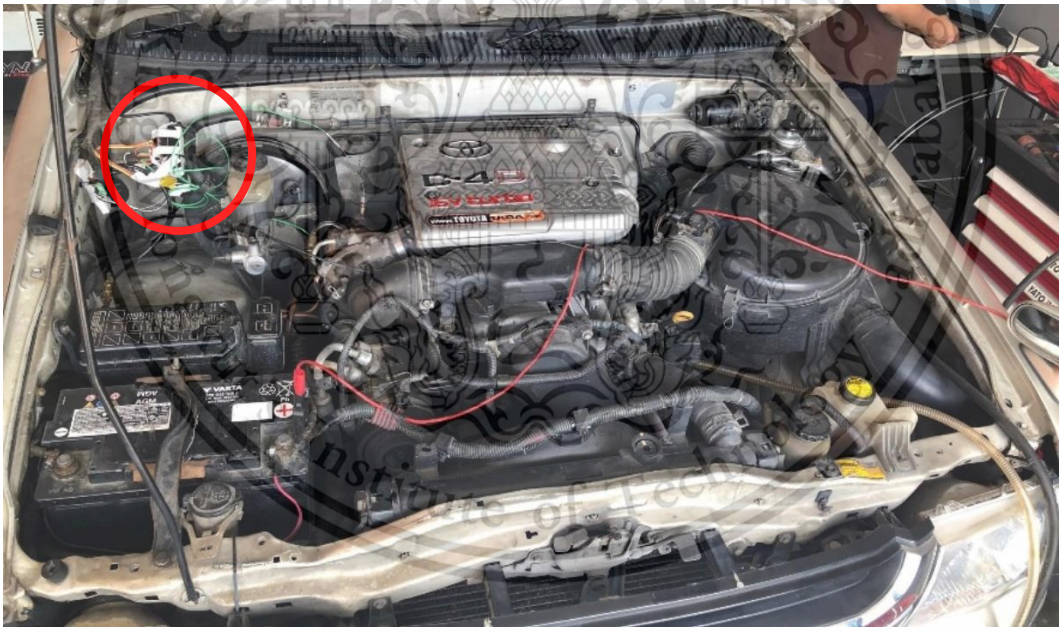

Figure 5.7 Actual position of Arduino board on the vehicle

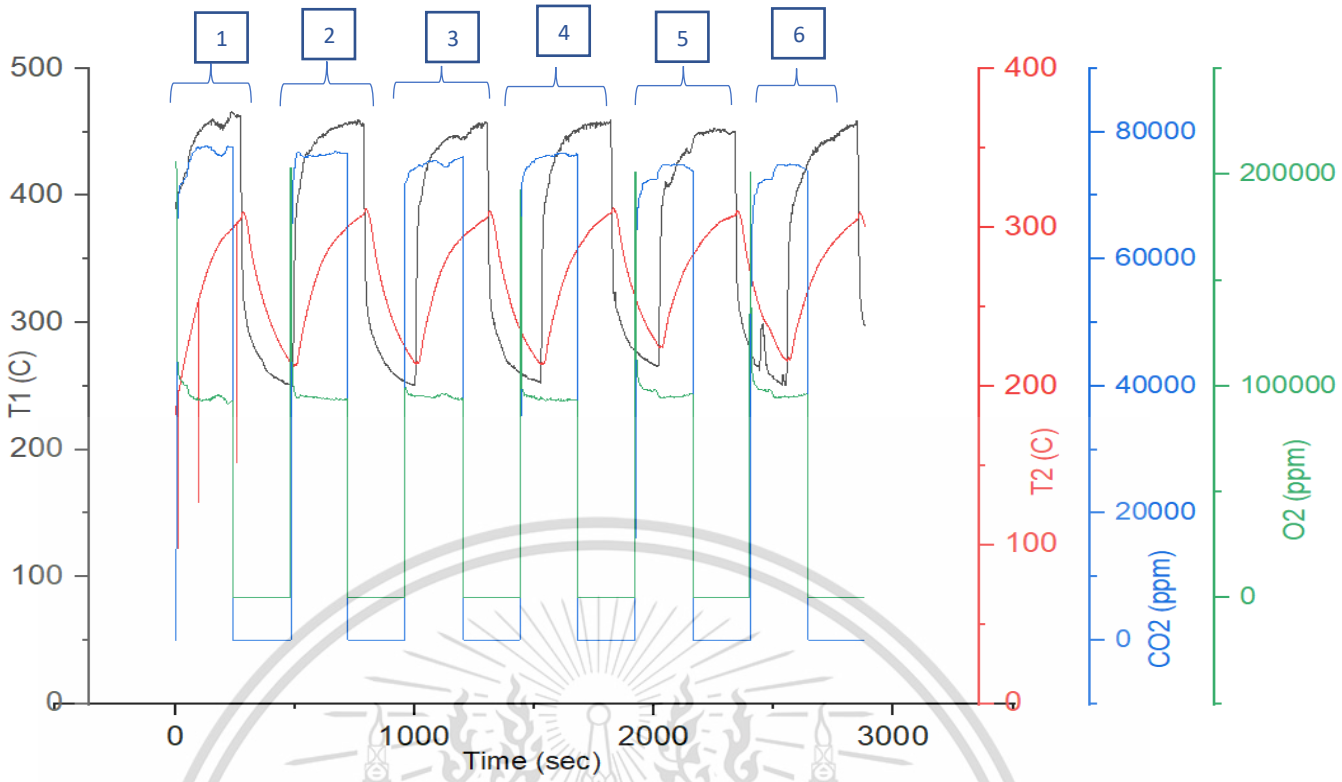

(a)

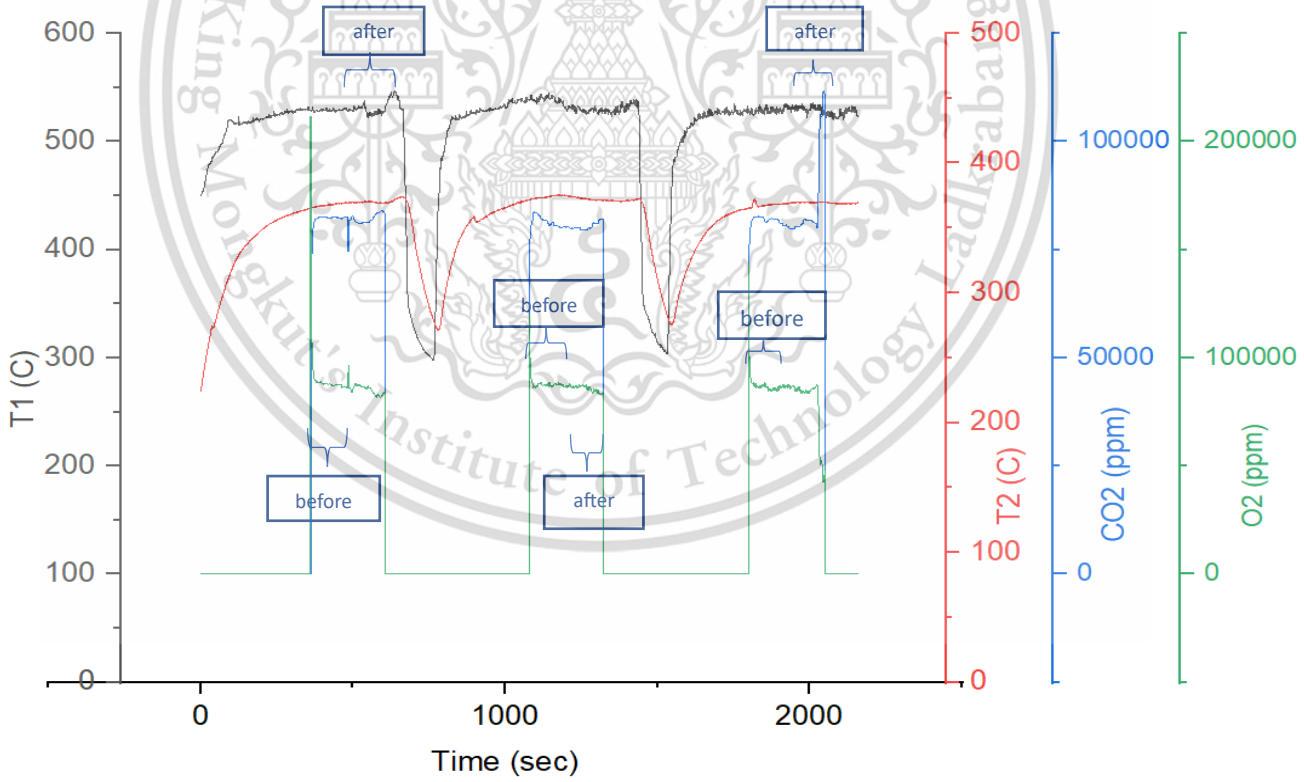

(b)

Figure 5.8 Real-time data of Temperature VS CO_2 and O_2 emissions at (a.) Vehicle speed:90 kph, Engine load: 140 Nm. (b) Vehicle speed: 120 kph, Engine load: 140 Nm.

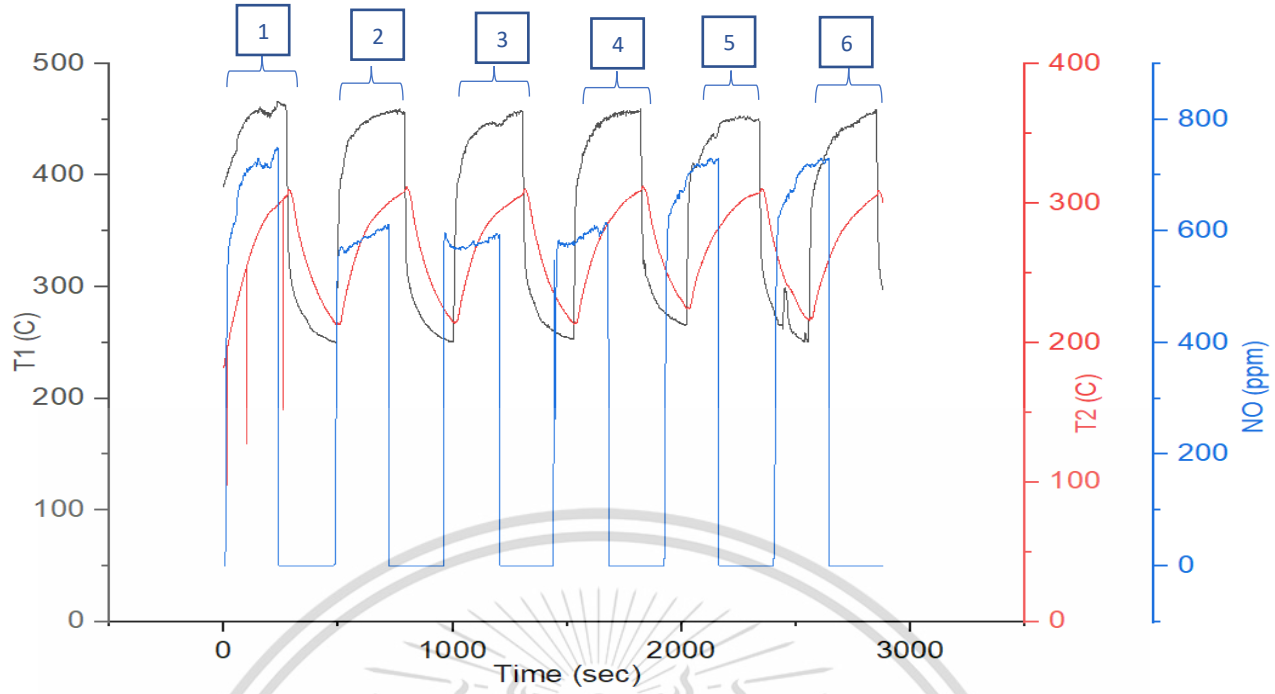

(a)

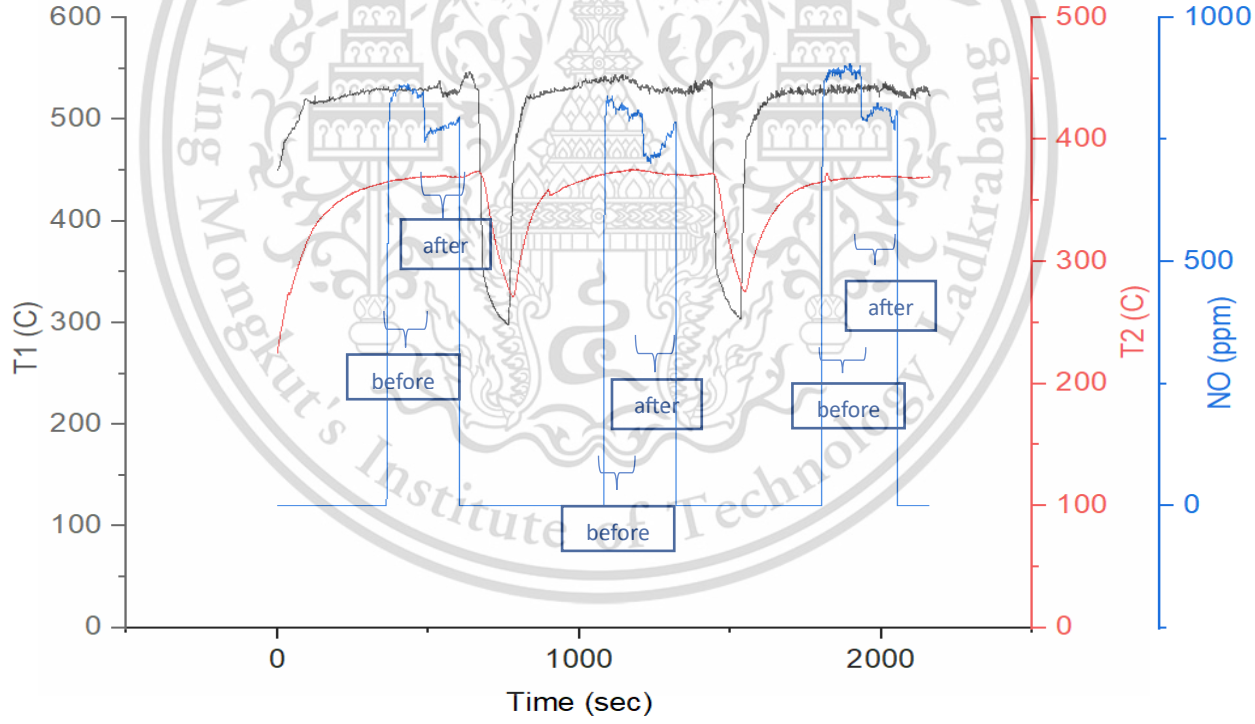

(b)

Figure 5.9 Real-time data of Temperature VS NO emissions at (a.) Vehicle speed:90 kph, Engine load: 140 Nm. (b) Vehicle speed: 120 kph, Engine load: 140 Nm.

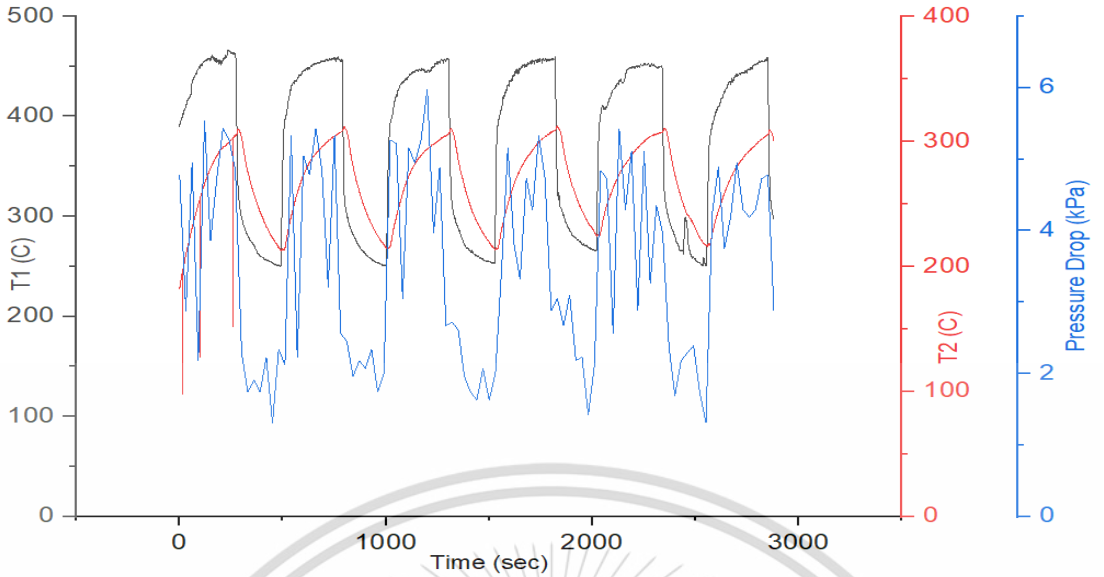

(a)

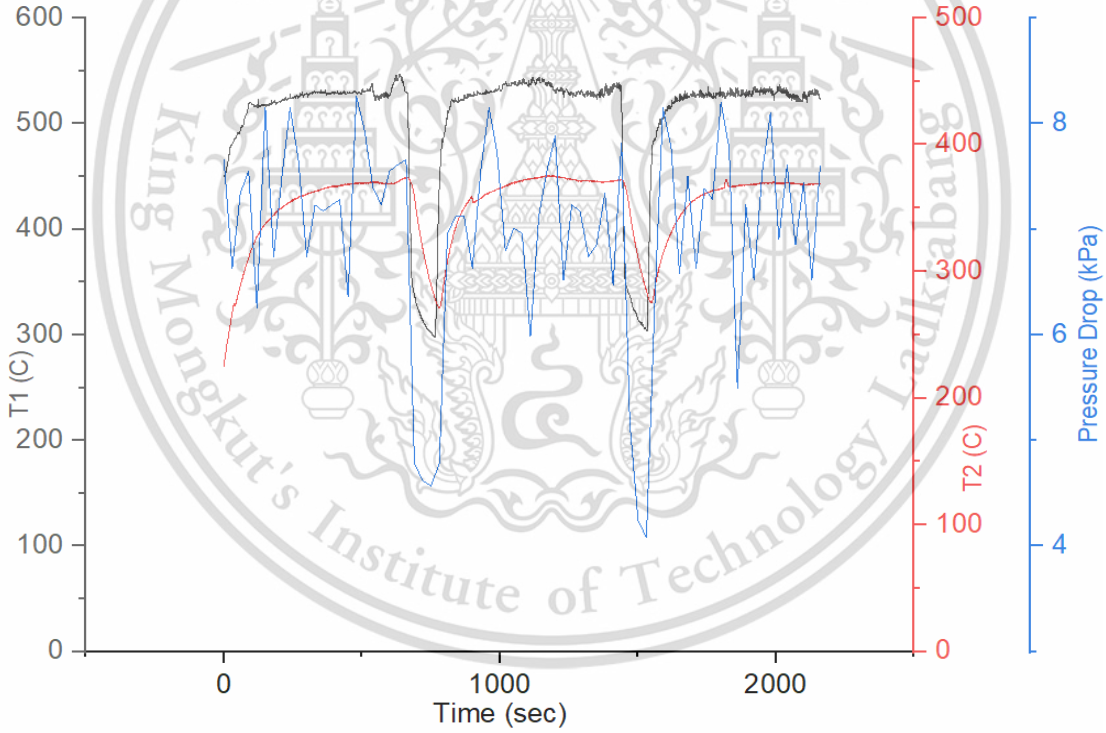

(b)

Figure 5.10 Real-time data of Temperature VS Pressure at (a.) Vehicle speed:90 kph, Engine load: 140 Nm. (b) Vehicle speed: 120 kph, Engine load: 140 Nm.

Reference

[1] Okawara, Seiji & Tsuji, Shinji & Inoue, Mikio & Itatsu, Toshiro & Nohara, Tetsuo & Komatsu, Kazunari. (2006). *Soot trapping and continuously oxidizing behavior by flow-through Metallic PM filter*. JSAE Review. 37(2). 91-96.

[2] Hay Mon Oo, Preechar Karin, Chinda Charoenphonphanich, Nuwong Chollacoop, Katsunori Hanamura, *Physicochemical characterization of direct injection Engines's soot using TEM, EDS, X-ray diffraction and TGA*, Journal of the Energy Institute, Volume 96, 2021, Pages 181-191, ISSN 1743-9671, https://doi.org/10.1016/j.joei.2021.03.009.

[3] Setiabudi, A., Makkee, M., Moulijn, J., *The role of NO2 and O2 in the accelerated combustion of soot in diesel exhaust gases*, Appl. Catal. B. Environ., Vol. 50, Issue 3, pp. 185–194, 2004, doi: 10.1016/j.apcatb.2004.01.004.

[4] Singh, M., Srilomsak, M., Wang, Y., Hanamura, K., Vander Wal, R., *Nanostructure Changes in Diesel Soot during NO2–O2 Oxidation under Diesel Particulate Filter-like Conditions toward Filter Regeneration*. International Journal of Engine Research 20, No. 8–9, pp. 953–66, 2019, doi:10.1177/1468087418807608.

[5] Allansson, R., Blakeman, P., Cooper, B., Hess, H. et al., *Optimising the Low Temperature Performance and Regeneration Efficiency of the Continuously Regenerating Diesel Particulate Filter (CR-DPF) System*, SAE Technical Paper 2002-01-0428, 2002, doi:10.4271/2002-01-0428.

[6] Gorsmann C., *Catalytic Coatings for Active and Passive Diesel Particulate Filter Regeneration*. Monatshefte fur Chemie - Chemical Monthly, 2005

[7] Lee, K., Seong, H., Choi, S., *Detailed analysis of kinetic reactions in soot oxidation by simulated diesel exhaust emissions*, Proceeding Combust. Inst., Vol. 34, Issue 2 pp. 3057–3065, 2013, doi:10.1016/j.proci.2012.06.121.

[8] Luo, J., Tie, Y., Tang, L. et al. *Effect of regeneration method and ash deposition on diesel particulate filter performance: a review*. Environ Sci Pollut Res **30**, 45607–45642 (2023). https://doi.org/10.1007/s11356-023-25880-2

[9] Pérez, V.R., & Bueno-López, A. (2015). *Catalytic regeneration of Diesel Particulate Filters: Comparison of Pt and CePr active phases*. Chemical Engineering Journal, 279, 79-85.

[10] Shiel, K., Naber, J., Johnson, J., and Hutton, C., "Catalyzed Particulate Filter Passive Oxidation Study with ULSD and Biodiesel Blended Fuel," SAE Technical Paper 2012-01-0837, 2012, https://doi.org/10.4271/2012-01-0837.

[11] The NATION, *Raise the speed limit of 120km/hr is no effect*, 2023, https://www.nationthailand.com/infocus/30403563?fbclid=IwAR0NheEdiKsheviyfnwjksz9dU8hYxJkUxFNxmnL2X8BknwzlVgKCHRsCcY

[12] Yongjin Jung, Young Dug Pyo, Jinyoung Jang, Gang Chul Kim, Chong Pyo Cho, Changho Yang, *NO, NO2 and N2O emissions over a SCR using DOC and DPF systems with Pt reduction*, Chemical Engineering Journal, Volume 369, 2019, Pages 1059-1067, ISSN 1385-8947, https://doi.org/10.1016/j.cej.2019.03.137.

[13] Ehrburger, P., Brilhac, J.F., Drouillot, Y., Logie, V., & Gilot, P. (2002). Reactivity of Soot With Nitrogen Oxides in Exhaust Stream.

[14] M. Schejbal, J. Štěpánek, M. Marek, P. Kočí, M. Kubíček, Modelling of soot oxidation by NO2 in various types of diesel particulate filters, Fuel, Volume 89, Issue 9, 2010, Pages 2365-2375, ISSN 0016-2361, https://doi.org/10.1016/j.fuel.2010.04.018.

[15] M. Jeguirim, V. Tschamber, J.F. Brilhac, P. Ehrburger, *Oxidation mechanism of carbon black by NO2: Effect of water vapour*, Fuel, Volume 84, Issues 14–15, 2005, Pages 1949-1956, ISSN 0016-2361, https://doi.org/10.1016/j.fuel.2005.03.026.

[16] Bermúdez, V., Serrano, J. R., Piqueras, P., & Campos, D. (2015). Analysis of the influence of pre-DPF water injection technique on pollutants emission. Energy, 89, 778–792. doi:10.1016/j.energy.2015.05.142

CHAPTER 6

CONCLUSION

6.1 Conclusion

In conclusion, this research focused on assessing the impact of biodiesel fuel (B20) with an installation of after-treatment systems, includes diesel oxidation catalyst (DOC) and partial-flow diesel particulate filter (P-DPF), on combustion characteristics, performance, and emissions using a real-engine real-vehicle setup. The experiment was conducted on a 2.5-liter four-cylinder common rail system, employing an engine dynamometer, and encompassed three different driving conditions. Firstly, the vehicle underwent testing under various loads ranging from 84 Nm to 160 Nm, while maintaining constant engine speeds of 1500 rpm, 2000 rpm, and 2500 rpm. This allowed for a comprehensive evaluation of the impact of vehicles with installation of after-treatment systems on engine performance and emissions across different load-speed combinations. Secondly, the New European Driving Cycle (NEDC) was employed to simulate real-world driving conditions, incorporating a range of speeds from 20 km/h to 120 km/h, while maintaining low engine load. This testing approach provided insights into the behavior of vehicles with installation of after-treatment systems during typical driving scenarios, further enhancing our understanding of their effects on combustion and emissions. Lastly, the vehicle was subjected to continuous running at two specific speeds: 90 km/h and 120 km/h, while maintaining a constant engine load of 140 Nm. This allowed for a focused analysis of the impact of soot oxidation in P-DPF on temperature, pressure drop, and emissions under sustained high-speed conditions.

The vehicle with the installation of after-treatment systems running at constant engine speeds of 1500, 2000, and 2500 rpm with variable engine loads of 84, 112, 140, and 160 Nm. The installation of after-treatment equipment (DOC and P-DPF, and Long P-DPF) and the use of B20 did not demonstrate any notable impact on vehicle thermal efficiency due to the fuel consumption not significantly different, which the calculation continue to brake thermal efficiency making it not significantly different and the pressure drop is related to the amount of soot trapped inside the P-DPF with the range between 3.97 - 7.24 kPa can cause higher

friction loss and higher exhaust temperature but not significantly effect to vehicle thermal efficiency.

Second chassis dynamometer testing the vehicle used the New European Driving Cycle (NEDC) for the simulation of an actual driving cycle of urban and highway driving. The implementation of DOCs and P-DPFs resulted in significant reductions in THC levels, achieving up to a 58% reduction. Additionally, the combination of ceria DOC with platinum P-DPF and the long P-DPF led to substantial reductions in CO emissions, with reductions of 81% and 89% respectively. Furthermore, the utilization of ceria DOC and platinum P-DPF contributed to notable PM and PN reductions, with reductions of up to 62% and 42% observed, respectively. When the long P-DPF was employed, PM and PN emissions were reduced by 69% and 45%, respectively. However, it is worth noting that the installation of the after-treatment system did not have a noticeable impact on carbon dioxide (CO_2) emissions. Considering the limited duration of the experiment for each scenario, the data suggests that the passive regeneration of PM within the filter occurs slowly or may not occur at all in terms of CO_2 emissions due to the exhaust temperature that is not high enough.

The third chassis dynamometer testing the vehicle was run continuously at two specific speeds: 90 km/h and 120 km/h, while maintaining a constant engine load of 140 Nm. The testing result provided insights into the impact of ceria and platinum coated DOCs and P-DPFs on the characteristics of soot oxidation. When the vehicle was operated at speeds of 90 and 120 km/h with no engine load, the exhaust temperature remained below 250 °C, particularly right after exiting the P-DPF. Consequently, under these conditions, passive regeneration through nitrogen dioxide (NO_2) was not possible. The analysis of CO_2, O_2, and NO emissions did not definitively indicate whether soot oxidation had taken place, except for a decrease in NO emissions after passing through the after-treatment systems. However, based on the exhaust temperature observations, it can be inferred that soot oxidation occurred when the temperatures exceeded 250 °C after exiting the P-DPF at speeds of 90 and 120 kph with an engine load of 140 Nm. This can be attributed to the presence of the Pt catalyst, which lowers the soot oxidation temperature. These findings collectively suggest that the soot trapped inside the P-DPF has been oxidized by NO_2.

Finally, the results revealed that it is possible to have passive regeneration occur inside P-DPF by NO_2 from these reasons. First, the Pt coating on the P-DPF facilitated a soot oxidation process where carbon-based soot interacted with nitrogen dioxide (NO_2), leading to a decrease in soot levels and according to the maximum inlet and outlet temperature were 550 ℃ and 375 ℃, respectively. Furthermore, CO_2 increased and O_2 decreased after leaving the after-treatment system, which were observed when the vehicle ran continuously with 90 and 120 km/h at 140 Nm. Secondly, the soot emissions result shows that after the installation of a Long P-DPF resulted in a significant reduction of up to 69% in particulate matter emissions, as observed through scanning electron microscopy (SEM) images can clearly seen that the soot aggregation decreases the most by using Long P-DPF. In addition, by observing from TEM and TEM-EDS analysis, single primary particles and their size distribution suggests that the after-treatment system plays a role in reducing the average fringe length, maximum fringe length, and particle size suggesting some surface oxidation by NO_2 and O_2. Furthermore, Carbon content also reduced after passing through after-treatment system suggesting the passive regeneration by NO_2 is occur inside the P-DPF.

In summary, this research demonstrated that the use of B20 in conjunction with after-treatment systems installed in the exhaust pipe has negligible effects on the performance of diesel engines and vehicles. However, as compared to utilizing B20 without any after-treatment systems, the adoption of these after-treatment systems resulted in a significant reduction in particulate matter emissions, maximum at 69%. Moreover, the findings provide evidence that the soot trapped inside the P-DPF undergoes oxidation through the action of NO_2, facilitated by exhaust temperatures exceeding 250 ℃ after exiting the P-DPF at speeds of 90 and 120 kph with an engine load of 140 Nm.

APPENDIX A

SCANNINNG ELECTRON MICROSCOPE

Fuel/ Equipment	10,000x magnification	50,000x magnification
B20 / -	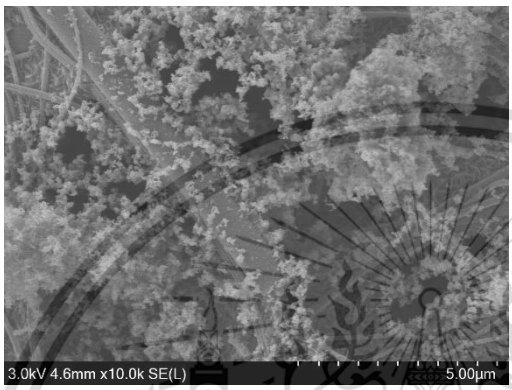	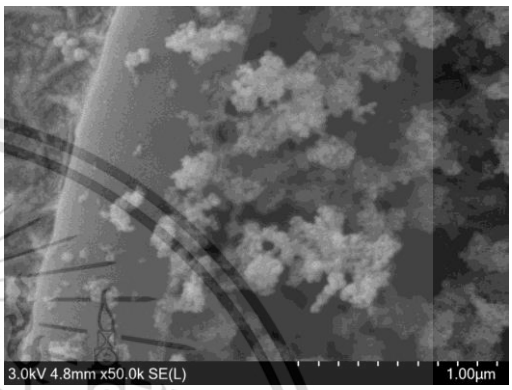
B20/ CeO_2 DOC + Pt P-DPF	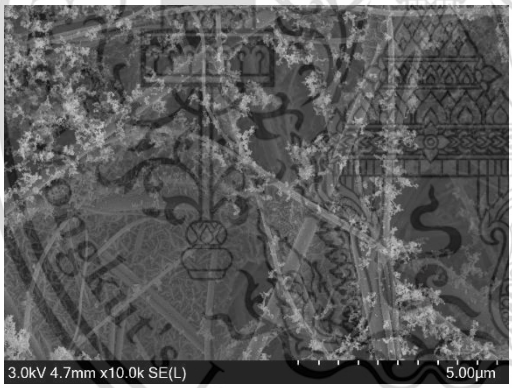	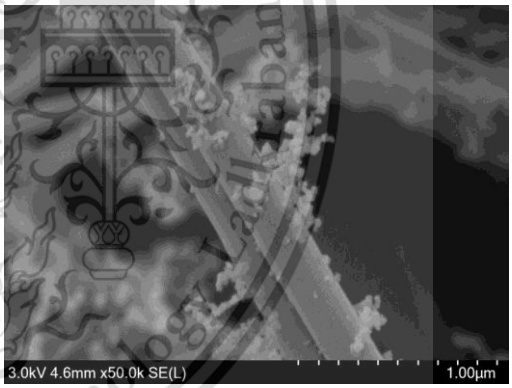
B20/Pt Long P-DPF		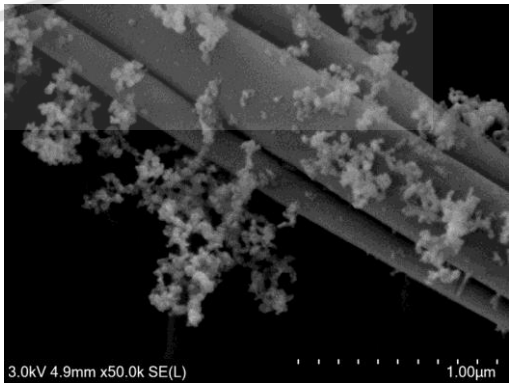

APPENDIX B

TEST REPORTS

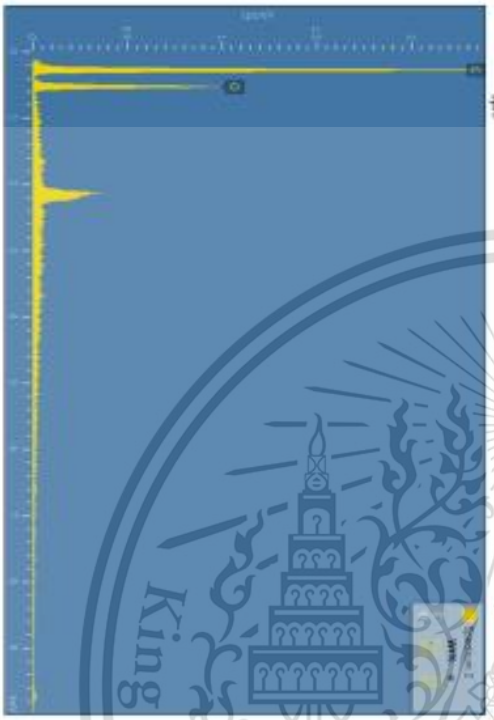

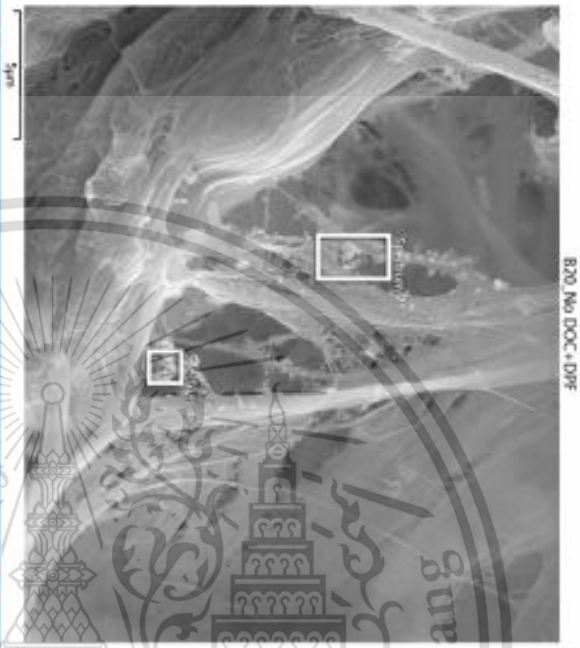

Label:	Spectrum 2
Source:	Acquired
Created:	8/17/2022 4:47:32 PM
Livetime:	50.3s
Process Time:	6
Accelerating Voltage:	15.00kV
Magnification:	5004 x
Working Distance:	10.7mm
Specimen Tilt (degrees):	0.0
Elevation (degrees):	35.0
Azimuth (degrees):	0.0
Number Of Channels:	2048
Energy Range (keV):	20 keV
Energy per Channel (eV):	10.0eV
Detector Type id:	28
Detector Type:	X-Max
Window Type:	SATW
Pulse Pile Up Correction:	Disabled
Primary Detector:	Horiba
Primary Detector Serial Number:	70527-X050

A-1 Test reports of EDS on B20 with no after-treatment system

Label:	Spectrum 10
Source:	Acquired
Created:	8/17/2022 5:19:17 PM
Livetime:	50.0s
Process Time:	6
Accelerating Voltage:	15.00kV
Magnification:	8001 x
Working Distance:	10.5mm
Specimen Tilt (degrees):	0.0
Elevation (degrees):	35.0
Azimuth (degrees):	0.0
Number Of Channels:	2048
Energy Range (kev):	20 kev
Energy per Channel (ev):	10.0eV
Detector Type Id:	28
Detector Type:	X-Max
Window Type:	SATW
Pulse Pile Up Correction:	Disabled
Primary Detector:	Horiba
Primary Detector Serial Number:	70527-X050

A-2 Test reports of EDS on B20 with CeO_2 DOC and Pt P-DPF

Label:	Spectrum 5
Source:	Acquired
Created:	8/17/2022 4:54:16 PM
Livetime:	50.3s
Process Time:	6
Accelerating Voltage:	15.00kV
Magnification:	4506 x
Working Distance:	10.6mm
Specimen Tilt (degrees):	0.0
Elevation (degrees):	35.0
Azimuth (degrees):	0.0
Number Of Channels:	2048
Energy Range (kev):	20 kev
Energy per Channel (ev):	10.0eV
Detector Type Id:	28
Detector Type:	X-Max
Window Type:	SATW
Pulse Pile Up Correction:	Disabled
Primary Detector:	Horiba
Primary Detector Serial Number:	70527-X050

A-3 Test reports of EDS on B20 with Pt long P-DPF

APPENDIX C

PUBLICATION

The 12th TSME International Conference on Mechanical Engineering
13th – 16th December 2022
Phuket, Thailand

AEC0011

Impacts of Partial Flow Diesel Particulate Filter on Vehicle's Brake Thermal Efficiency and Exhaust Emissions Characteristics

Plan Teekatasn Cosh[1], Poonnut Thaeviriyakul[1], Phyo Wai[1], Ban-seok Oh[1], Hai Liu[1], Myat Hsu Thin[1], Watanyoo Phairote[1], Mek Srilomsak[1*], Supat Kittiratsatcha[1], Preechar Karin[1], Chinda Charoenphonphanich[1], Kobsak Sriprapha[2], Sompong Srimanosaowapak[2], Katsunori Hanamura[3]

[1]School of Engineering, King Mongkut's Institute of Technology Ladkrabang, Bangkok 10520, Thailand
[2]National Energy Technology Centre, National Science and Technology Development Agency, Pathum Thani 12120, Thailand
[3]School of Engineering, Tokyo Institute of Technology, Tokyo 152-8552, Japan

* Corresponding Author: mek.sr@kmitl.ac.th

Abstract. This study provides an experimental investigation of the engine performance, diesel vehicle emissions, with the aim of reducing the smoke intensity of the after-treatment systems on commercial biodiesel fuels (B20 and B10). This paper investigates the combustion and emission characteristics of a B20 and B10 fuelled 2.5-liter direct injection diesel-engine pickup truck running at engine speed of 1500 rpm, 2000 rpm, and 2500 rpm with 84Nm, 112Nm, 140Nm, and 160Nm of torque. The vehicle was examined for its fuel economy, brake-specific energy consumption (BSEC), brake thermal efficiency (BTE), smoke intensity, and diesel emissions. The experiment includes an exhaust gas analysis and particulate matter (PM) emissions micro-scaled visualization using Digital Optical Microscopy and Scanning Electron Microscopy. Experimental results are discussed in three cases of after-treatment systems which are: without diesel oxidation catalyst (DOC) or partial flow diesel particulate filter (P-DPF), with DOC and P-DPF, and with Long P-DPF only. The case of with DOC and P-DPF results in lower fuel flow rate, increased BTE, and decreased BSEC. Smoke intensity in the exhaust gas can be reduced more than 50% compared to the case of without DOC or P-DPF, however, the greatest significant reduction in smoke intensity occurred under the Long P-DPF. Nevertheless, the smoke intensity and Diesel vehicle particle emission can be reduced not only by P-DPF through but also DOC. Lastly, the experiment result of NO increases due to the P-DPF mechanism.

Keywords: brake thermal efficiency, partial flow diesel particulate filter, brake-specific energy consumption

1. Introduction

Direct injection diesel-engines are widely used in automobiles because of their high thermal efficiency, torque, and longevity. However, the major drawback of diesel engines is that particulate matter (PMs) is high because fuel is injected directly into the combustion chamber of the diesel engine, which results in incomplete combustion and nonhomogeneous fuel and air mixture, which initiates soot formation.

Along with the rising human population, the usage of cars is also progressively rising. Future changes in the global ecology, temperature, and fossil fuel supplies will be caused by the increase in automobiles and excessive fuel usage. In many large population centers across the world, automotive exhaust emission is one of the main contributors to air pollution [4,5]. Diesel engine driven vehicles have important effects on human health due to their emissions, in terms of PMs and Oxide of Nitrogen (NOx) [6]. Untreated emissions from diesel engines contain harmful gas phase emission and solid phase PMs. Therefore, after-treatment systems are applied to vehicles, including Diesel Oxidation Catalysts (DOC) and Partial-Flow Diesel Particulate Filters (P-DPF) using a combination of flow mechanisms and chemical reactions to achieve near complete removal of PMs and harmful chemicals. In Thailand, heavy vehicles and buses are comparable to Euro 3, while for passenger cars and one-ton pickup trucks are equivalent to Euro 4. As a result, there is no need to construct after-treatment technology. Nevertheless, soon stronger pollution control regulations, equivalent to Euro 5, will be introduced to control pollution. This experiment and analysis will serve as more evidence and support of the importance of setting in an after-treatment system.

This research aims to investigate the effects of two different fuels (B10 and B20), as well as catalysts that coat DOC, P-DPF, and Long P-DPF after-treatment equipment, on diesel emissions, soot emissions, and engine performance. This study employs a real pickup vehicle with a 2.5-liter direct injection diesel engine to compare the engine performance. Additionally, a study of the soot emission was conducted at constant engine speeds (1500, 2000, and 2500 rpm) and varying engine loads (84, 112, 140, and 160 Nm) as this represents the practical range of speed and load in diesel engine applied on routes where peak performance is not required all the time.

2. Methodology

2.1 Preparation of fuel and operating conditions

Pure biodiesel (B100) production is conducted from based palm oil through acid-esterification and transesterification with methanol. To investigate and compare the engine performance and the exhaust emission of two different fuels, B20 (20% vol biodiesel and 80% vol diesel) and B10 (10% vol biodiesel and 90% vol diesel) were utilized. The fuel properties are as shown in Table 1. This experiment's operating conditions involved a range of engine loads (84, 112, 140, and 160Nm) at constant engine speeds (1500, 2000, and 2500 rpm).

Table 1. Properties of biodiesel. [3]

Properties (Units)	B10	B20	B100
Carbon (% mass)	84.6	82.6	76.7
Hydrogen (% mass)	13.5	13.4	12.4
Oxygen (% mass)	1.9	4.0	10.9
Low heating value (kJ/g)	43.1	42.4	37.4
Cetane Number	53.7	54.5	62.1
Flash Point (°C)	66	66	184.5
Density at 15 °C (kg/m3)	835	827	875
Viscosity at 40 °C (mm2/s)	3.0	3.1	4.5

2.2 Vehicle and test bench

A 2.5L 4-cylinder common rail direct injection diesel-engine vehicle (Toyota Hilux Tiger) was run at various engine speeds and loads on a chassis dynamometer. This experiment focuses on the effects of B20 and B10 fuels on the engine's performance and exhaust emission with three cases of after-treatment systems which are: without diesel oxidation catalyst (DOC) or partial flow diesel particulate filter (P-DPF), with DOC and P-DPF, and with Long P-DPF only. The vehicle specification is shown in Table 2. The vehicle test bench was positioned on the chassis dynamometer. The measurement of smoke intensity was measured by a BOSCH smoke intensity meter (DSM-240) with the measure accuracy of ±3%. Furthermore, exhaust emission such as Nitric Oxide (NO), Carbon Dioxide (CO_2) and Oxygen (O_2) as was monitored by the AVL exhaust gas analyzer (DITEST GAS 1000) with the accuracy of 0.001. On-board diagnostic (OBD), which is also connected to the engine control unit, all engine conditions were recorded, including emissions, mileage, and speed (ECU). Computer was using LabView programming software to measure the engine torque, speed, and fuel consumption under test circumstances. A schematic diagram of the equipment setup is shown in Fig. 1.

Table 2.Vehicle Specification.

Vehicle	Toyota Hilux Tiger
Engine Type	2KD-FTV (Diesel)
Number of cylinders & Arrangement	4 cylinders, In-line
Valve Mechanism	16 Valve DOHC
Bore x Stroke	92.0 mm x 93.8 mm
Displacement Volume	2500 cc
Compression Ratio	18.5 : 1
Fuel System	Common-rail type Direct Injection
Maximum Power (kW at rpm)	75 kW at 3600 rpm
Maximum Torque (Nm at rpm)	260 Nm at 1600 – 2400 rpm

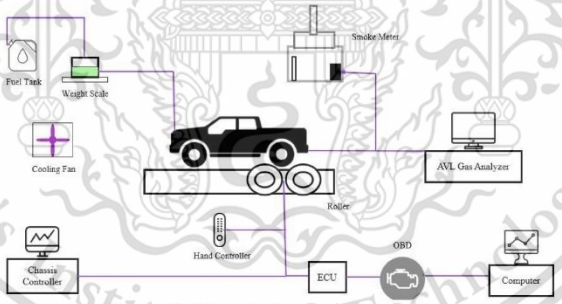

Figure 1. Chassis Dynamometer set up

2.3 After-treatment Systems

In this experiment, the after-treatment systems that include Cerium Dioxide (CeO_2) coating DOC and Platinum (Pt) coating P-DPF installed of downstream of the diesel engine. Fig.**2** illustrates the DOC and P-DPF systems when installed in the exhaust system. The DOC is locked at the upstream, followed by the P-DPF. By converting Carbon Monoxide (CO) also Hydrocarbon (HC) to Carbon Dioxide (CO_2) and Nitric Oxide (NO) to Nitrogen Dioxide (NO_2), which will be used further in the P-DPF equipment, most of gas phase exhaust emission can be treated at the DOC. P-DPF is used to trap particulate matters (PMs), then utilized with Oxygen (O_2) and NO_2 to oxide carbon element (soot) in the PMs to form CO_2

and NO. In addition, the oxidation of soot can be accelerated with the aid of Pt catalyst coating on P-DPF substrate. Therefore, NO and CO_2 levels rise when NO_2 and soot (the carbon form) are mixed in the P-DPF (the PMs are oxidized and the P-DPF is regenerated). In order to compare which was the best, P-DPF and Long P-DPF were tested under varying situations. Table **3**. shows the specification of DOC, P-DPF, and Long P-DPF.

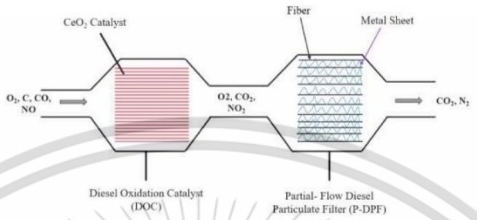

Fig 2. Exhaust gas flow through DOC and P-DPF

Table 3. DOC, P-DPF, and Long P-DPF Specifications.

Equipment	DOC	P-DPF	Long P-DPF
Element	CeO_2 (Cerium Dioxide)	Pt (Platinum)	Pt (Platinum)
Cell Density	300	200	200
Length (mm)	100	150	200
Diameter (mm)	144	144	144

2.4 Optical Microscopy (OM), and Scanning Electron Microscopy (SEM)

Paper filters were used with a smoke meter to collect PMs when testing the vehicle in real time. The PM samples on the paper filters were used to characterize the agglomerate particles in micro-scale through the OM (Nikon Model LV100) to enlarged images and viewed the original color of PMs and observed PMs morphology and microstructure through SEM (FE-SEM SU5000) under a magnification up to 10,000.

3. Calculation method

3.1. Engine Performance

The fuel consumption (g/s), engine speed (rev/min or rpm), and engine torque (Nm) were used to compute the brake specific fuel consumption (BSFC), brake specific energy consumption (BSEC), and brake thermal efficiency (BTE), which are all indicators of engine performance [3].

3.1.1. Brake Specific Fuel Consumption

The BSFC is calculated from the rate of fuel consumption to vehicle output power, which is measured in g/kWh.

3.1.2. Brake Specific Energy Consumption

The BSEC refers to the rate of energy consumption to vehicle output power, which is measured in kJ/kWh and Lower Heating Value (LHV) used to calculated in this equation were B20 LHV (42.42 kJ/g) and B10 LHV (43.10 kJ/g).

3.1.3. Brake Thermal Efficiency

The vehicle output power from heat energy supplied to a system is known as BTE.

4. Result and discussion

The following section will discuss the results in terms of engine performance, exhaust emission, oxygen, smoke intensity, and soot morphology.

4.1. Engine Performance

The results of the engine performance test for fuel consumption, BSFC, BSEC, and BTE were used to determine engine performance. Fuel consumption, BSFC, BSEC, and BTE data for both B20 and B10 fuels are shown in Fig. 3. At a constant engine speed, Fuel Consumption and BTE increased when the engine torque increased due to enhancing engine power as a result of increased fuel injection in support of the increased workload. On the other hand, BSFC and BSEC slightly decreased because there was more time for combustion and heat loss. At constant engine torque, Fuel Consumption, BSFC, and BSEC increased but BTE decreased when the engine speed increased due to more fuel being injected into the combustion chamber. The results of the engine performance test are not significantly impacted after the installation of DOC and P-DPF. The results of the engine performance test after switching to B10 biodiesel fuel were in the same direction, and the installation of after-treatment systems had no appreciable effects.

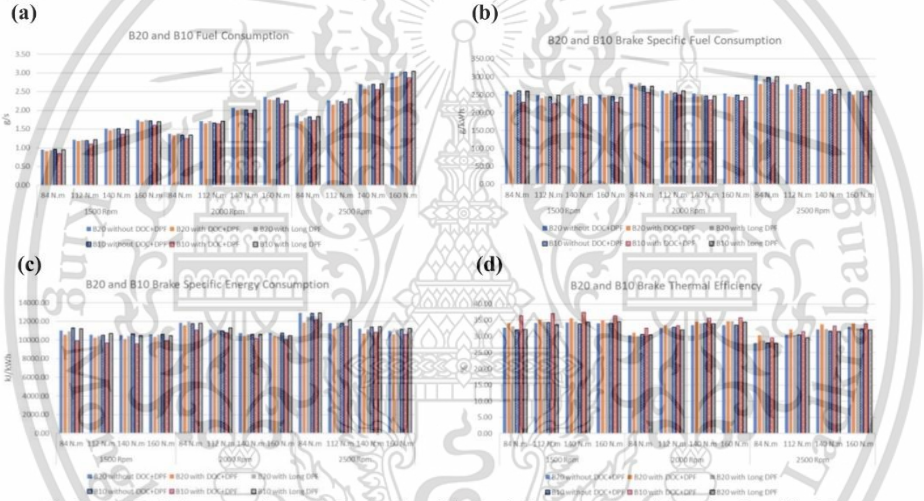

Fig 3. (a) Fuel Consumption, (b) Brake Specific Fuel Consumption, (c) Brake Specific Energy Consumption, and (d) Brake Thermal Efficiency

4.2. Exhaust Emission

4.2.1 Nitric Oxide and Carbon Dioxide

Fig. 4 shows a comparison of exhaust gas emissions, respectively. As a result, NO and CO_2 are increased due to the increases in engine torque at each constant engine speed. However, they are decreased due to the increase in engine speed. Nitrogen (N_2) and O_2 in the combustion chamber results in a rise in NO. CO_2 (the primary by-product of fuel and air consumption) rises as fuel injection into the combustion chamber increases. After installation of the after-treatment equipment, NO increases and CO_2 decreases due to the P-DPF mechanism, as explained in 2.3, Platinum (Pt) catalyst in P-DPF not only increases soot oxidation with NO_2 and soot (in the form of Carbon) but also converts CO into CO_2, which results in increased CO_2. The result of NO in conditions with DOC and P-DPF is highest due to DOC converts NO into NO_2 first then more NO_2 react with soot (Carbon form) inside P-DPF. The results of the NO and CO_2 fuel conversion from B20 to B10 followed the same trend consistent through all engine loads and speeds.

4.2.2 Oxygen

As shown in Fig. 4(c), O_2 slightly decreased with the output torque. This is due to more fuel injection into the combustion chamber to increase engine torque. This result is consistent across all engine speeds. However, there are no appreciable differences in the amount of O_2 in the exhaust gas across the three different cases of the after-treatment systems.

In comparison with the B20, B10 resulted in the same trend of O_2 concentration, except that the amount of O_2 is lower. This is because a higher percentage of biodiesel in diesel increases the proportion of O_2 molecule in the combustion chamber causing more complete combustion [2]. After installation of after-treatment systems, O_2 decreases due to oxidation reaction in DOC for the treatment of HC, CO, and NO.

4.2.3 Smoke Intensity

As shown in Fig. 4(d), smoke intensity is higher at low engine speeds, due to the resulting incomplete combustion. Because more fuel is being injected into the combustion chamber as engine torque increases, the smoke intensity likewise increases. Due to the after-treatment system, the smoke intensity can be reduced up to 74% by using DOC and P-DPF (greatest reduction up to 81% by using Long P-DPF) as measured from a BOSCH smoke intensity meter.

Smoke intensity fuel conversion from B20 to B10 followed the same trend, except that B10 had higher smoke intensity at low engine speeds than B20. This can be explained by a higher fraction of biodiesel in B20 fuel being effective in enhancing better combustion. Smoke intensity has decreased as a result of after-treatment systems. The Long P-DPF case provided the greatest smoke reduction.

4.3. Soot Morphology

The results are illustrated by images of paper filters taken with an optical microscope (OM, Nikon Model LV100) in Fig.5 and with a 10,000-magnification scanning electron microscope (SEM, FE-SEM SU5000) in Fig.6. In this experiment, B20 and B10 results of soot trapped on the paper filter follow the same trend. Therefore, only the result of B20 will be represented here. Without an after-treatment system, soot aggregation was shown in Figs. 5a and 6a. However, once an after-treatment system was installed, soot aggregation dramatically diminished, as is seen in Figs. 5b, 5c, 6b, and 6c, which were also consistent with the smoke intensity graph.

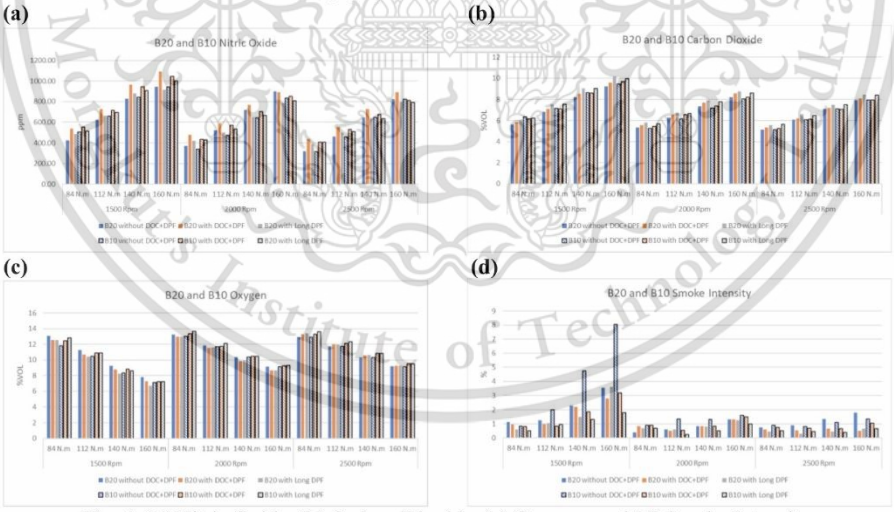

Fig. 4. (a) Nitric Oxide, (b) Carbon Dioxide, (c) Oxygen, and (d) Smoke Intensity

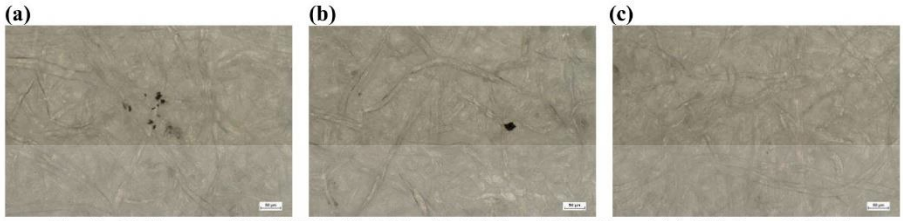

Fig. 5. OM images (a) B20 PM, (b) B20 with DOC and P-DPF, and (c) B20 Long P-DPF

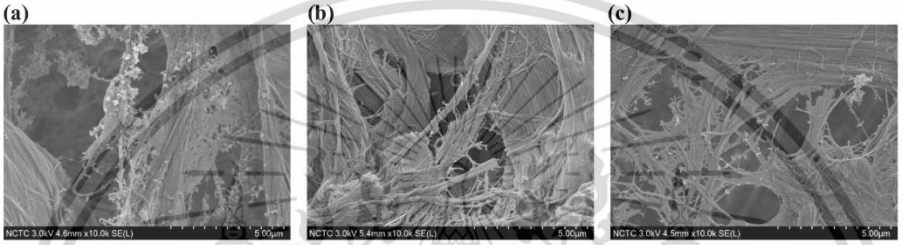

Fig. 6. SEM images (a) B20 PM, (b) B20 with DOC and P-DPF, and (c) B20 Long P-DPF

5. Conclusion

When compared to the three cases of after-treatment systems, the amount of smoke intensity (PM suspended gas) was reduced by up to 81% with the installation of Long P-DPF. A Pt coating on P-DPF can trigger a soot oxidation process in which carbon-based soot trapped inside the material reacts with NO_2 to reduce the quantity of soot while increasing the amount of NO. The comparison of SEM images between three different conditions shows that less soot is produced following the installation of after-treatment equipment. The results of the trials suggested that the installation of after-treatment equipment (DOC and P-DPF) and the use of biodiesel (B10 and B20) in the tests had no discernible effect on engine performance.

Acknowledgments

The authors would like to thank the National Research Council of Thailand (Diesel Engine's Particulate Matter Reduction using Ethanol-Biodiesel-Diesel Blends and Particulate Filter 398/2563) for their support.

References

[1] Wai P, Karin P, Phairote P, Chollacoop N, Kosaka H and Po-ngen W 2022 *Proc. Int. Conf. on Materials, Minerals and Polymer* vol 66 p 2830-2835
[2] Sethin A and Somnuk K 2022 *IOP Conf. Ser.: Earth and Environment Science* vol 1050
[3] Kanokkhanarat P, Karin P, Depaiwa N, Wongpattharaworakul V, Srisurangkul C and Yamakita M 2022 *Proc. Int. Conf. on Materials, Minerals and Polymer* vol 66 p 2862-2867
4] Azimi S, Rocher V, Muller M, Moilleron R and Thevenot D 2005 *J. Sci. Total Environ.* **337** 223-239
[5] Yusaf T, Yousif B and Elawad M 2011 *Conf. on Process Integration, Modelling and Optimisation for Energy Saving and Pollution Reduction, PRES 2010* vol 36 p 4871–4878
[6] Papadopoulos G, Ntziachristos L, Tziourtzioumis C, Keramydas C, Lo T S, Ng K L, Wong H L A and Wong C K L 2020 *J. Sci. Total Environ.* **731** 139137
[7] Jung Y, Pyo Y D, Jang J, Kim G C, Cho C P and Yang C 2019 *J. Chemical Engineering* **369** 1059-1067
[8] Caliskan H and Mori K 2017 *J. Energy Engineering* **128** 128-144

AUTHOR BIOGRAPHY

Author: Mr. Plan Teekatasn Cosh

Nationality: Thai

Date of Birth: 26th June 1998

Place of Birth: Chiang Mai, Thailand

Email: 64601180@kmitl.ac.th

Education:

2023 Master of Engineering in Automotive and Advanced Transportation Engineering, Faculty of Engineering,

King Mongkut's Institute of Technology Ladkrabang, Bangkok, Thailand

2021 Bachelor of Engineering in Mechanical Engineering,

Chiang Mai University, Chiang Mai, Thailand

Presentation and publication:

[1] P.T. Cosh, P. Thaeviriyakul, P. Wai, B. Oh, H. Liu, M.H. Thin, W. Phairote, M. Srilomsak, S. Kittiratsatcha, P. Karin, C. Charoenphonphanich, K. Sriprapha, S. Srimanosaowapak, K. Hanamura, *Impacts of Partial Flow Diesel Particulate Filter on Vehicle's Brake Thermal Efficiency and Exhaust Emissions Characteristics*, 2023, Proc. TSME Int. Conf. on Mechanical Engineering, p 63-69.